DEVELOPING A HEURISTIC OPTIMIZATION METHOD FOR SIMULTANEOUS CALIBRATION OF CAR FOLLOWING AND LANE CHANGING PARAMETERS UNDER NON-LANE BASED MIXED TRAFFIC

TARIQUL HASAN

MILITARY INSTITUTE OF SCIENCE AND TECHNOLOGY

2021

DEVELOPING A HEURISTIC OPTIMIZATION METHOD FOR SIMULTANEOUS CALIBRATION OF CAR FOLLOWING AND LANE CHANGING PARAMETERS UNDER NON-LANE BASED MIXED TRAFFIC

TARIQUL HASAN
(*BSc Engg., MIST*)

A THESIS SUBMITTED FOR THE DEGREE OF MASTER OF ENGINEERING

DEPARTMENT OF CIVIL ENGINEERING
MILITARY INSTITUTE OF SCIENCE AND TECHNOLOGY

2021

DEVELOPING A HEURISTIC OPTIMIZATION METHOD FOR SIMULTANEOUS CALIBRATION OF CAR FOLLOWING AND LANE CHANGING PARAMETERS UNDER NON-LANE BASED MIXED TRAFFIC

TARIQUL HASAN

2021

CERTIFICATION OF APPROVAL

The thesis titled "**DEVELOPING A HEURISTIC OPTIMIZATION METHOD FOR SIMULTANEOUS CALIBRATION OF CAR FOLLOWING AND LANE CHANGING PARAMETERS UNDER NON-LANE BASED MIXED TRAFFIC**", submitted by Tariqul Hasan, Roll No: 1017110003, Session: 2017-2022 has been accepted as satisfactory in partial fulfillment of the requirement for the degree of Master of Science in Civil Engineering.

BOARD OF EXAMINERS

Dr. Md. Hadiuzzaman Professor Department of Civil Engineering Bangladesh University of Engineering and Technology	Chairman (Supervisor)

Lieutenant Colonel Mohammed Russedul Islam, PhD Instructor Class A Department of Civil Engineering Military Institute of Science and Technology	Member (Co Supervisor)

Brigadier General Md Habibul Huq, psc Head Department of Civil Engineering Military Institute of Science and Technology	Member (Ex-officio)

Brigadier General (Retd) Shah Md Muniruzzaman, psc, PhD Professor Department of Civil Engineering Military Institute of Science and Technology	Member (Int)

Dr. Md Asif Raihan Assistant Professor ARI Bangladesh University of Engineering and Technology	Member (Ext)

DECLARATION

I hereby declare that this thesis is my original work and it has been written by me in its entirety. I have duly acknowledged all the sources of information which have been used in the thesis. The thesis (fully or partially) has not been submitted for any degree or diploma in any university or institute previously.

কর্নেল তারিকুল হাসান, পিএসসি
উপ মহাপরিচালক
এয়ার উইং
সদর দপ্তর বিজিবি, ঢাকা

18 March, 2021

Tariqul Hasan
Roll- 1017110003

ABSTRACT

Microscopic traffic simulation models have been widely used to analyze the traffic operation and management strategies on highways and urban streets primarily because the simulation is less disruptive to traffic, less expressive, and faster than the field experimentation. In order to provide accurate and meaningful results, simulation models must be calibrated and validated before real simulation is conducted. However, calibration methods differ in algorithm, level of accuracy, convergence time and level of effort. It is essential to choose a calibration method particularly suitable for a specific traffic and roadway condition.

In this research, a new approach has been proposed for calibration of microscopic traffic simulation model VISSIM. Wiedemann 99 car following model and lane changing model parameters were simultaneously calibrated for freeways. Drone was used to capture real time traffic data over a 2.6 km stretch segment of the Dhaka-Mymensingh Highway (N3) in Bangladesh for the calibration and validation through image processing technique. New mathematical equation, based on the fusion of microscopic and macroscopic traffic data, has been derived dynamically from Leader-Follower pair of simulated vehicle trajectory data to evaluate the measure of performance (MOP) between the observed and simulated traffic data. Root mean square error (RMSE) between the measurement of space headway of 1191 instances of observed lane change and space headway derived from the mathematical equation by evaluating simulated vehicle trajectory data has been considered as the fitness function for calibration, and sum of absolute error (SAE) for validation against average headway measurement. Three optimization techniques namely, Genetic Algorithm (GA), Simultaneous Perturbation Stochastic Approximation (SPSA) and Simulated Annealing (SA) were used to examine their performances in terms of level of accuracy and computational time in calibrating

the parameters. In the perspective of present study on non-lane based mixed traffic condition with MOP derived from new mathematical equation based on micro and macro data, SA proved to be efficient reducing RMSE to 93.90%, while GA reduced to 92.15% and SPSA 91.85%.

Though the microscopic simulation is getting increasingly common in traffic planning and operational research, the most important drawback of traffic simulation model is that the calibration and validation of such model can be very tedious. This invokes the necessity of a graphical user interface (GUI) for ease in calibration and result interpretation. In this study a user-friendly Optimization Program Control Interface (OPCI) has been demonstrated for auto calibration that controls the entire process of calibration and generates the desired graphical output for result interpretation and analysis.

ACKNOWLEDGEMENTS

All praise to Almighty Allah, the most beneficent and merciful, the blessings of Whom made the study a success.

The author feels extremely privileged to work under their most revered teacher, Dr. Md. Hadiuzzaman, Professor, Department of Civil Engineering, BUET for his encouragement, continuous guidance, invaluable suggestion and generous help at every stage of this concerted dissertation. His contribution to me can only be acknowledged but never be compensated. His consistent inspiration helped me to work diligently throughout the completion of this research work and also contributed my ability to approach and solve a problem. Without his assistance, advice and finely corrections this dissertation would not has been materialized and will always be remembered.

The author also expresses their gratitude to the Lieutenant Colonel Mohammed Russedul Islam, PhD, Instructor Class A, Department of Civil Engineering, Military Institute of Science and Technology for his continuous support and assistance in developing the traffic model in VISSIM.

The author also expresses their heartfelt thanks to the Nazmul Hoque, Research Assistant of Dr. Md. Hadiuzzaman, BUET, for his relentless support and assistance in undertaking the thesis activities.

Finally, the author can never forget the blessings, cooperation, great inspirations and unbound sacrifices of his family members to bring out this finished thesis.

TABLE OF CONTENTS

LIST OF FIGURES

LIST OF TABLES

TABLE OF ABBREVIATIONS

Serial	Abbreviated Form	Meaning
1	GA	Genetic Algorithm
2	SPSA	Simultaneous Perturbation Stochastic Approximation
3	SA	Simulated Annealing
4	MOPs	Measure of Performances
5	GUI	Graphical User Interface
6	MOE	Measure of Effectiveness
7	RMSE	Root Mean Square Error
8	SAE	Summation of Absolute Error
9	SSE	Summation of Square Error
10	PCU	Passenger Car Unit
11	LHD	Latin Hypercube Design
12	FHWA	Federal Highway Administration
13	OPCI	Optimization Program Control Interface
14	BGS	Background Subtraction
15	MAE	Mean Absolute Error
16	CALVIS	Calibration of VISSIM

CHAPTER 1
INTRODUCTION

1.1 General

In the last few decades traffic simulation model has grown into a major planning tool for transportation engineers. One of the supreme advantages of using such tools is to assess different alternates and scenarios of any projects prior to their field implementations and thereby enhancing scope for significant improvements of the projects. Traffic simulation models could be divided into three categories including microscopic, macroscopic, mesoscopic simulation models. First category simulates the movement of individual vehicles in a traffic stream. It is helpful in capturing the more detailed aspects of the system. Car-following and lane-changing models are the two fundamental components in traffic micro-simulations. The second (macroscopic) category simulates transportation network section-by-section rather than by tracking individual vehicles. The relationships between flow, speed, and density of traffic stream form the fundamental basis of this category. Mesoscopic traffic simulation models combine the properties of the first and second models (TRB, 2000).

Along with the increasing popularity and use of traffic simulations, an essential concern has been raised about their appropriate calibration and validation. Microscopic simulation models contain numerous independent parameters that can be used to describe traffic flow characteristics, driver behavior, and traffic control operations. These models provide a default value for each parameter, but they also allow users to change the values to represent local traffic conditions. The process of adjusting and fine-tuning model parameters by using field data to reflect local traffic conditions is model calibration. The findings based on the uncalibrated or inappropriately calibrated models could be misleading and even erroneous. Thus, proper calibration is a crucial step in simulation applications.

The calibration process, especially for microscopic simulations, could be a complex and time-consuming task because of the large number of unknown parameters and significant computational load associated with large-scale traffic simulation runs (Toledo, 2004). Although there are numerous optimization procedures that have been used to calibrate microsimulation traffic models, the manual search, gradient approach, simplex-based approach, and artificial intelligence techniques have been used most frequently.

Three widely practiced optimization algorithms are Genetic Algorithm (GA), Simultaneous Perturbation Stochastic Approximation (SPSA) and Simulated Annealing (SA) in which the former one is an artificial intelligence technique as mentioned earlier, SPSA is gradient based and SA is search based algorithm. These three optimization methods are based on different algorithm but serve the same purpose i.e. calibrating the parameters, at different level of accuracy and computational time. Generally, users demand that an optimization technique should fulfill three requirements. First, the method should be able to find the optimum values of parameter set to simulate real traffic scenario with minimum difference. Second, the convergence should be fast. Third, the program should have a minimum of control parameters so that it will be easy to use. In this thesis, an endeavor has been taken to compare above mentioned three methods of optimization and examine their performance in terms of applicability, accuracy, computational time and level of effort.

While recent research has indicated that the accuracy of a simulation model can significantly improve through the use of automated calibration procedures, but this is not a typical practice.

Many engineers lack in tools or the skill necessary to easily program and implement such procedures. A graphical user's interface (GUI) is necessary to make automated calibration more accessible to professional engineers.

This chapter presents a brief overview of the history and background of traffic simulation models, addresses the specific problems associates with model calibration and data requirement, identifies the objectives and significances of the study and summarizes the remaining chapters to address the problems identified.

1.2 Background of the Study

In a developing country like Bangladesh there is a rapid development in communication and transport infrastructures. But neither the government agencies nor the private consultancy firms commonly use traffic simulation model for transportation planning and traffic management. It is well established that the traffic simulation models are much safer, less expressive, and faster than the field implementation tests. Unfortunately, in our traffic context, transportation engineers and professional lack adopting state-of-art technologies.

In order to provide accurate and meaningful results, a simulation model must be calibrated and validated before a real simulation is conducted. Researches have shown that calibration of simulation model parameters using any of the optimization algorithm can efficiently improve the accuracy of simulation model output. However, practicing engineers rarely take this approach. Many of them do not have the tools or the skill to carry out calibration procedures which have been performed by researchers. Furthermore, a GUI for an automated calibration procedure is necessary to make these tools more available to students and professionals.

Hence it is essential to make extensive use of traffic simulation model in national transportation planning and traffic management. It is also necessary to calibrate the simulation model before its implementation in order to improve its accuracy following any of the calibration techniques. Finally, a GUI for automated calibration will certainly help the users in analyzing and interpreting the results.

1.3 Problem Statement

In a developing country like Bangladesh there is a rapid infrastructure development in communication sector like mass rapid transit (MRT), elevated expressway, and subway. An operational traffic simulation model is required to evaluate its anticipated impact on traffic parameters of roadway. In order to depict the real traffic scenario, the driving behavior parameters of any micro simulation model including both the car following and the lane changing parameters are to be adequately calibrated. Most of the previous studies (Duong, Saccomanno & Hellinga 2010, Park & Kwak 2011, Crowe 2009, Menneni, Sun, & Vortisch 2008, Park, Jongsun & Ilsoo 2006, Lownes & Machemehl 2006, Park & Qi 2005, Kim, Kim & Rilett 2004, Fellendorf & Vortisch 2001, Lee, Xu & Chandrasekar 2001) calibrated car following parameters and few literatures were found calibrating the lane changing parameters only (Park & Schneeberger 2003). Though significant number of researchers calibrated both the car following and lane changing parameters (Karakikesa, Spanglera & Margreiter 2017, Lidbe, Hainen & Jones 2017, Leyn & Vortisch 2015, Miller 2009, Park, Won & Yun 2006, Gomes, May & Horowitz 2004) but they did that at different stages/steps of simulation process appropriate for particular types of networks and compared against separate measure of performances (MOPs) using mostly macro traffic data like vehicle count, speed, flow, volume, queue length, delay, capacity etcetera. But none applied for simultaneous calibration of car following and lane changing parameters. Car following parameters were also focused in few literatures for simulation of heterogeneous or mixed traffic (Siddharth & Ramadurai 2013, Manjunatha, Mathew & Vortisch 2012, Mathew & Radhakrishnan 2010) where lane changing parameters were completely ignored. Complex maneuvers commonly adopted by the drivers in mixed traffic condition makes the calibration process of lane changing parameters more erroneous, which is further aggravated in non-lane- based traffic condition. Large and detailed microscopic vehicle trajectory data sets are needed to calibrate and validate lane changing models more accurately. Absence of vehicle trajectory data will compensate the accuracy of simulation result which will mislead the transport planners. Simultaneous calibration of car following and lane changing parameters by incorporating the fusion of macro and micro traffic data will invariably improve the simulated model to represent the real world more reliably.

1.4 Thesis Objectives and Scope of Work

This study aims to develop a methodology for calibration of microscopic simulation models by simultaneous optimization of car following and lane changing parameters with the fusion of both macro and micro traffic data using heuristic optimization algorithms under non-lane based mixed traffic condition. The specific objectives are:

a) To develop an efficient traffic simulation calibration method by simultaneous optimization of parameters related to car following and lane changing sub-models.

b) To formulate an objective function by the fusion of macroscopic and microscopic traffic flow data.

c) To investigate a robust heuristic optimization algorithm to be used for mixed traffic condition.

It is expected that the calibrated parameters will produce an accurate simulation model that will be used in deciding the operational impact of different infrastructural development projects.

The scope of this thesis is restricted to uninterrupted arterials. The test site is the Tongi Diversion Road, a section of the Dhaka-Mymensingh Highway (N3) in Bangladesh (shown in Figure 6-1). The GUI has been developed to calibrate any number of driving behavior parameters of VISSIM microsimulation model. However, the calibration process is expected to accurately estimate and predict the complex nature of the prevailing heterogeneous traffic condition of the test site through appropriate modifications and extensions of programming codes for other traffic simulation models of VISSIM.

1.5 Significance of the Study

Understanding the consequences of a highway or traffic operations improvement before project implementation is essential to traffic engineers and planners. Decision- makers are hesitant to invest in highway projects that promise to improve safety and reduce congestion without some evidence that these promises are realizable. Experimenting with the transportation system can be costly, traffic disruptive, and impractical. Engineers have been able to avoid such experiments by turning to computer software for a comparatively low-cost method of analyzing transportation projects.

In North America and Europe, use of traffic simulation model for traffic management has become a common practice. It is much more time and cost effective with enhanced accuracy than any other field implementation tests. Bangladesh is yet to adopt such technology in transportation planning. Whereas, the utility of such modeling software can be maximized in developing country like Bangladesh where there is a continuous growth of traffic infrastructures with inherent deficiency in efficient traffic management. Few of the government and private universities are presently in possession of VISSIM simulation software for the purpose of pure academic research. It is envisaged that the use of VISSIM will be commercialized within next five years with a greater number of professionals and expertise on this modeling software. And use of simulation model will be of limited utility until and unless it is properly calibrated. The model must be calibrated basing on existing roadway and traffic condition. Hence the importance of method of calibration cannot be under emphasized.

1.6. Outline of Methodology/ Experimental Design

1.6.1 General procedures

Calibration of a micro simulation model for mixed traffic requires special procedures to address the unique characteristics of such traffic. Accordingly, a methodology will be proposed which will include representation of vehicles, geometry and traffic, followed by identification of car following and lane changing calibration parameters by sensitivity analysis, setting their ranges heuristically and determining the parameter values by an optimization model. The traffic representation addresses several distinct features of mixed traffic. First, to ascertain the need for calibration, the model will be simulated with the default setting (pre-calibration) and will be compared with field values against the appropriate MOPs; if the error is insignificant (which is generally unlikely), then the model with default settings can be adopted without any further calibration. If the error is significant, the calibration steps will be followed.

1.6.2 Data collection

A minimum of 7200 seconds of video data will be collected using drone on Dhaka-Mymensingh Highway. The video will be analyzed through software module to get the macro and vehicle trajectory data.

1.6.3 Vehicle representation

Simulation models typically come with a set of standard types of vehicles such as car, bus, truck, and motorcycle. However, in the case of mixed traffic, several non-standard vehicle types such as motorized and non-motorized three wheelers exist and these can significantly affect the simulation results. Therefore, the first step in the simulation will be to accurately define the static and dynamic characteristics of every vehicle type in terms of length, width, acceleration and deceleration, and speed ranges.

1.6.4 Geometric representation

The next step will be accurate representation of the geometry of freeway defined by the number of lanes and width of each lane.

1.6.5 Traffic representation

This phase involves identifying the local characteristics of the traffic and fine tuning the elements of networks so that the traffic in the simulation behaves similar to the one in the reality. One can observe different additional movements in terms of lane changes, smaller vehicles seeping through etc. The available parameters in the simulation model may not be sufficient to replicate certain special movements by the vehicles in mixed traffic, but depending on the flexibility of network modeling, one can try to bring the behavior in the simulation as close as possible to reality.

1.6.6 Selection of parameters

Parameters that influence the safety distance, space headway, drivers' aggressiveness, safe and relative speed, time to collision and gap acceptance between subject vehicle and following vehicle will be the primary preference for calibration. A sensitivity analysis will be conducted to identify the key parameters for calibration of particular type of network.

1.6.7 Optimization algorithm

Three state-of-art heuristic optimization algorithms namely Genetic Algorithm (GA), Simultaneous Perturbation Stochastic Approximation (SPSA) and Simulated Annealing (SA) will be applied for calibration of parameters and their performance will be compared in terms of applicability, accuracy, computational time and level of effort for simultaneous calibration of car following and lane changing parameters.

1.6.8 Measures of Performances (MOPs) and objective function

Microscopic traffic variable for lane changing maneuver like space headway between a pair of leader-follower vehicles is dependent on their speed, and density around the roadway which is macroscopic traffic variable. As such both the aggregated and disaggregated MOPs will be selected and blended together to derive a mathematical equation for the objective function.

1.7 Thesis Outline

This thesis consisting of eight chapters as follows:

Chapter 1 gives an introduction of the relevant research background, problems statement, objectives and scope, significance of the study and outline of methodology of this thesis work.

Chapter 2 comprehensively reviews previous works on calibration of microscopic traffic simulation models with respect to their categories in terms of use of micro simulation tools, calibration methodology, and use of objective functions and MOPs.

Chapter 3 presents the salient aspects of microscopic simulation model VISSIM with special emphasis on Wiedemann's 99 car following and lane changing driving behavior parameters.

Chapter 4 presents three widely used stochastic optimization algorithm GA, SPSA and SA and makes a comparative study on their approaches in optimization.

Chapter 5 derives the mathematical equation for the measurement of MOP and objective function. It also discusses the conceptual framework of the thesis work along with computer coded VISSIM interface 'Optimization Program Control Interface (OPCI) that controls the entire automation of calibration process.

Chapter 6 proposes a seven steps calibration procedure which includes field data collection and processing, VISSIM model development, determination of MOPs and Objective function, selection of parameter and range, sensitivity analysis and the calibration approaches based on three optimization techniques i.e. GA, SPSA & SA.

Chapter 7 presents the OPCI generated calibration and validation results in accordance with three optimization techniques along with relevant interpretation and analysis.

Chapter 8 summarizes the main conclusions of this thesis and discusses recommendations for future thesis works related to calibration of macroscopic traffic simulation mode in different traffic and roadway condition.

Annexure A presents numerous figures and tables explaining the relationship between headway and speed of following vehicle that has been established by analyzing each pair of Leader-Follower vehicles trajectory data obtained from each VISSIM simulation output file.

Annexure B orients with the various features of OPCI and the automation of calibration process.

CHAPTER 2

REVIEW OF LITERATURE

Many studies about calibration of traffic simulation models have been published. These studies adopted different traffic microsimulation tools and model parameters, heuristic optimization methodologies and suitable objective function against numerous MOPs. This chapter briefly reviews the literatures based on mentioned categories.

2.1 Traffic Microsimulation Tools

Car following and lane changing models of few widely used microsimulation tools are reviewed in Table-2.1:

Table 2.1: Car Following and Lane Changing Model of Various Traffic Microsimulation Tools

Tools	Car Following Model	Lane Changing Model
VISSIM	Model based on the psycho-physical behavior suggested by Wiedemann in 1974 and subsequently developed in 1999. The model constituted by different thresholds that form four regimes; Free driving, Following, Approaching and Braking.	It classifies lane changes into free lane change and necessary lane change. The free lane change uses lag time to collision in the target lane as the decision variable. For necessary lane change, the model also checks the lead time to collision and maximum deceleration.
AIMSUN	Safety distance model based on the model developed by Gipps (1981). When constrained by the vehicle in front, the follower tries to adjust its speed in order to obtain safe space headway to its leader. When free, the	AIMSUN describes a vehicle's motivation to change lane in terms of necessity, desirability, and possibility to change lanes following the Gipps lane changing model.

	vehicle's speed is constrained by its desired speed and its maximum acceleration.	
MITSIM	Three regimes with different follower behavior; free driving, following and emergency deceleration. The behavior in the following regime is based on an The Gazis-Herman-Rothery (GHR) model which states that the follower's acceleration is proportional to the speed of the follower, the speed difference between follower and leader, and the space headway.	The model distinguishes between mandatory and discretionary lane changes. These models assume three levels of decision making: decision to change lane, choice of lane to change to, and execution of the lane change (gap acceptance).
TRANSIMS	The model uses cellular automata which divides a roadway into cells of equivalent size. Each cell can hold either a part of a vehicle (for large trucks or buses) or a single vehicle. No parts of any two distinct vehicles can occupy the same cell.	Cellular automata model assumes that vehicle changes to another lane if the number of empty cells ahead and backward of the current and target lane satisfy favorable speed conditions, then, the lane change potential is expressed with certain probability, depending on availability of sufficient space to perform the lane change.
PARAMICS	The acceleration model is based on the psycho-physical model developed by Fritzsche (1994). The model accounts for human perception in the definitions of the five model regimes; Danger, Closing in, Following I, Following II and Free driving.	The model is based on the gap acceptance theory, which has front gap and rear gap (both in distance unit) in the target lane as the decision variables.

CORSIM	CORSIM Uses the Pitt's car following model that incorporates the vehicle spacing and speed differential between the lead and following vehicle as two independent variables. Follower will maintain safe gap from leader and decelerate while insufficient gap prevails.	Halati (1997) developed the model which are classified as mandatory lane changing, discretionary lane changing, and random lane changing. Lane changing maneuvers depend on the availability of acceptable lead and lag gaps in the target lane.

Cheu (1998) used FRESIM to calibrate twelve global parameters. Kim & Rilett (2001) illustrated simulation model CORSIM and TRANSIMS by ITS data. GENOSIM was developed by Ma & Abdulhai (2002) in combinatorial parametric optimization to calibrate the micro-simulation model PARAMICS. Schultz & Rilett (2004) introduced statistical method for normal distribution of data using CORSIM. Park & Qi (2005) chose VISSIM to calibrate eight driving behavior parameters. Turley (2007) developed a GUI for automated calibration in CORSIM. Cunto & Saccomanno (2008) described the procedure for calibrating and validating safety performance in VISSIM. Mathew & Radhakrishnan (2010) proposed a methodology to calibrate VISSIM for heterogeneous traffic. Park & Kwak (2011) presented a case study on TRANSIMS to calibrate and validate fourteen parameters related to car following and lane change behavior model. Omrani & Kattan (2013) calibrated the driver behavioral and route choice parameters in PARAMICS. Manjunatha, Vortisch & Mathew (2013) used VISSIM to calibrate thirteen parameters (four parameters after sensitivity analysis) in a mixed traffic environment at two signalized intersections in Mumbai.

2.2 Calibration Approach

Cheu (1998) was the first one to apply the GA to the parameter calibration of FRESIM. Kim & Rilett (2001) illustrated GA based approach for simulation model CORSIM and TRANSIMS by ITS data. GENOSIM was developed by Ma & Abdulhai (2002) in combinatorial parametric optimization using GA as the core algorithm. Park & Schneeberger (2003) used Latin Hypercube sampling along with a linear regression model to generate scenarios. However, they did not consider the correlations among the parameters. Schultz & Rilett (2004) introduced methodologies for lognormal and normal distribution of data (i.e., mean and variance) for calibration. Park & Qi (2005) used Latin Hypercube Design (LHD) algorithm and statistical method 'Analysis of Variance' (ANOVA), to identify the appropriate parameters and their acceptable ranges. Kim, Kim & Rilett (2005) developed a statistically based objective function based on nonparametric statistical techniques like the Moses' distribution free rank-like test, Wilcoxon rank-sum test and the Kolmogorov-Smirnov test to compare the simulated result.

Egami, Mon-Ma, Setti & Rilett (2006) proposed a system for GA based automatic calibration of two-lane traffic simulation models using several different highway sections to find the set of calibrated parameters. Turley (2007) developed a GUI for automated calibration in CORSIM using GA as the core algorithm. Omrani & Kattan (2013) has developed multi-criteria optimization framework for the simultaneous calibration of demand and supply parameters in dynamic traffic assignment (DTA). They applied GA to estimate origin-destination (OD) flows. Mathew & Radhakrishnan (2013) applied GA to obtain optimal parameters in heterogeneous traffic environment. Manjunatha (2013) applied GA in the unique features of mixed traffic at signalized intersections.

Hee-Sang, Kwang & Ho-Chan (2008) introduced free model concept as an alternative intelligent system technique to design a controller for complex dynamic system and calibrated the parameters of the free model by simultaneous perturbation stochastic approximation (SPSA) method. Wang, Jian, Guanglin & Xiaowei (2013) optimized transit operation strategies. The penalty function method was adopted to simplify the optimization model into a general programming model with linear constraints. GA and the SA algorithm were used to obtain near-optimum solutions. Kuo, Yiyo, Luo & Chi-Ming (2011) proposed a SA based circular route optimization procedure to optimize the driving route for buses.

2.3 Objective Functions and MOPs

Cheu (1998) used the mean absolute error ratio (MAER) as the fitness function which were10.68% and 15.32% respectively for AVI OD and CORSIM OD. Kim & Rilett (2001) obtained TRANSIMS MAER values as 0.72% for the AVI OD and 12.16% for CORSIM OD. Ma & Abdulhai (2002) used queue length as MOP for validation and 90% accuracy with field data was obtained. MAER was used as the objective function against volume and travel time by Schultz & Rilett (2004). Volume MAER resulted a difference of 8.5% and 8.4% and travel time MAER yielded 15.2% and 15.9% for lognormal and normal distribution alternatives respectively. Kim, Kim & Rilett (2005) observed distribution of travel time rather than mean time with MAER ranged from 0.7% to 6.7%. Park & Qi (2005) chose average travel time, Park & Kwak (2011) used travel times and vehicle count, Cunto & Saccomanno (2008) and Duong, Saccomanno & Hellinga (2010) chose safety performance as MOP.

Turley (2007) considered average content and speed during sensitivity analysis and volume and travel time during calibration. Volume MAER ranges from 12.1% to 24.0% and travel time

MAER ranges from 87.6% to 88.2% resulted in difference between values of default and calibrated parameters. Mathew & Radhakrishnan (2010) considered absolute error value as the objective function. Omrani & Kattan (2013) chose normalized root mean square error (NRMSE) and the Geoffrey E. Havers statistic (GEH) as the fitness function against OD flow. The NRMSE between the observed and simulated results were found to be 17.7% & 15.4% in AM peak, and 20.3% & 19.3% in PM peak for count data and speed values respectively.

2.4 Lane Changing Parameters

There were numerous literatures that had worked on lane changing parameters. Karakikesa, Spanglera & Margreiter (2017) describes a systematic calibration process of a motorway network in VISSIM, based on travel time measurements that were derived from limited number of Bluetooth detectors. Model's systematic calibration and validation under the suggested approach show very good results in 96.5% of the created intervals, for both cars and heavy vehicles. After a reasonable adjustment of desired speeds of vehicle classes in first stage, they calibrated cc1 & cc2 of Wiedemann 99 car following model, and maximum deceleration (trailing vehicle), safety distance reduction factor and maximum deceleration for cooperative braking of lane changing model in second stage of calibration.

Lidbe, Hainen & Jones (2017) made a comparative study to evaluate three meta-heuristics (GA, SA, and Tabu Search (TS)) optimization techniques for calibration of microsimulation models in VISSIM by calibrating Wiedemann 74 car following and lane changing parameters, and concluded that TS gives better calibration results compared to the GA and SA.

Yeom, Rouphail, Rasdorf, & Schroeder (2016) proposed a methodology to simulate freeway work zone capacity in VISSIM under various scenarios of work zone lane closure and calibrated car following parameters cc1 and cc2 and lane changing parameters like maximum deceleration for a necessary lane change (own and trailing), for a necessary lane change, −1 meter/sec2 per distance (own and trailing), safety distance reduction factor and maximum deceleration for cooperative braking. It can replicate any work zone queue discharge flow rate value consistent with the empirical model predictions.

Essa & Sayed (2015) used Surrogate Safety Assessment Model (SSAM) for measurement of conflict (e.g., time to collision) and finding their locations and compared with simulated conflicts in VISSIM. They followed a two-step calibration procedure to enhance correlation between simulated and field-measured conflicts. The first calibration step was matching actual field conditions (desired speed and arrival type) to ensure that VISSIM gives real average delay values. The second step was the use of sensitivity analysis followed by a genetic algorithm procedure to calibrate the VISSIM parameters that had effect on the simulated conflicts. The results highlighted the importance of model calibration and identified several limitations of the SSAM.

Leyn & Vortisch (2015) simulated German highway capacity and calibrated VISSIM driving behavior parameters for basic freeway segments. They successfully calibrated cc1, cc4, cc8 and cc9 of Wiedemann 99 car following parameters and cooperative lane change maximum speed difference, maximum collision time, −1 meter/sec2 per distance (own), accepted deceleration (trailing vehicle) and to slower lane if collision time above of lane changing parameters. They recommended that a separate parameter set for every behavior type and vehicle class (e.g., passenger cars and heavy vehicles) is crucial, as certain passenger car driving characteristics are inappropriate for heavy vehicles.

Siddharth & Gitakrishnan (2013) simulated Indian heterogeneous traffic conditions in Chennai with calibration of five Wiedemann 74 and car following, one lane changing, one lateral driving behavior parameters and four desired accelerations using GA optimization technique. Calibrated parameters yielded 8.19% flow MAPE during calibration and 10.2% flow MAPE during validation.

2.5 Summary

VISSIM, AIMSUN, MITSIM, TRANSIMS, PARAMICS and CORSIM have relatively different presentation of their car following and lane changing models. The parameter sets, though not discussed in this chapter, are significantly different. The resulting car following trajectories of a follower – leader vehicle pair and lane changing behavior will not be similar. However, the speed difference between follower and leader, and the space headway (or gap) are two important aspects of roadway parameters that have been focused in all the microsimulation tools for modeling both the car following and lane changing behavior.

From the above review it is revealed that though different micro simulation tools have been used for modeling, VISSIM is the widely used latest trend in micro simulation model. A look at the method of calibration studies revealed that GA and SPSA were frequently used. The relevant literature lacks the use of SA optimization in traffic simulation calibration. Again, the concept of GA has been applied vastly by different researchers to calibrate their desired parameters in their respective geographic locations basing on different roadway and traffic configurations. The obtained optimal parameter values will not be similar in the context of Bangladesh with heterogeneous traffic mix and unconventional physical elements of roadways. Though significant number of researchers calibrated both the car following and lane changing parameters but they did that at different stages/steps of simulation process appropriate for particular types of networks and compared against separate measure of performances (MOPs) using mostly macro traffic data like vehicle count, speed, flow, volume, queue length, delay, capacity etcetera. But none applied for simultaneous calibration of car following and lane changing parameters. Car following parameters were also focused in few of the literatures for simulation of heterogeneous or mixed traffic where lane changing parameters were completely ignored. Complex maneuvers commonly adopted by the drivers in mixed traffic condition makes the calibration process of lane changing parameters more erroneous, which is further aggravated in non-lane- based traffic condition.

CHAPTER 3

MICROSCOPIC SIMULATION MODEL VISSIM

3.1 General

VISSIM was developed in Germany at the University of Karlsruhe in the early 1970s, but the software was not made commercially available until 1993. Because of its European roots, VISSIM was designed to model a variety of modes, including general traffic, buses, light rail, heavy rail, trucks, pedestrians, and bicyclists. VISSIM is a microscopic, time step and behavior-based simulation model developed to model urban traffic and public transport operations and flows of pedestrians. The program can analyze private and public transport operations under constraints such as lane configuration, vehicle composition, traffic signals, public transport stops, thus making it a useful tool for the evaluation of various alternatives based on transportation engineering and planning measures of effectiveness (PTV VISSIM 7 User Manual).

VISSIM comprises a traffic simulator and a signal state generator. The traffic simulator is a microscopic traffic flow simulation model including the car following and lane change logic. It contains network geometry and generates traffic. As in CORSIM, VISSIM uses links to represent roadway segments. VISSIM does not, however, have the traditional node structure found in CORSIM. The signal state generator contains the signal control logic that can be used to can model virtually any control logic, including fixed time, actuated, adaptive, transit signal priority, and ramp metering. The node-less network structure and separate signal state generator both give the user greater flexibility in defining the traffic environment.

3.2 Car following logic (The Wiedemann Approach)

VISSIM uses the psycho-physical driver behavior model developed by Wiedemann (1974). The basic concept of this model is that the driver of a faster moving vehicle starts to decelerate as he reaches his individual perception threshold to a slower moving vehicle. Since he cannot exactly determine the speed of that vehicle, his speed will fall below that vehicle's speed until he starts to slightly accelerate again after reaching another perception threshold. This results in an iterative process of acceleration and deceleration. Different thresholds and regimes of Wiedemann car following model is shown in Figure-3.1.

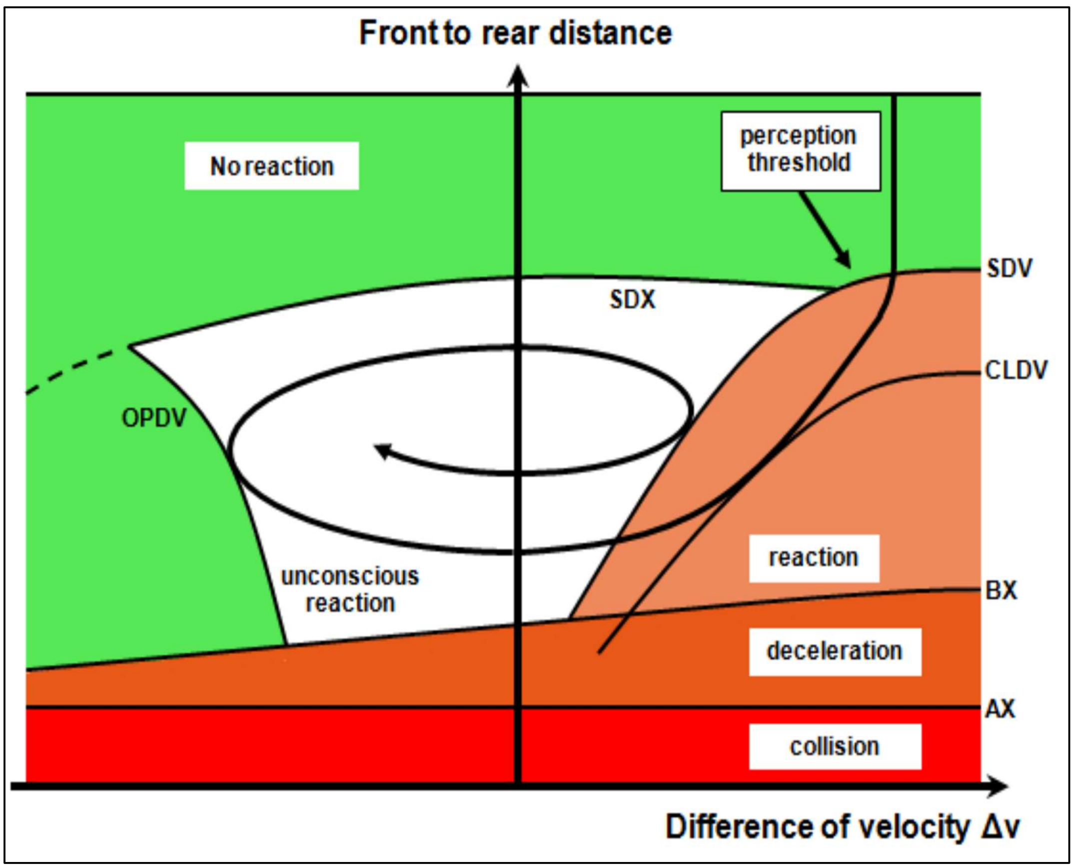

Figure 3.1: Different Thresholds and Regimes of Wiedemann Car Following Model
Source: PTV VISSIM 7 User Manual

The basic idea of the Wiedemann model is the assumption that a driver can be in one of four driving modes:

3.2.1 Free driving

Free driving has no influence of preceding vehicles. In this mode the driver seeks to reach and maintain a certain speed, his individually desired speed. The vehicle is located above all thresholds in the Figure-3.1.

3.2.2 Approaching

It is the process of adapting the driver’s own speed to the lower speed of a preceding vehicle. While approaching (passing the SDV threshold of Fgure-3.1), a driver applies a deceleration so that the speed difference of the two vehicles is zero in the moment he reaches his desired safety distance.

3.2.3 Following

The driver follows the preceding car without any conscious acceleration or deceleration. He keeps the safety distance more or less constant, but again due to imperfect throttle control and imperfect estimation the speed difference oscillates around zero. The thresholds SDV, SDX, OPDV and BX constitute the Following regime (Figure-3.1).

3.2.3 Braking

It is the application of medium to high deceleration rates if the distance falls below the desired safety distance (Threshold BX of Figure-3.1).

3.3 Driving Behavior Model

A driving behavior model is the core of any traffic simulation model. It determines how the vehicles will behave within the network. In VISSIM, the driving behavior models contain a psycho-physical car following model for longitudinal vehicle movement and a rule-based algorithm for lateral movements.

3.3.1 Car-following Models

The car following model contains the following parameters:

3.3.1.1 The look ahead distance

It defines the distance that a vehicle can see forward in order to react to other vehicles either in front or to the side of it (within the same link). This parameter is in addition to the number of Observed Vehicles.

3.3.1.2 The number of observed vehicles

This parameter affects how well vehicles in the network can predict other vehicles' movements and react accordingly. As some of the network elements are internally modeled as vehicles it might be useful to increase this value if there are several cross sections of network elements within a short distance. However, the simulation will run slower with higher values.

3.3.1.3 The look back distance

It defines the distance that a vehicle can see backwards in order to react to other vehicles behind (within the same link). The minimum value is important when modeling lateral vehicle behavior.

3.3.1.4 Temporary lack of attention

It defines a period of time for which vehicles will not react to a preceding vehicle (except for emergency braking) for a certain amount of time.

3.3.2 Basic models for car following behavior and their parameters

Car following model selects the basic model for the vehicle following behavior. Depending on the selected model the model parameters change. ‘Wiedemann 74’ model is mainly suitable for urban traffic and ‘Wiedemann 99’ model is used for freeways traffic. ‘No Interaction’ model is used for simplified pedestrian behavior where vehicles do not recognize any other vehicles. Depending on the selected Car following model a different number of model parameters are available.

3.3.2.1 Wiedemann 74 model parameters

This model is an improved version of Wiedemann’s 1974 car following model. The following parameters are available:

a) Average standstill distance (ax) defines the average desired distance between stopped cars. It has a fixed variation of ± 1m.

b) Additive part of desired safety distance (bx_add) and Multiplication part of desired safety distance (bx_mult) affect the computation of the safety distance. The distance d between two vehicles is computed using the formula:

$d = ax + bx$

where ax is the standstill distance

$bx = (bx\_add + bx\_mult * z) * v$

v is the vehicle speed (m/s)

z is a value of range [0,1] which is normal distributed around 0.5 with a standard deviation of 0.15.

3.3.2.2 Wiedemann 99 model parameters

This model is based on Wiedemann's 1999 car following model. The following parameters are available:

a) CC0 (Standstill distance) defines the desired distance between stopped cars. It has no variation.

b) CC1 (Headway time) is the time (seconds) that a driver wants to keep. The higher the value, the more cautious the driver is. Thus, at a given speed v (m/s), the safety distance dx_safe is computed to:

$dx\_safe = CC0 + CC1 \cdot v.$

The safety distance is defined in the model as the minimum distance a driver will keep while following another car. In case of high volumes this distance becomes the value with the strongest influence on capacity.

c) CC2 (‘Following’ variation) restricts the longitudinal oscillation or how much more distance than the desired safety distance a driver allows before he intentionally moves closer to the car in front. The default value is 4.0m which results in a quite stable following process.

d) CC3 (Threshold for entering ‘Following’) controls the start of the deceleration process, i.e. when a driver recognizes a preceding slower vehicle. In other words, it defines how many seconds before reaching the safety distance the driver starts to decelerate.

e) CC4 and CC5 (‘Following’ thresholds) control the speed differences during the ‘Following’ state. Smaller values result in a more sensitive reaction of drivers to accelerations or decelerations of the preceding car, i.e. the vehicles are more tightly coupled. CC4 is used for negative and CC5 for positive speed differences. The default values result in a fairly tight restriction of the following process.

f) CC6 (Speed dependency of oscillation) value indicates the influence of distance on speed oscillation while in following process. If the value set to 0 the speed oscillation is independent of the distance to the preceding vehicle. Larger values lead to a greater speed oscillation with increasing distance.

g) CC7 (Oscillation acceleration) is the actual acceleration during the oscillation process.

h) CC8 (Standstill acceleration) is the desired acceleration when starting from standstill.

i) CC9 (Acceleration at 80 km/h) is the desired acceleration at 80 km/h

3.3.3 Lane change

There are basically two kinds of lane changes in VISSIM:

a) Necessary lane change (in order to reach the next connector of a route)

b) Free lane change (because of more room / higher speed)

3.3.3.1 Necessary lane change

In case of necessary lane change, the driving behavior parameters contain the maximum acceptable deceleration for the vehicle and the trailing vehicle on the new lane, depending on the distance to the emergency stop position of the next connector of the route.

3.3.3.2 Free lane change

In case of free lane change, VISSIM checks for the desired safety distance of the trailing vehicle on the new lane. This safety distance depends on its speed and the speed of the vehicle that wants to change to that lane. There is currently no way for the user to change the "aggressiveness" for these lane changes. However, changing the parameters for the desired safety distance (which are used for the vehicle following behavior) will affect the free lane changes as well.

In both cases, when a driver tries to change lanes, the first step is to find a suitable gap (time headway) in the destination flow. The gap size is dependent on the speed both of the lane changer and the vehicle that "comes from behind" (on that lane where the lane changer changes to). In case of a necessary lane change it is also dependent on the deceleration values of the "aggressiveness".

3.4 Summary

VISSIM is a microscopic, time-step and behavior-based simulation model developed to model urban traffic and public transit operations. A driving behavior model is the core of any traffic simulation model. It determines how the vehicles will behave within the network. In VISSIM, the driving behavior models contain a psycho-physical car following model for longitudinal vehicle movement and a rule-based algorithm for lateral movements. The models are based on the continued work of Wiedemann. In this study, Wiedemann 99 car following model for freeways and lane changing model have been used and sensitive driving behavior parameters of VISSIM are calibrated which will be discussed in later section.

CHAPTER 4

STOCHASTIC OPTIMIZATION ALGORITHM

4.1 General

Stochastic optimization algorithms have been growing rapidly in popularity over the last decade or two, with a number of methods now becoming standard approaches for solving challenging optimization problems. Stochastic optimization plays a significant role in the analysis, design, and operation of modern systems. Methods for stochastic optimization provide a means of coping with inherent system noise and coping with models or systems that are highly nonlinear, high dimensional, or otherwise inappropriate for classical deterministic methods of optimization. Many traffic simulation models require the user to define characteristics for several different driver types. Since an engineer cannot quantify a priori how courteous or aggressive the drivers on a particular system might be, these driver behavior characteristics must often be reverse engineered based on field data. Some method of optimization must be used to find a set of parameters that best reflects observed characteristics of the system. Three popularly used stochastic optimization algorithms SPSA, SA and GA lend them well to this task and is accepted as efficient and robust optimization and search methodologies used in a variety of fields. This section will briefly discuss the concept of these three optimization methods.

4.2 Genetic Algorithm (GA)

Genetic algorithm is a heuristic search method that belongs to the larger class of evolutionary algorithms (Goldberg 1989, Holland 1975). GA optimization is a stochastic search process that mimics the natural process of the survival of the fittest through the manipulation of a population of chromosome. GA starts with a population with random "chromosomes" (initial population of parameter values), where each chromosome represents a vector of parameters containing a solution for the optimization problem. Fitness is a subjective measure used by Charles Darwin to describe how likely an organism is to survive and produce offspring. A fitness value is assigned to each chromosome according to the quality of the solution. Based on the fitness value of individuals that contribute to the population of the next generation, selection rules select individuals with probabilities. Afterwards, a random decision to either "mutate" or "crossover" is executed.

In case of mutation decision, a random "chromosome" is elected from the current population and the parameter values are then changed to create an "offspring" chromosome by random process, based on predefined probabilities. For crossover decision, two random "chromosomes" are elected and random information (parameter values) are swapped to create an offspring chromosome. The chromosome (parameter set) that yields the worse fitness results (e.g., higher RMSE) from either "mutation" or "crossover" operation is then dropped. This process is continued until the maximum number of iterations is achieved or there are no changes in parameter sets between iterations.

One limitation of GA is that, while they tend not to converge on local extrema, they have no way of determining whether a solution is the absolute best possible. Rather, they can only compare a solution to others that have been tried. Thus, GA is most appropriate in situation where a "good enough" solution is desired, rather than an absolute optimum

4.3 Simultaneous Perturbation Stochastic Approximation (SPSA)

Simultaneous perturbation stochastic approximation (SPSA) is well known for its application to tackle optimization problems where the direct measurement of gradient g(θ) is impossible, such as in the case of micro-simulation calibration (Spall, 1998). For a system, L(θ) is a scalar-valued performance measure, and θ is a continuous-valued ρ-dimensional vector of the system parameters that can be manipulated to achieve a better system performance. It is common that a noise Ɛ could occur when observing L(θ) and then the observation z(θ) is described as follows:

$$z(\theta) = L(\theta) + \mathcal{E} \quad (4.1)$$

It is assumed that L(θ) is differentiable over θ and that the minimum θ* is obtained at a zero point of the gradient, i.e., in Eq. (2):

$$g(\theta) = \left|\frac{\delta L}{\delta \theta}\right|_{\theta=\theta*} = 0 \quad (4.2)$$

SPSA algorithm starts with an initial guess θ_0 (e.g., the default parameter values in the simulation software). It then applies a series of "simultaneous perturbation" over the successive steps until the approximation of the gradient g(θ) almost surely converges to zero. Along the successive steps, default parameters in simulation will get replaced with the estimated parameters θ_k. θ_k is updated recursively in the standard form.

$$\hat{\theta}_{k+1} = \hat{\theta}_k - a_k\, \hat{g}_k(\hat{\theta}_k) \quad (4.3)$$

where the gained sequence {a_k} needs to satisfy the regularity conditions, and $\hat{g}_k(\hat{\theta}_k)$ is the estimated gradient at $\theta = \theta_k$ at k^{th} iteration.

The perturbation is performed upon deriving $\hat{g}_k(\hat{\theta}_k)$. At iteration step k, a ρ-dimensional random perturbation vector Δ_k is generated. Each of the ρ components of Δ_k is independently generated form a zero-mean probability satisfying certain conditions. Each component of Δ_k is usually generated from the Bernoulli (±1) distribution.

$$z_k^{(+)}(\theta_k) = L(\hat{\theta}_k + c_k \Delta_k) + \varepsilon_k^{(+)} \tag{4.4}$$

$$z_k^{(-)}(\theta_k) = L(\hat{\theta}_k - c_k \Delta_k) + \varepsilon_k^{(-)} \tag{4.5}$$

where c_k is a positive scalar, and $z_k^{(+)}(\theta_k)$, $z_k^{(-)}(\theta_k)$ are the measurements of the system under the perturbation $\hat{\theta}_k + c_k \Delta_k$, $\hat{\theta}_k - c_k \Delta_k$, respectively.

According to Spall (1998), SPSA uses the following formula to obtain the approximation of $\hat{g}_k(\hat{\theta}_k)$:

$$\hat{g}_k(\hat{\theta}_k) = \frac{z_k^{(+)} - z_k^{(-)}}{2c_k} \begin{bmatrix} \Delta_k^{-1} \\ \cdot \\ \cdot \\ \cdot \\ \Delta_{kp}^{-1} \end{bmatrix} \tag{4.6}$$

The gained sequences of a_k and c_k are used to balance the algorithm stability and the desired forms of the gain sequences are shown below:

$$a_k = \frac{a}{(1+A+k)^{\alpha}}, \quad c_k = \frac{c}{(1+k)^{\gamma}} \tag{4.7}$$

where A is a constant that is applied to stabilize the optimization process. Spall (1998) recommended some general guidelines regarding the choices of a_k and c_k. If a is small, the calculations are stable initially. However, this may result in sluggish performance for large calculations. On the other hand, a large numerator, a_k>0, which is used to produce non-negligible step sizes, leads to instability early in the calculation. It is most effective to set the numerator c to a small positive number.

4.4 Simulated annealing (SA)

SA imitates the annealing process used in metallurgic. The term ‘annealing’ refers to the process in which a solid, that has been brought into liquid phase by increasing its temperature, is brought back to the solid phase by slowly reducing the temperature in such a way that all the particles are allowed to arrange themselves in a perfect crystallized state. Such a crystallized state represents the global minimum of certain energy function (Ledesma, Aviña & Sanchez, 2008).

In order for annealing to occur properly, the two conditions have to be met. First, the initial temperature has to be high enough to ensure that the process will start from a state in which all the particles are randomly arranged into the liquid phase. Second, the subsequent cooling process has to be slow enough in order to ensure that the particles will have time to rearrange themselves and reach thermal equilibrium at each temperature. Otherwise, if the initial temperature is not high enough or the cooling process is too fast, the annealing process will result in an unstable glass instead of a perfect crystal. This represents a suboptimal situation in which a local minimum instead of global minimum of the energy function has been reached.

Simulated annealing (SA) was first introduced by Metropolis (1953). It imitated the annealing process used in metallurgic, specifically where a solid that has been brought into liquid phase by increasing its temperature has been brought back to the solid phase by slowly reducing the temperature. This conversion was carried out in such a way that all the particles were allowed to arrange themselves in a perfect crystallized state, resembling the global minimum of certain energy function. Kirkpatrick (1983) introduced the application of SA for deterministic optimization problems as an analogy of the annealing process for a thermodynamic system. In emulating the physical annealing process, SA treated the feasible solutions as the possible energy states in a physical system, and the fitness value in the optimization problem as the energy of a physical system.

The parameters to be calibrated are denoted by vector θ_i, and $F(\theta_i)$ is the associated fitness value and i is the iterative index. The current solution is randomly perturbed to obtain a new feasible solution θ_j. The new solution is accepted with a probability of p_j^k.

$$p_j^k = \begin{cases} 1 & F(\theta_i) \leq F(\theta_j) \\ exp^{\left[\frac{F(\theta i)-F(\theta j)}{T_k}\right]}, & otherwise \end{cases} \tag{4.8}$$

where T_k is a monotonically decreasing scalar sequence, imitating the cooling of temperature in the physical annealing process. As the sequence number k increases, the probability of accepting an inferior solution (compared with the previous solution) decrease.

Based on the above process, SA avoids being trapped at local minima to find the best fitness value by accepting not only the changes that decrease objective function, but also some changes that increase it. Generally, the escape from local minima in SA is dependent on the annealing schedule, the choice of initial temperature, the number of perturbations at each temperature, and the amount of temperature reduction (Venkataraman, 2001).

4.5 Summary

There are a large number of methods for numerical optimization in multivariate problems. Hence, a user with a challenging optimization problem faces the daunting task of determining which algorithm is appropriate for a given problem. This choice is made more difficult by the large amount of "hype" and dubious claims that are associated with some popular algorithms. An inappropriate approach may lead to a large waste of resources, both from the view of wasted efforts in implementation and from the view of the resulting suboptimal solution to the optimization problem of interest.

Methods involving a population of candidate solutions, such as GA, may be useful for a broad search over the domain of the parameters being optimized and subsequent initialization of more powerful local search algorithms. One of the weaknesses of a GA is the inability to determine if a particular solution is the best possible. Stopping criteria define when a solution is “good enough.” Generally, this will either be a predefined minimum fitness value or a maximum number of iterations.

SPSA is generally used in nonlinear problems having many variables where the objective function gradient is difficult or impossible to obtain. SPSA is designed explicitly for noisy measurements unlike GA and SA. SPSA to be competitive (and possibly more efficient) in terms of the overall cost of the optimization process (Spall, 1998) in comparison with GA and SA, especially the case when only noisy values of the objective function are available.

Simulated annealing (SA) employs a stochastic approach in the search of global optima. In contrast to GA's stochastic manipulation of a whole pool of candidate solutions, the SA algorithm avoids being trapped in the neighborhood of local optima by allowing for temporary increases in the “cost”, namely the difference between the simulated outputs and their corresponding field measurements. SA algorithm does not require direct gradient information. This algorithm is designed to traverse local minima enroute to a global minima. Since this method can address both discrete and continuous optimization problems, there is no need to assume the existence of a loss-function gradient. SA is based on intriguing analogy to the cooling of materials and the achievement of an optimal state for the material by cooling neither too fast nor too slow. While some positive experience has been reported with optimization by SA, it appears that there exist more efficient algorithms for many problems.

However, a problem common to all stochastic optimization techniques is that values must be specified for algorithm's tunable coefficients. All stochastic optimization techniques have such coefficients (the gain sequence is SPSA, probability of crossover and mutation in GA, cooling schedule and probability of accepting a step in SA). These coefficient values are typically problem-dependent and can have a profound effect on the performance of an algorithm. No search algorithm is uniformly better than all other algorithms across all possible problems. It is clear, however, that some algorithms may work better than others on certain classes of problems as a consequence of being able to exploit the problem structure.

CHAPTER 5

DERIVATION OF MATHEMATICAL MODEL AND CONCEPTUAL FRAMEWORK

5.1 General

Microscopic traffic simulation utilizes car following and lane changing models to represent each driver's behaviors in a roadway for studying the transportation systems as a cost-effective alternative to field tests. Lane changing model is as important as car-following model that govern the second-to-second motion of vehicles in microscopic traffic simulation tools (FHWA 1995, PTV 2007, Quadstone 2009, TSS 2002, Caliper 2011). In car following models, the behavior of the leading vehicle is relatively unaffected by the lag one, while the lane changing decision depends on many parameters, and hence is more complex. Lane changes involve a high level of interaction between vehicles, and the behavior of each vehicle is largely influenced by others. Thus, it is essential for any researcher to study the microscopic vehicle details in order to understand the interactions of vehicles. The objective of this study is simultaneous calibration of car following and lane changing parameters considering a mix of microscopic and macroscopic traffic data. In this chapter a new mathematical model will be derived to meet the above objective.

5.2 Relation between Headway and Speed in Microscopic Traffic Data

Car following model has been studied by researchers for more than 50 years and there are numerous models on lane changing behavior. A lane change involves the interaction of several vehicles. The variables that describe the interactions between these vehicles may be divided into three groups: (i) Space Headway; (ii) Time Headway; and (iii) Speed (Balal, Cheu & Gyan, 2015). Space Headway is defined as the distance between corresponding points of two successive vehicles at any given time. It involves the measurement of the distance from rear bumper of lead vehicle to rear bumper of following vehicle at a point of time. If all the space headways in distance x over which the density has been measured are added then,

$$\sum_{1}^{n_x} h_{si} = x \tag{5.1}$$

But the density (k) is the number of vehicles n_x at a distance of x, that is

$$k = \frac{n_x}{x} = \frac{n_x}{\sum_{1}^{n_x} h_{si}} = \frac{1}{\bar{h}_s} \tag{5.2}$$

Where, $\overline{hs}$ is average space headway. The average space headway is the inverse of density which is true for aggregated data.

Space headway is an important measure of performance which is affected by both the car following and lane changing parameters in any microscopic traffic simulation model. Again, in a car following model, it can be easily visualized that space headway is affected by speed of Leader-Follower vehicle pair; higher the speed, greater the safety distance or headway between them. Similarly, minimum gap (synonymously headway) for lane change also depends on the speed of the subject vehicle (Mizanur, Mashrur, Xie, & He, 2013). Therefore, in microscopic traffic simulation, space headway being an important traffic measurement, is influenced by speed variable in both the car following and lane changing model. Speed is not only the factor that influences headway. The microscopic driving behavior is also related to macroscopic property of traffic stream (Laval and Daganzo 2006) e.g. density. As discussed before, average headway is inverse of average density for aggregated data. For disaggregated vehicles trajectory data like second-to-second motion of vehicles, average density will still have some effect on headway, but may not be in depiction of fundamental relationship between them for aggregated data. A pattern may be drawn between both the measurements while performing the regression analysis between each pair of Leader-Follower vehicle.

The observations from NGSIM US101 and I80 data (Figure 5.1 and 5.2) show a fairly linear relationship among the following distance/space headway (h_s) and following speed (v) of the Leader-Follower car pair with quite a bit of scatter (Menneni & Carlos, 2008). But examining the traffic data for this study it can be suggested that relationship can better be fitted with second or third order polynominal curve (Figure A.1, Table A.1 & A.2 of Annexure A). For the microscopic disaggregated vehicle trajectory data, relationship between following space headway (h_s) and following speed (v) of the Leader-Follower car pair is largely influenced by the average density ($\bar{k}$) of the roadway. As such a new mathematical model can be derived basing on the analysis of VISSIM simulated data where space headway (h_s) between the Leader-Follower car pair will be the function of following speed (v) and average density ($\bar{k}$) of the roadway, a fusion of both macro and micro data.

$$h_s = f(v, \bar{k}) \tag{5.3}$$

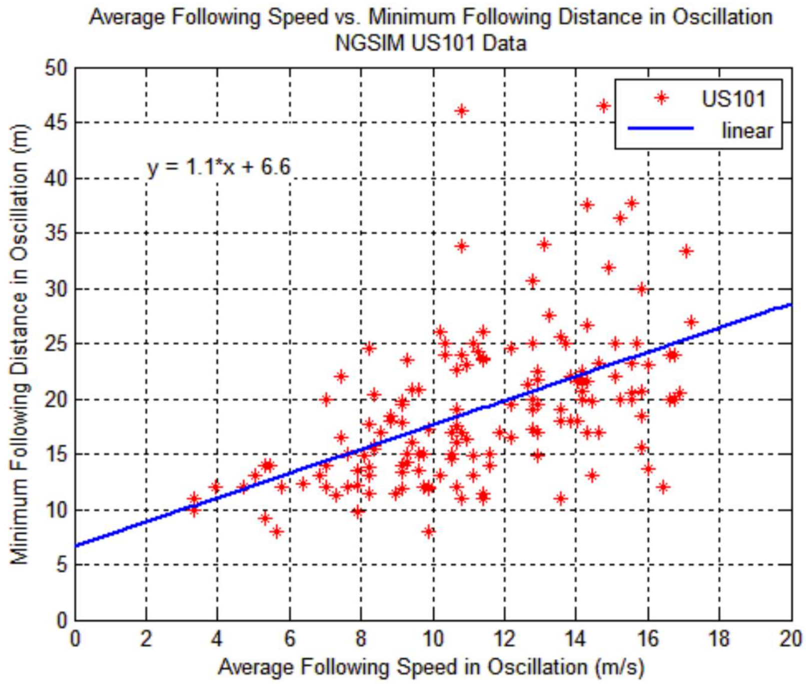

Figure 5.1: Average following speed vs following distance (NGSIM US101 Data)
Source: Menneni & Carlos (2008)

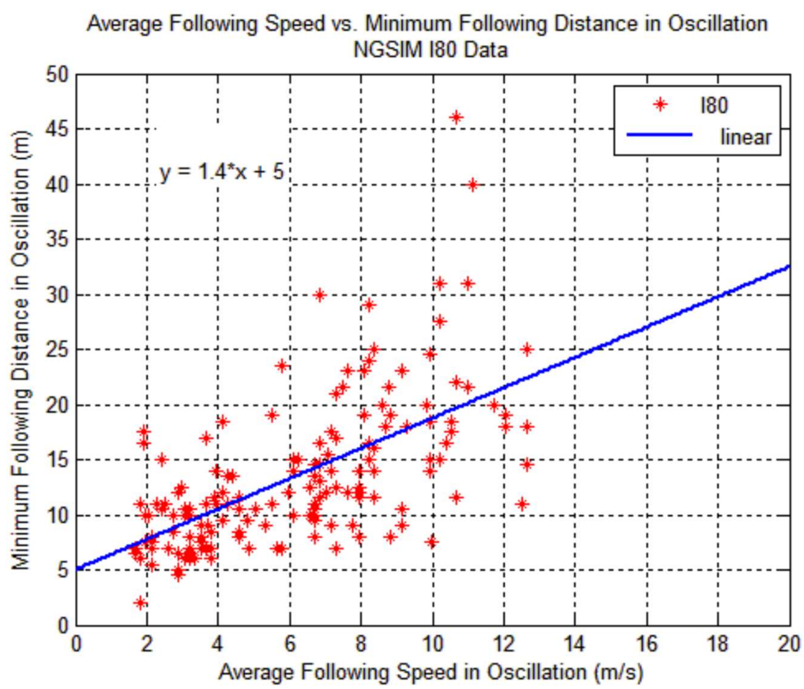

Figure 5.2: Average following speed vs following distance (NGSIM US I80 Data)
Source: Menneni & Carlos (2008)

5.3 Mathematical Model

Regression analysis of NGSIM vehicle trajectory data indicated that a fairly linear relationship exists between space headway (h_s) and the speed (v) of following vehicle of the Leader-Follower car pair with some scattered variation (Figure 5.1 and 5.2).

$$h_s = f(v) \tag{5.4}$$

Again, for aggregated macroscopic data,

$$\bar{h}_s = \frac{1}{\bar{k}} \tag{5.5}$$

The linear regression relationship between space headway (h_s) and the speed (v) can further be smoothen by incorporating second order or third order polynominal equation where all the coefficients will be dependent on average density ($\bar{k}$) of the roadway. As such

$$h_s = f(v, \bar{k}) \tag{5.6}$$

$$h_s = a_2 v^2 + a_1 v + a_0 \quad \text{(second order polynominal)} \tag{5.7}$$

or

$$h_s = a_3 v^3 + a_2 v^2 + a_1 v + a_0 \quad \text{(third order polynominal)} \tag{5.8}$$

Where,

h_s = Space headway (m)

v = Speed of following vehicle of Leader-Following vehicle pair (m/sec).

a_0, a_1, a_2, a_3 = Coefficients dependent on average density ($\bar{k}$) of the roadway.

$$a_0 = f(\bar{k}) \tag{5.9}$$

$$a_1 = f(\bar{k}) \tag{5.10}$$

$$a_2 = f(\bar{k}) \tag{5.11}$$

$$a_3 = f(\bar{k}) \tag{5.12}$$

By plotting the value of a_0, a_1, a_2, a_3 for each pair of Leader-Follower vehicle against their corresponding average density ($\bar{k}$), it is revealed that linear/polynominal relationship exist between each coefficient and average density with some noisy data. It can easily be visualized that a discrete relation between them will be difficult to obtain due to presence of highly variable data. However, for simplicity, assuming a linear relationship, the 'Box and Whiskers Plot' is used to remove the noisy data. The box and whisker diagram (or box plot) is a way to visually organize data into fourths or quartiles. The diagram is made up of a "box," which lies between the first and third quartiles, and "whiskers" that are straight lines extending from the ends of the box to the maximum and minimum data values. Thus, the middle two-fourths are enclosed in a "box" and lower and upper fourths are drawn as whiskers. The length of the box itself, equal to the third quartile minus the first quartile, is called the interquartile range. The population interquartile range is the difference between the 0.75 and 0.25 quartiles. To be more aggressive in defining the relation, we have used semi-interquartile range where the data between the 0.75 and 0.50 quartiles have been considered for defining an equation and data beyond the range have been discarded. The comparative improvement of curve fitting after removal of noisy data for 2nd degree and 3rd degree polynominal relation between each coefficient and the average density is shown in Figure A.2 and A.3 at Annexure. We can draw the 2nd order polynominal relationship between each of the coefficients and average density through following equations (equation 5.13, 5.14, 5.15 and 5.16):

$$a_0 = f(\bar{k}) = m_0\bar{k}^2 + n_0\bar{k} + p_0 \quad (5.13)$$

$$a_1 = f(\bar{k}) = m_1\bar{k}^2 + n_1\bar{k} + p_1 \quad (5.14)$$

$$a_2 = f(\bar{k}) = m_2\bar{k}^2 + n_2\bar{k} + p_2 \quad (5.15)$$

$$a_3 = f(\bar{k}) = m_3\bar{k}^2 + n_3\bar{k} + p_3 \quad (5.16)$$

Replacing the values of coefficient in Equation 5.7 and 5.8 we get,

$$h_s = v^2(m_2\bar{k}^2 + n_2\bar{k} + p_2) + v(m_1\bar{k}^2 + n_1\bar{k} + p_1) + (m_0\bar{k}^2 + n_0\bar{k} + p_0) \quad (5.17)$$

or

$$h_s = v^3(m_3\bar{k}^2 + n_3\bar{k} + p_3) + v^2(m_2\bar{k}^2 + n_2\bar{k} + p_2) + v(m_1\bar{k}^2 + n_1\bar{k} + p_1) + (m_0\bar{k}^2 + n_0\bar{k} + p_0) \quad (5.18)$$

Where, v and $\bar{k}$ are the independent variables, and m_0, m_1, m_2, m_3, n_0, n_1, n_2, n_3, p_0, p_1, p_2, p_3 are the coefficients whose values are obtained from the equation 5.13, 5.14, 5.15 and 5.16. This equation of space headway (h_s) has been drawn from each VISSIM simulated output data (output file *.fzp) with different combination of parameters. In each iteration of optimization algorithm with different combination of parameters, values of simulated headway (h_s) which are dependent on the independent variable v & $\bar{k}$ and the coefficients, will be directed towards the observed headway values. An objective function of difference in space headway (h_s) between the actual and simulated trajectory data derived by above mathematical equation will able to calibrate the desired parameters more precisely.

5.4 Conceptual Framework

5.4.1 Optimization Program Control Interface (OPCI)

An Optimization Program Control Interface (OPCI) has been coded in Visual Studio 2015 integrates the Visual Basic 2015 and VISSIM 7.0 to implement the calibration approach by three optimization methods. A snap shot of OPCI is shown in figure 5.3 and 5.4.

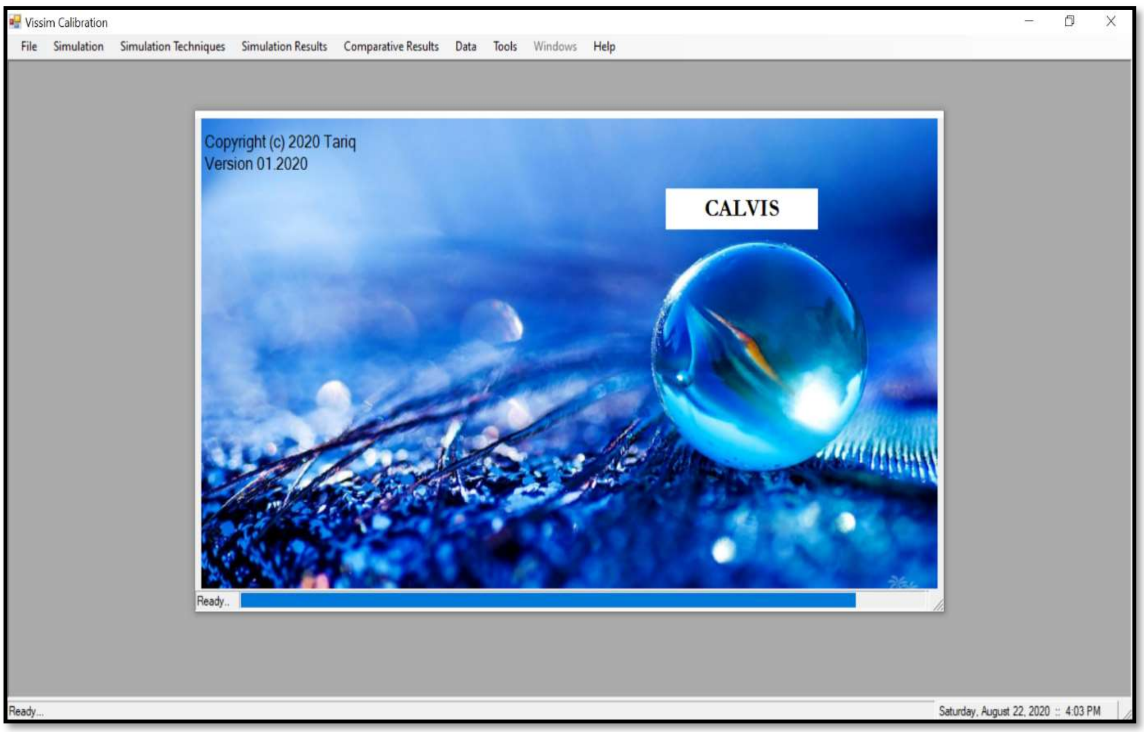

Figure 5.3: Snap Shot of Optimization Program Control Interface

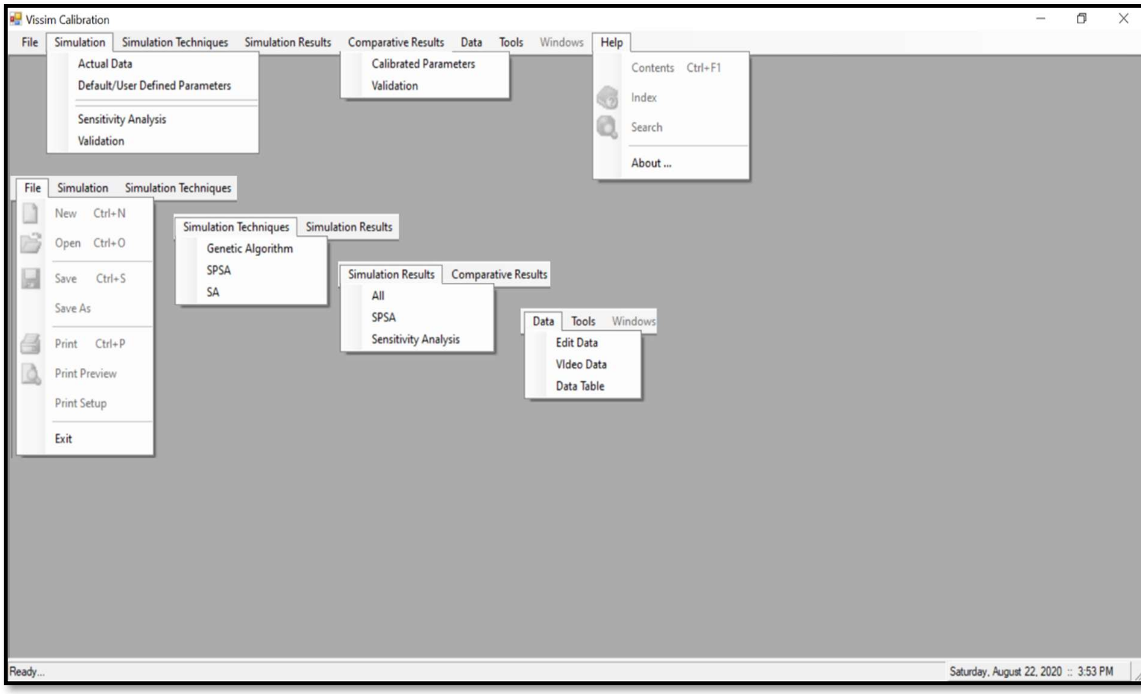

Figure 5.4: Sub Menu Bar of Optimization Program Control Interface

New program for GA, SPSA and SA algorithm has been coded in Visual Basic 15 for the OPCI. OPCI capture the observed video data, analyze and organize the vehicle trajectory data for comparison with simulation data. It communicates with VISSIM through COM interface, customize the input parameters and run simulation for specific number of iterations as per user's choice. After every simulation, OPCI gets the simulation result from VISSIM, analyze and formulate equation for MOP, and compare with observed data as per objective function. Guided by the selected optimization algorithm it suggests new set of parameters for the subsequent simulation. Finally, OPCI produces the output of optimal parameters resulting from lowest value of objective function. OPCI also has the provision of preserving vehicle trajectory data and displays result in the forms of graphs and charts for further analysis.

5.4.2 Conceptual flow diagram

The conceptual flow diagram for the complete optimization process illustrated in figure 5.5.

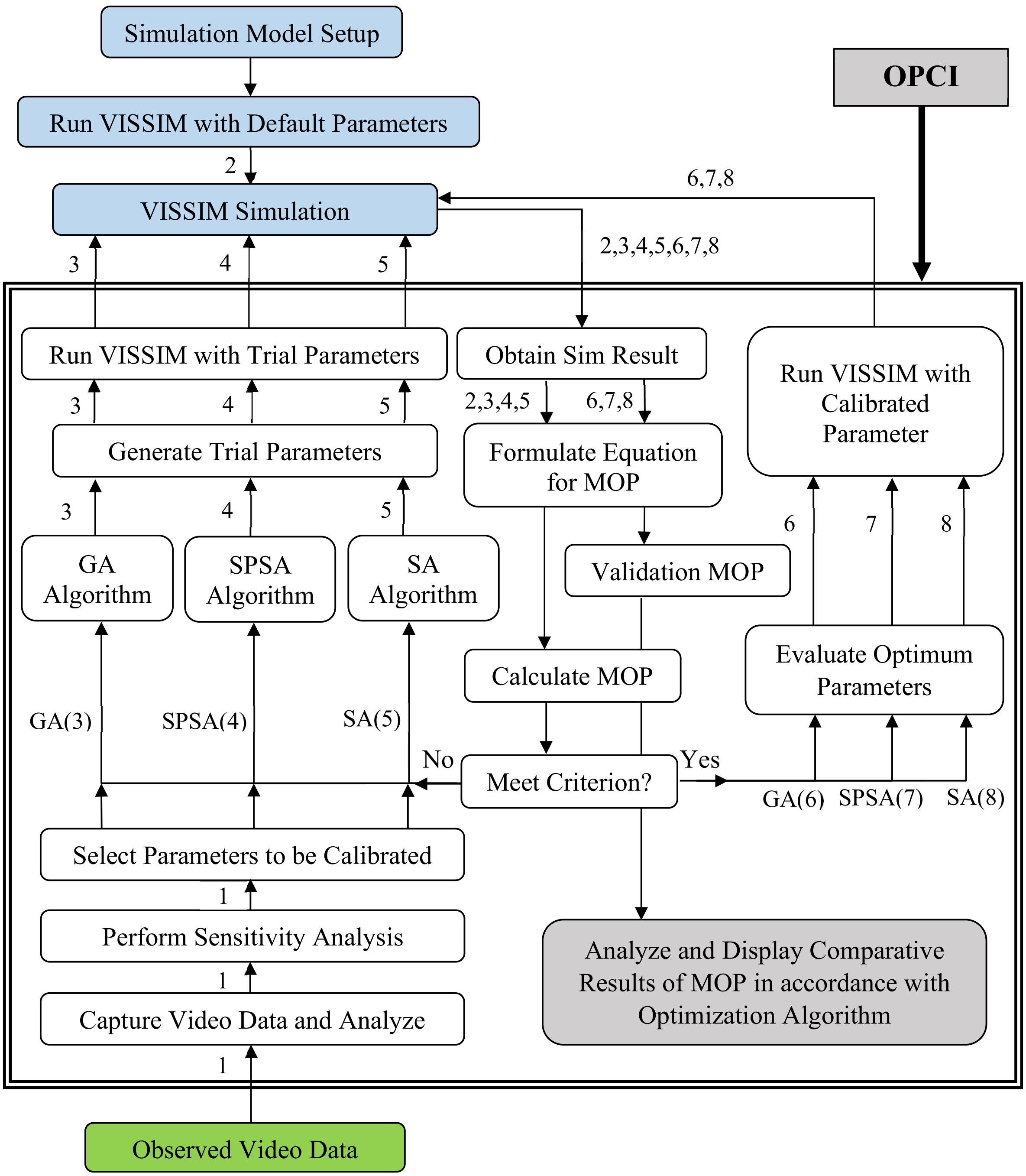

Figure 5.5: Conceptual Flow Diagram

5.5 Summary

This chapter presented derivation of mathematical model and conceptual framework. The conceptual framework elaborately demonstrated how OPCI controls the entire calibration process.

CHAPTER 6

CALIBRATION AND VALIDATION PROCEDURES ALONG WITH A CASE STUDY

6.1 General

The proposed procedure developed for the calibration and validation of microscopic simulation models is similar to those presently in practiced. The main innovation lies in the simultaneous calibration of car following and lane changing parameters, mathematical formulation of new equation for comparing of MOP in the objective function, fusion of macroscopic and microscopic vehicle trajectory data and comparison of the performance of three optimization techniques in calibration of parameters. Moreover, an interface software OPCI has been developed to assist users in calibration of micro simulation model VISSIM incorporating above innovations. The proposed procedure for calibrating microscopic simulation models consists of seven main steps: field data collection and processing, VISSIM model development, determination of MOPs and Objective function, selection of parameter and range, sensitivity analysis, parameter calibration using optimization techniques, and model validation. This chapter presents the proposed calibration and validation approach step-by-step in more details describing on a particular case study. In this research, all simulation work was carried out with Version 7. 0 of VISSIM on a personal computer with a Pentium 2.53-GHz central processing unit and 4.00 GB of random-access memory.

6.2 Data Collection and Processing

6.2.1 Study area

At the beginning of the study a suitable site has been selected and a high-resolution data collection and processing techniques has been adopted for the research. The collected data will serve as the basis for the calibration and validation for traffic simulation model VISSIM. The study site is the Tongi Diversion Road, a section of the Dhaka-Mymensingh Highway (N3) in Bangladesh (shown in Figure 6.1). It is an 8-lane major arterial road in Dhaka, which connects the capital city with the Shahjalal International Airport. A straight 400 meters long uninterrupted section has been selected. There are exactly 4 through lanes on each direction of the test site totaling up to a width of 14.48 meters (m). The test section experiences a directional average annual daily traffic (AADT) of about 11451 vehicles. The traffic stream consists of 40% cars, 12% microbuses or jeeps, 10% motorcycles, 8% buses, 10% utility vehicles and 20% auto-rickshaws. Such geometric and traffic characteristics make the test site an ideal study location for non-lane-based heterogeneous uninterrupted traffic condition.

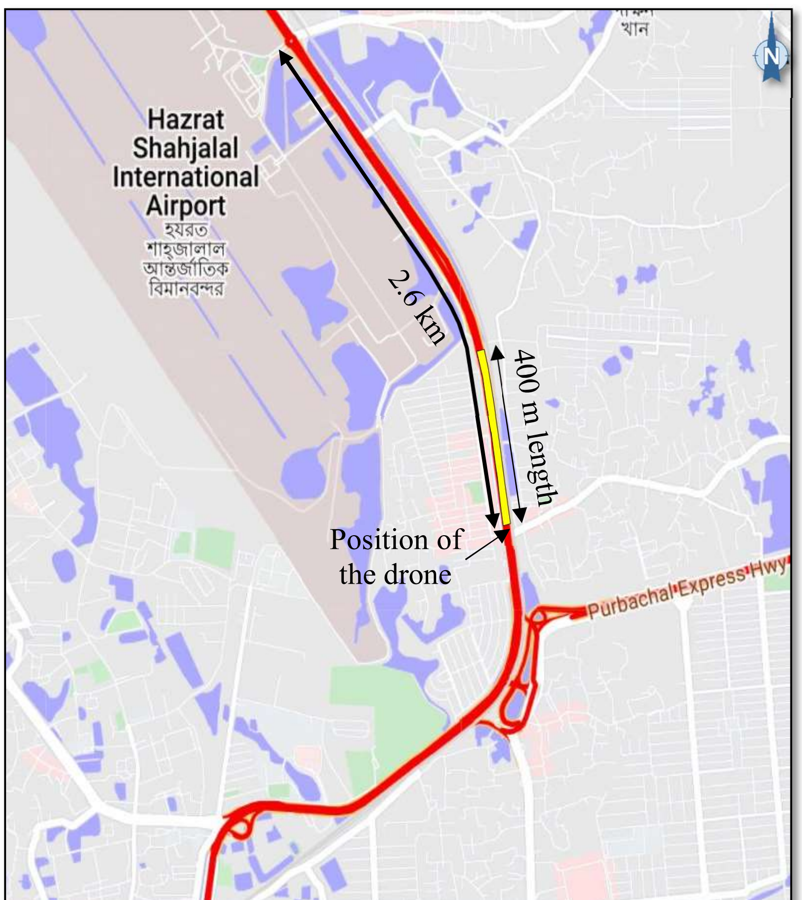

Figure 6.1: The study site (courtesy: https://snazzymaps.com)

6.2.2 Data collection

Collection of high-resolution traffic data required for the development of an accurate macroscopic model is a very challenging task under the existing traffic condition of the study area. This is mainly because loop detectors are unsuitable for the test site due to measurement errors caused by non-lane-based movement of vehicles activating either both or neither of two adjacent detectors. Small Unmanned Aerial Vehicles (drones) have been one of the latest tools for monitoring transportation infrastructure and operations. Their lower cost compared to current fixed location camera systems or Manned Aerial Vehicles (MAV) and their ability to cover a large length of road arterials depending on viewing angle and altitude, make them a promising tool of collecting both macroscopic and microscopic data (Emmanouil, Eleni, Golias and Adam 2017). Moreover, drones' ability to hover over any area gives the ability to collect data from places that would be considered unavailable by other fixed cameras. Considering such advantageous, DJI Mavic drone has been used in this study to record traffic stream which was flown at a height of 25 meters at a fixed location shown in figure 6.1. At this height the drone has clearly captured the traffic stream up to 400 meters length of the roadway. The drone offers gimbal support system for the camera with 3-axis stabilization. Therefore, there was no shakiness or movement of camera during video recording. The drone has the hovering accuracy of ±0.1 meters vertically and ±0.3 meters horizontally. A snapshot of the recorded traffic stream by the drone is shown in figure 6.2. The data obtained from drone is considered representative of the traffic condition of the roadway up to 2.6 kilometer as there is no ingress or egress within this section of Dhaka-Mymensingh Highway.

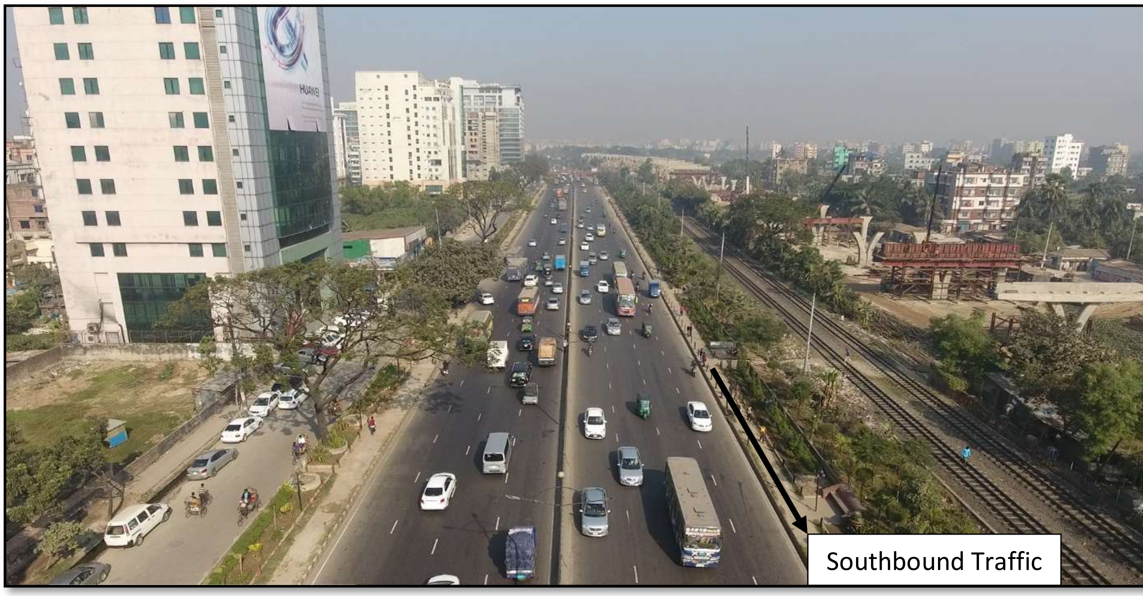

Figure 6.2: Snapshot of Captured Traffic Stream by Drone

Only the southbound vehicle stream was recorded. Although the non-lane-based heterogeneous behavior becomes more acute with the increase of traffic volume in the roadway, the test site was videoed from 11:00 AM to 2:00 PM on 19 July 2018. These videos were processed and the extracted data was filtered for anomalies. Ultimately, 7200 seconds data of 19 July was used for calibration and validation of the model parameters. During this period, total 1191 instances of lane changing event have been detected.

6.2.3 Data processing

OPCI has provision for built-in data processing. It uses OpenCV (Open Source Computer Vision Library), an open source computer vision and machine learning software library. OpenCV was built to provide a common infrastructure for computer vision applications and to accelerate the use of machine perception in the commercial products. The library has more than 2500 optimized algorithms, which includes a comprehensive set of both classic and state-of-the-art computer vision and machine learning algorithms. These algorithms can be used to detect and recognize faces, identify objects, classify human actions in videos, track camera movements, track moving objects, extract 3D models of objects, produce 3D point clouds from stereo cameras, stitch images together to produce a high-resolution image of an entire scene, find similar images from an image database, etc. (website, https://opencv.org). For extracting high resolution traffic data from the video footages of the drone cameras, OpenCV Background Subtraction (BS) technique of image processing was used for coding the algorithm in Visual Basic 2015. BS is a common and widely used technique for generating a foreground mask (namely, a binary image containing the pixels belonging to moving objects in the scene) by using static cameras. As the name suggests, BS calculates the foreground mask performing a subtraction between the current frame and a background model, containing the static part of the scene or, more in general, everything that can be considered as background given the characteristics of the observed scene.

The algorithm can successfully detect non-lane-based movement of vehicles. It can also identify non-motorized traffic, and distinguish between dark car and car shadow quite accurately. Video data and vehicle geometry are provided as input to the algorithm and it gives vehicle position at 0.2 sec of interval of each vehicle of the traffic stream along the roadway in following format (Table-6.1):

Table 6.1: Sample Data Extraction by OpenCV Algorithm

Ser	Time (sec)	Vehicle No	Lane No	Position (meter)	Speed (km/hr)	Leader Vehicle No	Following Vehicle No	Headway (meter)	Density (veh/km)
245	9.2	5	1	123.27					
243	9.2	6	1	100.01					
241	9.2	7	4	50.21					
258	9.4	5	1	126.78					
256	9.4	6	1	103.5					
254	9.4	7	4	52.47					
253	9.4	8	2	49.78					
284	9.6	5	1	130.28					
282	9.6	6	1	106.97					
280	9.6	7	4	54.73					
279	9.6	8	2	52.21					

Once OpenCV algorithm extracts data in above format, OPCI puts up an algorithm to fill up the rest of the fields using SQL Server 14.0. After each simulation in VISSIM, the OPCI also extracts data from VISSIM output file *.fzp and fill up the fields in the similar format (Table-6.2).

Table 6.2: Sample Data Extraction by SQL Server Algorithm

Ser	Time (sec)	Vehicle No	Lane No	Position (meter)	Speed (km/hr)	Leader Vehicle No	Following Vehicle No	Headway (meter)	Density (veh/km)
245	9.2	5	1	123.27	63	1	6	58.73	72
243	9.2	6	1	100.01	63.18	5	10	23.26	72
241	9.2	7	4	50.21	40.5	4	11	75.84	72
258	9.4	5	1	126.78	63.18	1	6	59.22	71
256	9.4	6	1	103.5	62.82	5	10	23.28	71
254	9.4	7	4	52.47	40.68	4	11	77.07	71
253	9.4	8	2	49.78	43.74	2	12	74.19	71
284	9.6	5	1	130.28	63	1	6	59.72	71
282	9.6	6	1	106.97	62.46	5	10	23.31	71
280	9.6	7	4	54.73	40.68	4	11	78.31	71
279	9.6	8	2	52.21	43.74	2	12	74.7	71

6.3 VISSIM Model Development

The VISSIM model was constructed by tracing the roadway network over the aerial photographs which served as a background. Scale was established on the aerials by matching landmarks with the scaled aerials from the study site, and was also verified from field measurements. The number of lanes and other roadway geometry were confirmed by field visits. Driver behavior parameters like driver aggressiveness and saturation flow rates were calibrated based on field observations. The distribution of vehicle types was also calibrated to local conditions so that the percentage of cars, heavy trucks, and buses matched the traffic counts. 3D models of non-standard vehicles like motorized three wheelers were drawn and incorporated in the VISSIM model to replicate reality. Non lane-based traffic movement is achieved in VISSIM by placing the vehicles anywhere on the lane by setting the 'Desired position at free flow' to 'any' and permitting the vehicles to overtake along the left or right of a slower vehicle by setting the option overtaking to all. To keep the record of the attribute values for each vehicle per time step, 'saving vehicle records to a file option' in VISSIM was selected. In this case study, only the southbound network was modelled in VISSIM.

6.4 Measure of Performance (MOP)

It is important to clearly identify all MOPs before proceeding forward in the calibration and validation process. Calibration of parameters will be performed based on microscopic data and with these set of calibrated parameters validation of model will be conducted by macroscopic data. As such, space headway derived from mathematical equation during lane change has been considered as MOP for calibration and average headway for validation. To formulate the mathematical equation for space headway, each pair of Leader-Follower vehicles trajectory data have been analyzed and a relation between headway and speed of following vehicle has been established. OPCI has used the Gauss-Jordan Elimination algorithm to solve any systems of linear/polynominal equations. Figure-A.1 at Annexure A to this thesis explains the relationship obtained from one of the VISSIM simulation output file. From the figure, it can preferably be concluded that 3rd degree polynominal relationship will have smoother curve fitting. Comparative tables of coefficient values along with their degree of reliability for all 384 pairs of Leader-Follower vehicles are also presented in Table A.1 and A.2 at Annexure A to support the above statement.

After finalizing the degree of polynominal function, when we plot the coefficient a_0, a_1, a_2 and a_3 each against the average density, we find that liner/polynominal relationship exist between each coefficient and average density with some noisy data. OPCI has used the 'Box and Whiskers Plot' to remove the noisy data. The comparative improvement of curve fitting after removal of noisy data for 2nd degree and 3rd degree polynominal relation between each coefficient and the average density is shown in Figure A.2 and A.3 at Annexure. A 2nd degree polynominal functions between each of the coefficient and average density have been considered in this thesis.

6.5 Objective Function

6.5.1 Calibration of parameters

A good objective function plays a critical role in obtaining good results. A widely used error measure that can provide a fairly good initial estimate of the degree of fit between the simulated and the actual traffic measurements is the Root Mean Squared Error (RMSE). In this thesis the objective function has been designed to be RMSE of space headway (h_s) between the actual data, and actual data modified by above mathematical equation obtained from simulation during lane changes. During the simulation, space headway (h_s) of each pair of Leader-Follower vehicles is influenced by the car following parameters whereas, the lane change events are dictated by the lane changing parameters. As such an objective function that combines only those data of space headway (h_s) during any event of lane changes will invariably ensure simultaneous calibration of both car following and lane changing parameters. The objective of the calibration is to minimize the RMSE which is expressed as the following equations:

$$\mathrm{RMSE}_{\mathrm{headway}} = \frac{1}{m}\sum_{i=1}^{m}\sqrt{(O_i - S_i)^2} \tag{6.1}$$

Where,

O_i= Observed space headway (m)

S_i = Space headway (m) obtained by the mathematical equation derived from Simulated microscopic trajectory data

m = Number of lane changes

6.5.2 Validation

Regardless of the exact calibration procedure employed its success and efficiency depends on the measurements used during the validation as well as the MOP employed. The measurements used to compare reality with simulation cannot be easily defined because they depend on the given site to be modeled and the available instrumentation. In freeways the most common measurements are volume, speed or occupancy, and rather infrequently density which can be derived from occupancy (Hourdakis, Michalopoulos & Kottommannil, 2003). In this thesis, space headway (h_s) which was equated based on simulated microscopic trajectory data, has been used as MOP for calibration of parameters. As such an aggregated macroscopic measurement, like average headway, has been considered as the MOP with Sum of Absolute Error (SAE) of simulated and observed data on average headway over every 10 meters interval along the roadway on each second as the objective function for validation. This objective function will actually allow us to examine the performance of parameters calibrated on microscopic data to depict the actual output while validating through macroscopic data. The objective function for validation will be expressed as follows:

$$\mathrm{SAE}_{\mathrm{headway}} = \sum_{\mathrm{i=1}}^{\mathrm{m}} Abs(S_i - O_i) \tag{6.2}$$

Where,

S_i = Simulated average headway (m) on each sec of time over every 10 m interval of the roadway

O_i= Observed average headway (m) on each sec of time over every 10 m interval of the roadway

m = Number of data

6.6 Selection of Parameters

6.6.1 Simulation with default parameters

Once the vehicle population has been defined, the simulation should be tested with the default Driver Behavior parameters. This defines the global calibration step in micro-simulation modeling. This initial calibration is performed with default parameters values as suggested in different literatures to check how the model reproduces observed traffic conditions in the field. In this study, the initial calibration for the VISSIM models failed to reproduce field observations with default driver behavior settings with RMSE of headway 30.32 meter during lane change. Thus, fine tuning of the model parameters was necessary.

6.6.2 Selection of parameters

Initial selection of parameters depends on the type of model being calibrated. Certain parameters can be eliminated immediately. The decision to eliminate a parameter in this step should be based on a priori knowledge that the parameter will not meaningfully impact the simulation accuracy. Parameters may also be eliminated if the model they are associated with is not used. For example, Wiedemann 74 is related to arterial operations and Wiedemann 99 to freeway operations. This case study was implemented on a freeway and as such, the parameters related to Wiedemann 74 were not be included for calibration. Similarly, as there was no signalized intersection in the test site, signal model parameters were not considered for calibration. The rest parameters had to pass through the sensitivity analysis to prove its worthiness in affecting the simulation result while eliminated parameters were assigned with their default values.

6.6.3 Defining parameters range

There is no exact method to determine the ranges for the parameters. The ranges must be determined through a combination of past experience, information from the VISSIM documentation, and engineering judgment. The goal should be to make the range of a parameter large enough to cover all feasible values of the parameter without including values which introduce impossible or flawed behavior in the model. Impossible or flawed behavior could include things such as drivers running red lights or vehicles driving over the top of one another in an intersection. When the analyst is uncertain of a reasonable parameter range it is recommended to use a larger rather than smaller range and if necessary, narrow the ranges later in the process. Finally, engineering judgment must be used to modify the ranges used in other literatures or from the VISSIM documentation to tailor ranges to the specific model. Default, minimum and maximum parameter values in respect of Wiedemann 99 car following and lane change driver behavior are given in Table A.2 and A.3.

6.7 Sensitivity Analysis

Due to the complexity of the microscopic simulation models, the number of calibration parameters has a significant effect on the computation time. The objective of the sensitivity analysis is to identify key model parameters affecting MOPs. In a sensitivity analysis, parameters chosen from the step parameter selection are tested to assess their level of influence on MOPs. A baseline scenario is first developed using default values for all initially selected parameters. Afterward, the value of parameters is changed one at a time, while other parameters are kept to default values. Values of MOPs are collected for all scenarios. The trend of how the MOPs change over the varying parameter value demonstrates the intensity of the relationship between MOP and this parameter. Based on the sensitivity analysis results, parameters with low effect on MOP are excluded.

To ascertain the influence of a parameter on the space headway values derived from equation 26, a sensitivity analysis is to be conducted. Each parameter will be evaluated at four levels: low, medium, default, and high. The magnitude of these levels is chosen so that the likely useful range of the parameters is represented in the analysis. The results for the low, medium, and high levels will then be tested to determine whether a significant difference between the MOP results of each relative to the default state exists or whether they all appear to belong to the same distribution. During sensitivity analysis all parameters except the one being studied were held at their respective default values. The default values used in this analysis do not represent the optimal values of the parameters for all simulations. Student's t-test was conducted to test if there is a significant change in the value of MOP at 95% confidence level (α-level of 0.05) with comparison to default values. All averages and standard errors for sensitivity runs are based on 10 replicate runs at different random seeds of simulation. In this study, Wiedemann 99 car following model for freeways and Lane change model have been used and sensitivity analysis has been performed to determine most influential driving behavior parameters, affecting the model output, to be calibrated. Total 9 parameters are found to be sensitive to this model. These are w99cc0, w99cc1, w99cc2, w99cc3, w99cc4, w99cc5, w99cc7, w99cc8 and coopDecel. Table 6.3 provides a summary of the sensitivity findings for each of the driver behavior parameters:

Table 6.3: Summary of Headway Sensitivity to Parameters Modification

Parameters	Level	Value	Avg Headway Difference (m)	Standard Deviation	t-Statistic	Degree of Freedom	Critical t-Value	Significance
w99cc0	Default	1.5	1304	1273.02	0	0	0	
	Low	0	1305.79	1273.22	0	3	3.182	No
	Med	2	33.16	3.2	794.53	3	3.182	Yes
	High	4	31.77	2.57	990.06	3	3.182	Yes
w99cc1	Default	0.9	1304.2	1800.47	0	0	0	
	Low	0	1941.21	1102.87	1.16	3	3.182	No
	Med	2	25.22	7.16	357.26	3	3.182	Yes
	High	4	3803.58	1292.5	3.92	3	3.182	Yes
w99cc2	Default	4	1304.2	2205.17	0	0	0	
	Low	0	26.61	3.79	674.19	3	3.182	Yes
	Med	5	666.4	1100.12	1.16	3	3.182	No
	High	10	1305.2	1272.23	2	3	3.182	No
w99cc3	Default	-8	1304.2	2546.34	0	0	0	
	Low	-30	2573.25	3.82	668.58	3	3.182	Yes
	Med	-19	2571.07	9.45	270.47	3	3.182	Yes
	High	-8	1304	1273.02	0	3	3.182	No
w99cc4	Default	-0.35	1304.4	2847.01	0	0	0	
	Low	-1	29.59	4.54	561.59	3	3.182	Yes
	Med	-0.5	667.79	1102.99	1.16	3	3.182	No
	High	0	667.99	1101.04	1.16	3	3.182	No
w99cc5	Default	0.35	1304.2	3118.74	0	0	0	
	Low	0	1306.19	1273.22	0	3	3.182	No
	Med	0.5	668.19	1103.22	1.15	3	3.182	No
	High	1	32.57	2.02	1260.61	3	3.182	Yes

Parameters	Level	Value	Avg Headway Difference (m)	Standard Deviation	t-Statistic	Degree of Freedom	Critical t-Value	Significance
w99cc6	Default	11.44	1304	3368.55	0	0	0	
	Low	0	1303.21	1272.63	0	3	3.182	No
	Med	10	1305	1273.22	0	3	3.182	No
	High	20	668.39	1103.1	1.16	3	3.182	No
w99cc7	Default	0.25	1304.2	3601.14	0	0	0	
	Low	0	30.98	1.95	1305.87	3	3.182	Yes
	Med	0.5	670.17	1102.07	1.15	3	3.182	No
	High	1	29.59	4.57	557.82	3	3.182	Yes
w99cc8	Default	3.5	1304.2	3819.6	0	0	0	
	Low	1	35.35	1.82	1397.4	3	3.182	Yes
	Med	4.5	1304.6	1273.22	0	3	3.182	No
	High	8	1304.6	1272.83	0	3	3.182	No
w99cc9	Default	1.5	1304.2	4026.21	0	0	0	
	Low	0.5	1305.39	1274.02	0	3	3.182	No
	Med	1.75	1304.4	1273.42	0	3	3.182	No
	High	3	1305	1273.22	0	3	3.182	No
decelRedDistOwn	Default	200	1304.4	4222.79	0	0	0	
	Low	200	1304.2	1273.22	0	3	3.182	No
	Med	200	1304.2	1273.22	0	3	3.182	No
	High	200	1304.2	1273.22	0	3	3.182	No
accDecelOwn	Default	-1	1304.2	4410.56	0	0	0	
	Low	-1	1304	1273.02	0	3	3.182	No
	Med	-1	1304.2	1273.22	0	3	3.182	No
	High	-1	1304	1273.02	0	3	3.182	No
MaxDecelOwn	Default	-4	1304.2	4590.66	0	0	0	
	Low	-4	1304.2	1273.22	0	3	3.182	No
	Med	-4	1304	1273.02	0	3	3.182	No
	High	-4	1304.2	1273.22	0	3	3.182	No
accDecelTrail	Default	-0.5	1304	4763.9	0	0	0	
	Low	-0.5	1304.2	1273.22	0	3	3.182	No
	Med	-0.5	1304.2	1273.22	0	3	3.182	No
	High	-0.5	1304.4	1273.42	0	3	3.182	No
decelRedDistTrail	Default	200	1304.2	4931.11	0	0	0	
	Low	100	1304.2	1273.22	0	3	3.182	No
	Med	175	1304.2	1273.22	0	3	3.182	No
	High	250	1304.2	1273.22	0	3	3.182	No
MaxDecelTrail	Default	-3	1304	5092.78	0	0	0	
	Low	-3	1304.2	1273.22	0	3	3.182	No
	Med	-3	1304.2	1273.22	0	3	3.182	No
	High	-3	1304	1273.02	0	3	3.182	No
minHdwy	Default	0.5	1304.2	5249.53	0	0	0	
	Low	0.5	1304.4	1273.42	0	3	3.182	No
	Med	0.5	1304.2	1273.22	0	3	3.182	No
	High	0.5	1304.2	1273.22	0	3	3.182	No

Parameters	Level	Value	Avg Headway Difference (m)	Standard Deviation	t-Statistic	Degree of Freedom	Critical t-Value	Significance
diffusTm	Default	60	1304.2	5401.72	0	0	0	
	Low	60	1304.2	1273.22	0	3	3.182	No
	Med	60	1304	1273.02	0	3	3.182	No
	High	60	1304.2	1273.22	0	3	3.182	No
coopDecel	Default	-3	1304.2	5549.75	0	0	0	
	Low	-3	33.56	2.99	849.93	3	3.182	Yes
	Med	-3	1303.8	1274.02	0	3	3.182	No
	High	-3	667.99	1101.5	1.16	3	3.182	No
safDistFactLnChg	Default	0.6	1304	5693.88	0	0	0	
	Low	0.6	1304.2	1273.22	0	3	3.182	No
	Med	0.6	1304.2	1273.22	0	3	3.182	No
	High	0.6	1304	1273.02	0	3	3.182	No

6.8 Parameter Calibration Using Optimization Algorithm

6.8.1 GA based calibration approach

GA resembles the biological process of evolution and natural selection. The basic idea of the GA is that a population of individuals, each representing a possible solution to a given problem, is compared to an assigned fitness value to get the best individuals. Selecting the best individuals from the current generation and mating them to produce a new set of individuals using genetic manipulation like genetic crossover and genetic mutation, the optimal individual is obtained after many iterations of GA.

6.8.1.1 Defining chromosomes to represent the parameters

In GA gene is represented by a binary digit 0 or 1. One chromosome is defined as a group of genes used to represent a value of each parameter. Generation is the specified number of chromosomes and the population size is defined as the number of chromosomes included in one generation.

6.8.1.2 Determining number of genes for each parameter

Numbers of genes for each parameter vary according to domain of parameter and the increment of parameter values. An equation is derived by Yu Lie (2006) and later used by many researchers to determine the number of genes needed for each parameter. Table 6.4 illustrate the suggested number of genes for driving behavior parameters.

Table 6.4: Number of Genes for Each Parameter

Serial	Driving Behavior Parameters	Unit	Number of Genes
1	CC0 (Standstill distance)	meter	5
2	CC1 (Headway time)	second	4
3	CC2 (‘Following’ variation)	meter	3
4	CC3 (Threshold for entering ‘Following’)	-	5
5	CC4 (Negative ‘Following’ thresholds)	-	4
6	CC5 (Positive ‘Following’ thresholds)	-	4
7	CC7 (Oscillation acceleration)	m/ s^2	3
8	CC8 (Standstill acceleration)	m/ s^2	4
9	Maximum deceleration for cooperative braking	m/ s^2	3
Total number of Genes			35

6.8.1.3 Population of Chromosomes

Table 6.4 shows total 35 genes will represent the nine parameters for calibration. So, a chromosome with any combination of 35 genes will represent all nine parameters. The population size is therefore the number of chromosomes in one generation which is considered

16 in this thesis. We can recall here that holding the number of iterations constant, larger populations tends to reach higher fitness values than smaller populations.

6.8.1.4 Decoding each chromosomes to parameter values

The equations derived by Yu Lie (2006) have been used in this thesis for decoding each chromosome to parameter values.

6.8.1.5 Selection, crossover and mutation of chromosome

In GA, select, crossover and mutate are three operators needed in creating the next generation of chromosome. Selection is based on probability, and the chromosomes with higher fitness values will most likely be selected. In the study 50 percent of the total of 16 populations is reproduced for the next generation. Again, above mentioned 50 percent of chromosomes are recombined in the next generation with a crossover rate of 0.7 (i.e. 70 percent of the total 35 genes). Two chromosomes interchange part of their genes to create two new chromosomes during crossover. One chromosome is mutated to create a new chromosome by changing one of its genes from 1to 0 or from 0 to 1. The probability of any element of a chromosome being mutated is approximately 1 percent.

6.8.1.6 Creation of new generation

After the operators of selection, crossover and mutation are carried out to the chromosomes of the former generation, more chromosomes will be produced to form the new generation while keeping the same population size. The whole iteration process will continue for 20 times in the program. Finally, the chromosome that will be ranked with highest fitness value (meaning lowest RMSE) will represent the optimal parameter set.

6.8.2 SPSA based calibration approach

SPSA is based on highly efficient gradient approximation that relies on measurement of objective function, not on measurements of gradient of objective function (Spall, 1998). It is particularly advantageous when complete knowledge on the relationship between the parameters to be optimized and the objective function are not available or difficult to compute. Optimization in SPSA is based only two function measurements regardless of the dimension of the gradient vector. In the micro simulation calibration context in general, the objective function is the Loss (θ) which is a scalar valued MOP and θ is a continuous-valued ρ-dimensional vector of parameters to be optimized. With an initial guess of θ which is in our case is the default parameter values of VISSIM, SPSA method applies a series of "simultaneous perturbation" over the successive steps until the approximation of the gradient converges to zero.

6.8.2.1 Number of iteration and coefficient selection

In our study we have examined the convergence of gradient for 100 iterations with an initialization of counter k set to zero. A, c, a, α and γ are the non-negative coefficient in SPSA algorithm. The algorithm gain sequences are a_k and c_k which are expressed in the following equations:

$$a_k = \frac{a}{(A+K+1)^{\alpha}} \quad \text{and} \quad c_k = \frac{c}{(K+1)^{\gamma}}$$

Recommended coefficient values of are given in the Table 6.5.

Table 6.5: Recommended Values of Coefficients-SPSA

Serial	Coefficient	Value	Remarks
1	α	0.602	
2	γ	0.101	
3	a	0.0017	$\frac{a}{(A+1)^{\alpha}}$ * value of elements in $\hat{g}_k(\hat{\theta}_k)$ = smallest value of change in the elements of θ in the first iteration.
4	c	1.89	Standard deviation of the measurement noise in y(θ) which can be estimated by collecting several y(θ) values at the initial guess of θ.
5	A	10	≤ 10% of number of iterations

6.8.2.2 Generation of simultaneous perturbation vector

A ρ-dimensional random perturbation vector Δ is generated by using Bernoulli ± 1 distribution with probability of 1/2 for each ± 1 outcome.

6.8.2.3 Evaluation of objective function

Two measurements of objective function based on the simultaneous perturbation of current θ_k are obtained which can be expressed as $y(\hat{\theta}_k + c_k * \Delta)$ and $y(\hat{\theta}_k - c_k * \Delta)$.

6.8.2.4 Gradient approximation

Simultaneous perturbation is applied to all components in $\hat{\theta}_k$ of an unknown gradient $g_k(\hat{\theta}_k)$ and the gradient approximation can be shown as:

$$\hat{g}_k(\hat{\theta}_k) = \frac{y(\hat{\theta}_k + c_k * \Delta) - y(\hat{\theta}_k - c_k * \Delta)}{2c_k} \begin{bmatrix} \Delta_k^{-1} \\ \cdot \\ \cdot \\ \cdot \\ \Delta_{kp}^{-1} \end{bmatrix}$$

6.8.2.5 Updating θ Estimates

In every iteration $\hat{\theta}_k$ is updated as $\hat{\theta}_{k+1}$ recursively in the standard stochastic approximation form.

$$\hat{\theta}_{k+1} = \hat{\theta}_k - a_k * \hat{g}_k(\hat{\theta}_k)$$

Where a_k is a positive gain sequence of step sizes, and $\hat{g}_k(\hat{\theta}_k)$ is the approximation of $g(\theta)$ at each iteration.

6.8.2.6 Imposing constraints

The above optimization form is adapted to accommodate a constraint of upper and lower bound for each component of θ and updated θ is modified, if necessary.

6.8.2.7 Termination of algorithm

The algorithm will terminate after 100 iterations with a value of k = k+1 in successive iterations.

6.8.3 SA based calibration approach

The SA optimization technique bases it operation in considering the objective function of MOP as the equivalent energy function of an illusory annealing process. In this way a control parameter '*t*', which is referred as the *'temperature'*, is used to control the randomness of the optimization process. '*temperature*' is used to determine how and when new solutions are perturbed and accepted.

The algorithm is defined in such a way that for high values of *'t'*, the search is performed totally at random; and then, when *'t'* is decreased, the search becomes more and more directive. The algorithm is basically a three steps process: perturb the solution, evaluate the quality of the solution, and accept the solution if it is better than the new one (Ledesma, Aviña & Sanchez, 2008).

The SA annealing algorithm can be described as an iterative procedure composed by two nested loops. The inner loop simulates the achievement of thermal equilibrium at a given temperature, so it is going to be referred as the thermal equilibrium loop. The outer loop performs the cooling process, in which the temperature is decreased from its initial value towards zero until certain convergence criterion is achieved and the search is stopped. This loop is going to be referred as the cooling loop or annealing loop.

6.8.3.1 Thermal equilibrium loop

Starting with an initial model, 20 iterations were made inside the thermal equilibrium loop. Each iteration of the inner loop computes a new model that may or may not be accepted according to certain probability.

6.8.3.1.1 Perturbation scheme

It defines the way in which the model is updated. The parameters to be calibrated are denoted by vector θ_i, and $F(\theta_i)$ is the associated fitness value and i is the iterative index. The current solution is randomly perturbed using a uniform distribution over the feasible set in the model space to obtain a new set of parameters θ_j with feasible solution $F(\theta_j)$. The new solution is accepted with certain probability.

6.8.3.1.2 Acceptance criterion

Metropolis algorithm is used to determine the acceptance criterion. In the algorithm, a measurement 'ΔE' is computed by subtracting the measurement of the objective function at the initial model from the updated model.

$$\Delta E = F(\theta_j) - F(\theta_i)$$

If $\Delta E < 0$ then updated model θ_j is always accepted. But, if $\Delta E \geq 0$ then updated model is accepted with probability:

$$p = e^{\frac{-\Delta E}{t}}$$

Where 'p' is the probability of acceptance of updated model and 't' is '*temperature*'. On the other hand, if the updated model is not accepted, the new iteration will proceed with the same initial model θ_i. It is important to note that, at high values of temperature, the probability presents a uniform preference for any model; while, at very low temperatures, only those models for which 'ΔE' is very small will have a substantial chance of occurrence. The probability of accepting worse solution $p_0 = 0.7$ at the start and $p_n = 0.001$ at the end of the model optimization has been considered.

6.8.3.2 Cooling loop

The cooling or annealing loop, constitutes the outer loop of the algorithm. It starts with an initial model selected at random and an initial value of temperature t_0. At each iteration, the temperature is decreased in a progressive manner towards zero until certain convergence criterion is achieved. 20 iterations were made inside the cooling loop.

6.8.3.2.1 Initial temperature

The initial value of the temperature parameter is of critical importance to the success of the algorithm. A low initial temperature can result in a loss of the global character of the search by restricting the search to the region of the model space around the starting point. On the other hand, a too high initial temperature will keep the algorithm performing ‘random walks’ over the model space during a large number of iterations. This will result in an unnecessary waste of valuable computational time; and, what is worse, it can result in an unsuccessful search if the total number of iterations is limited. According to this, the initial temperature value must be defined in such a way that almost any perturbation must be accepted during the first iteration of the cooling loop. Initial temperature $t_0 = -1.0/log(p_0)$ and final temperature $t_n = -1.0/log(p_n)$ has been considered in this study.

6.8.3.2.2 Cooling schedule

It defines the way in which the temperature is going to be decreased. It is also of crucial importance in the success of the search. A very low cooling schedule will take too much iteration to reach the global minimum and, if the total number of iterations is limited, an unsuccessful search can result. On the other hand, a too fast cooling schedule can get the algorithm trapped in a local minimum or even in any smooth region of the error surface. In this study, after each iteration of outer loop, temperature is decreased by a factor and replaces the existing temperature by,

$$t_{k+1} = t_k * (\frac{t_n}{t_0})^{\frac{1}{n-1.0}}$$

Where t_k is the value of the temperature at iteration k, t_0 is the initial temperature, t_n is the final temperature and n is the number of outer loop.

6.9 Summary

This chapter presented an overview of the execution part of the thesis. Seven steps of proposed calibration procedure were sequentially explained on this subject case study. Data collection and processing, selection of MOPs and objective functions for parameter calibration and validation, and the calibration approaches based on three optimization techniques i.e. GA, SPSA & SA have been elaborately discussed.

CHAPTER 7
CALIBRATION RESULTS AND VALIDATION

7.1 General

This chapter describes the detail analysis of calibration and validation results of the calibrated parameters against the three optimization algorithms generated by OPCI.

7.2 Measurement of Objective Functions with Default Parameters

With default parameters the measurement of RMSE with respect to space headway at any instances of lane change between the field data and simulated data was found 30.32 meter. Such unusual simulated result with default parameter indicates the necessity of model calibration.

7.3 Calibration Results

7.3.1 Genetic Algorithm (GA)

7.3.1.1 Measurement of objective function

The measurement of objective functions (i.e RMSE of space headway during lane change) in each generation of GA is presented in Table 7-1. The initial value of the objective function was 6.35 meter and after calibration process the RMSE decreased to 2.38 meter (62.52% reduction). In comparison with default parameters this change is equivalent to a decrement in the RMSE of 92.15%. Table 7-1 shows the calibrated parameters and RMSE values at each generation of GA.

Table 7.1: RMSE Values at each Generation of GA

Gen No	w99cc0	w99cc1	w99cc2	w99cc3	w99cc4	w99cc5	w99cc7	w99cc8	coopDecel	RMSE
1	0.26	1.07	4.29	-25.74	-0.4	0.87	1	6.6	-6.1	6.35
2	0.65	2.4	2.86	-12.26	0	0.53	0.29	6.6	-4.53	6.36
3	0.52	2.4	2.86	-12.97	-0.87	0.2	0.71	1	-2.96	3.35
4	0.52	2.4	2.86	-12.97	-0.87	0.2	0.71	1	-2.96	3.35
5	0.52	2.4	2.86	-12.97	-0.87	0.2	0.71	1	-2.96	3.35
6	0.52	2.4	2.86	-12.97	-0.87	0.2	0.71	1	-2.96	3.35
7	0.52	2.4	2.86	-12.97	-0.87	0.2	0.71	1	-2.96	3.35
8	0.52	2.4	2.86	-12.97	-0.87	0.2	0.71	1	-2.96	3.35
9	0.52	2.4	2.86	-12.97	-0.87	0.2	0.71	1	-2.96	3.35
10	3.61	1.6	1.43	-24.32	0	0.4	1	2.87	-5.58	2.38
11	3.61	1.6	1.43	-24.32	0	0.4	1	2.87	-5.58	2.38
12	3.61	1.6	1.43	-24.32	0	0.4	1	2.87	-5.58	2.38
13	3.61	1.6	1.43	-24.32	0	0.4	1	2.87	-5.58	2.38
14	3.61	1.6	1.43	-24.32	0	0.4	1	2.87	-5.58	2.38
15	3.61	1.6	1.43	-24.32	0	0.4	1	2.87	-5.58	2.38
16	1.55	1.6	1.43	-22.19	0	0.4	1	1	-5.05	2.38
17	1.55	1.6	1.43	-22.19	0	0.4	1	1	-5.05	2.38
18	1.55	1.6	1.43	-22.19	0	0.4	1	1	-5.05	2.38
19	1.55	1.6	1.43	-22.19	0	0.4	1	1	-5.05	2.38
20	3.61	1.6	1.43	-24.32	0	0.4	1	2.87	-5.58	2.38

7.3.1.2 Convergence of Objective Functions

The convergence of GA in respect of calibrated parameters and the objective function are shown in following figures. The figure shows the improvement of the objective function at each generation of the calibration process based on GA algorithm. It took 10 generations to get the optimized parameter set for GA based calibration. A close examination of the successive solutions indicates that, in the beginning of the calibration, the population includes randomly generated individuals; over the iterations, the population evolves towards better solutions and in the very last iteration, the majority of the population individuals are virtually identical.

cc0	**cc1**	**cc2**
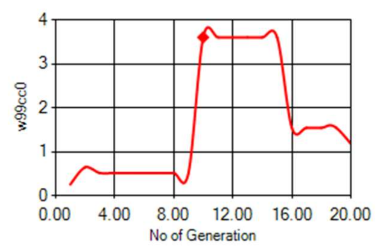	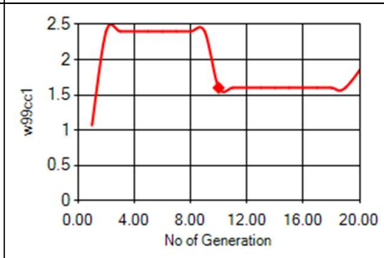	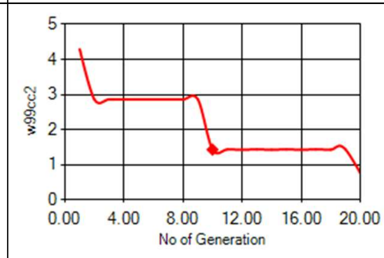
cc3	**cc4**	**cc5**
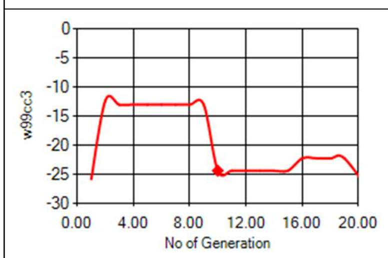	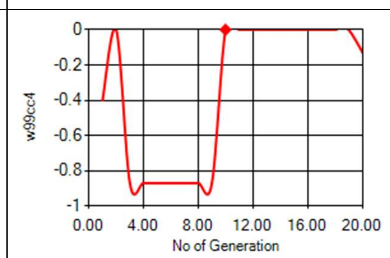	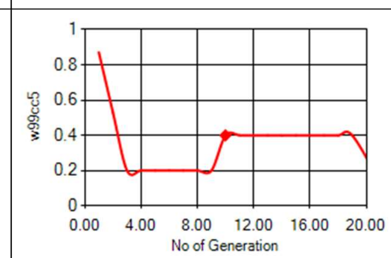
cc7	**cc8**	**coopDecel**
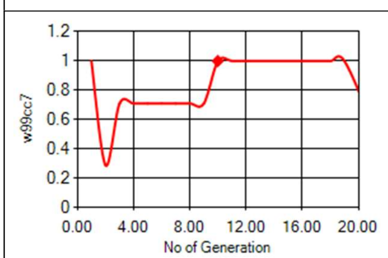	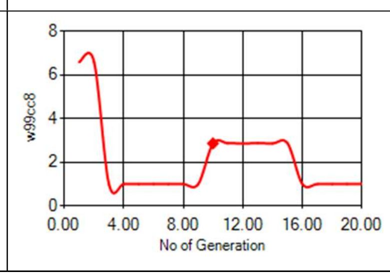	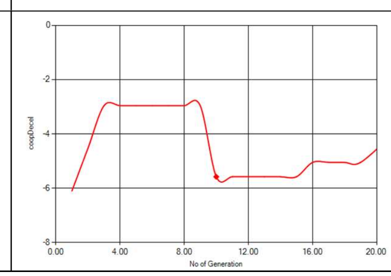

Objective Function (Headway Difference during Lane Change)

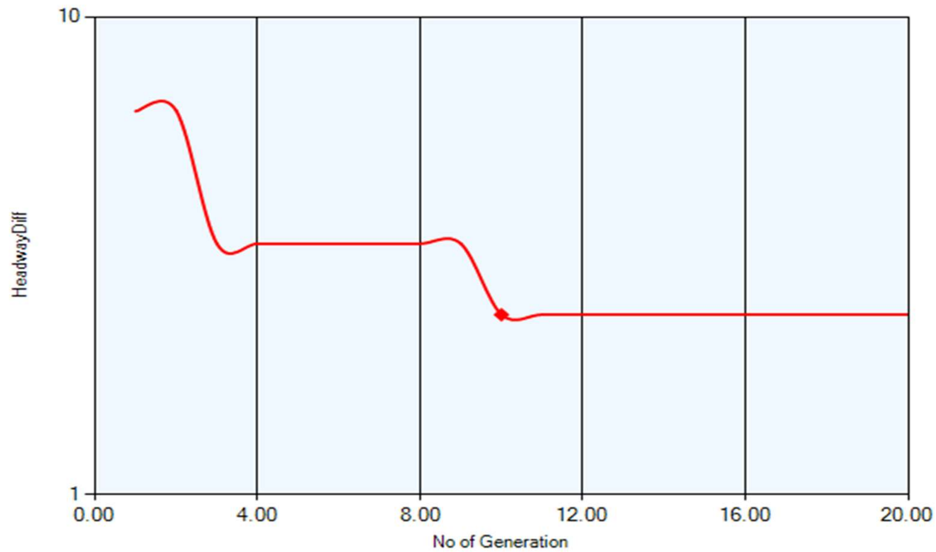

Figure 7.1: Convergence of GA Parameters and Objective Function (Generated from CALVIS)

7.3.2 Simultaneous Perturbation Stochastic Approximation (SPSA)

7.3.2.1 Measurement of objective function

With 100 iteration in SPSA, the initial value of the objective function was 45.28 meter and after calibration process the RMSE decreased to 2.47 meter (95.55% reduction). In comparison with default parameters this change is equivalent to a decrement of 91.85% RMSE. Table 7-2 shows the calibrated parameters and RMSE values at each iteration of SPSA.

Table 7.2: RMSE Values at each Iteration of SPSA

Iteration	w99cc0	w99cc1	w99cc2	w99cc3	w99cc4	w99cc5	w99cc7	w99cc8	coopDecel	RMSE
1	1.36	0.52	3.63	-8	0	0	0.14	3.12	-3.11	45.28
2	2.63	1.79	4.9	-9.27	-0.01	0	0	4.39	-1.84	43.46
3	0	2.6	5.7	-9.7	-2.05	2.05	0	1.8	-1.3	44.48
4	1.37	0.77	3.87	-8	-0.22	0.22	0.38	3.37	-2.87	48.45
5	1.37	0.77	3.87	-8	-0.22	0.22	0.38	3.37	-2.87	40.51
6	1.37	0.77	3.87	-8	-0.22	0.22	0.38	3.37	-2.87	40.51
7	1.37	0.77	3.87	-8	-0.22	0.22	0.38	3.37	-2.87	48.45
8	1.37	0.77	3.87	-8	-0.22	0.22	0.38	3.37	-2.87	40.51
9	1.36	0.52	3.63	-8	0	0	0.14	3.12	-3.11	34.16
10	1.37	0.77	3.87	-8	-0.22	0.22	0.38	3.37	-2.87	40.51
11	2.73	1.89	2.26	-9.37	-1.37	0	0	1.75	-1.74	36.71
12	2.74	1.9	2.27	-9.38	-1.38	0	0	1.76	-1.75	36.72
13	1.37	0.77	3.87	-8	-0.22	0.22	0.38	3.37	-2.87	40.51
14	2.74	1.9	2.27	-9.38	-1.38	0	0	1.76	-1.75	36.72
15	2.74	1.9	2.27	-9.38	-1.38	0	0	1.76	-1.75	36.72
16	2.74	1.9	2.27	-9.38	-1.38	0	0	1.76	-1.75	36.72
17	1.36	0.52	3.63	-8	0	0	0.14	3.12	-3.11	34.16
18	1.36	0.52	3.63	-8	0	0	0.14	3.12	-3.11	34.16
19	1.36	0.52	3.63	-8	0	0	0.14	3.12	-3.11	33.36
20	1.36	0.52	3.63	-8	0	0	0.14	3.12	-3.11	33.36
21	3.02	2.42	2.22	-9.65	-1.87	1.87	2.03	1.72	-4.52	31.77
22	3.02	2.42	2.22	-9.65	-1.87	1.87	2.03	1.72	-4.52	31.77
23	1.24	0.64	3.75	-8.12	-0.1	0.09	0.26	3.24	-2.99	28.6
24	1.24	0.64	3.75	-8.12	-0.1	0.09	0.26	3.24	-2.99	28.6
25	1.24	0.64	3.75	-8.12	-0.1	0.09	0.26	3.24	-2.99	28.6
26	1.24	0.64	3.75	-8.12	-0.1	0.09	0.26	3.24	-2.99	28.6
27	1.36	0.52	3.63	-8	0	0	0.14	3.12	-3.11	27.01
28	1.36	0.52	3.63	-8	0	0	0.14	3.12	-3.11	27.01
29	1.36	0.52	3.63	-8	0	0	0.14	3.12	-3.11	27.01
30	1.36	0.52	3.63	-8	0	0	0.14	3.12	-3.11	27.01
31	1.37	0.77	3.87	-8	-0.22	0.22	0.38	3.37	-2.87	26.21

Iteration	w99cc0	w99cc1	w99cc2	w99cc3	w99cc4	w99cc5	w99cc7	w99cc8	coopDecel	RMSE
32	1.24	0.64	3.75	-8.12	-0.1	0.09	0.26	3.24	-2.99	25.42
33	1.24	0.64	3.75	-8.12	-0.1	0.09	0.26	3.24	-2.99	25.42
34	1.24	0.64	3.75	-8.12	-0.1	0.09	0.26	3.24	-2.99	25.42
35	1.36	0.52	3.63	-8	0	0	0.14	3.12	-3.11	25.57
36	1.36	0.52	3.63	-8	0	0	0.14	3.12	-3.11	25.57
37	1.36	0.52	3.63	-8	0	0	0.14	3.12	-3.11	25.57
38	1.36	0.52	3.63	-8	0	0	0.14	3.12	-3.11	25.57
39	2.78	0	2.21	-6.58	-1.64	0	1.8	1.7	-1.45	24.62
40	2.78	0	2.21	-6.58	-1.64	0	1.8	1.7	-1.45	24.62
41	1.36	0.52	3.63	-8	0	0	0.14	3.12	-3.11	23.83
42	0.01	0	4.98	-9.35	-0.01	1.35	1.49	4.47	-1.76	23.04
43	2.83	0	2.16	-6.53	-1.47	1.47	1.61	1.65	-4.58	22.24
44	0	0	5.11	-6.52	-0.01	1.48	1.62	4.6	-4.59	21.45
45	1.5	0.9	4	-8	-0.35	0.35	0.25	3.5	-3	20.65
46	1.5	0.9	4	-8	-0.35	0.35	0.25	3.5	-3	20.65
47	1.5	0.9	4	-8	-0.35	0.35	0.25	3.5	-3	20.65
48	2.64	1.8	2.35	-9.28	-1.28	1.28	0	1.84	-4.39	19.95
49	2.76	0	2.23	-9.4	-1.4	1.4	0	4.52	-1.71	19.86
50	2.87	0	2.12	-9.51	-0.01	1.51	1.65	1.61	-4.62	19.06
51	0.09	1.79	2.36	-6.73	-1.27	1.27	1.41	4.39	-1.84	18.27
52	1.36	0.52	3.63	-8	0	0	0.14	3.12	-3.11	17.69
53	3.02	0	2.22	-6.35	-1.87	0	0	5.02	-4.52	16.68
54	1.36	0.52	3.63	-8	0	0	0.14	3.12	-3.11	15.63
55	1.36	0.52	3.63	-8	0	0	0.14	3.12	-3.11	15.09
56	0.07	1.81	4.92	-9.29	-0.01	1.29	0	4.41	-1.82	12.35
57	0.03	1.85	2.3	-6.67	-0.01	0	0	4.45	-1.78	11.32
58	1.36	0.52	3.63	-8	0	0	0.14	3.12	-3.11	11.12
59	0	1.94	5.05	-9.42	-0.01	0	0	4.54	-1.69	10.74
60	0.01	1.87	4.98	-9.35	-1.35	1.35	1.49	1.77	-4.46	10.33
61	1.36	0.52	3.63	-8	0	0	0.14	3.12	-3.11	9.55
62	2.72	1.88	2.27	-9.36	-0.01	0	0	4.48	-1.75	9.02
63	1.36	0.52	3.63	-8	0	0	0.14	3.12	-3.11	8.91
64	0.09	1.79	2.36	-6.73	-1.27	1.27	0	1.85	-1.84	8.82

Iteration	w99cc0	w99cc1	w99cc2	w99cc3	w99cc4	w99cc5	w99cc7	w99cc8	coopDecel	RMSE
65	0.05	1.83	4.94	-9.31	-0.01	0	0	1.81	-4.42	5.84
66	1.36	0.52	3.63	-8	0	0	0.14	3.12	-3.11	5.8
67	0.11	1.77	4.88	-9.25	-0.01	1.25	0	4.37	-1.86	5.78
68	2.61	1.77	2.38	-6.75	-0.01	0	0	1.87	-1.86	5.65
69	1.36	0.52	3.63	-8	0	0	0.14	3.12	-3.11	5.56
70	1.36	0.52	3.63	-8	0	0	0.14	3.12	-3.11	3.99
71	1.36	0.52	3.63	-8	0	0	0.14	3.12	-3.11	3.97
72	1.36	0.52	3.63	-8	0	0	0.14	3.12	-3.11	3.37
73	0	1.89	2.26	-9.37	-1.37	0	0	1.75	-1.74	3.26
74	0	1.95	2.2	-9.43	-1.43	0	1.57	4.55	-4.54	3.18
75	0.03	1.85	2.3	-9.33	-0.01	0	0	4.45	-1.78	2.49
76	1.36	0.52	3.63	-8	0	0	0.14	3.12	-3.11	2.47
77	1.36	0.52	3.63	-8	0	0	0.14	3.12	-3.11	2.47
78	1.36	0.52	3.63	-8	0	0	0.14	3.12	-3.11	2.47
79	1.36	0.52	3.63	-8	0	0	0.14	3.12	-3.11	2.47
80	1.36	0.52	3.63	-8	0	0	0.14	3.12	-3.11	2.47
81	1.36	0.52	3.63	-8	0	0	0.14	3.12	-3.11	2.47
82	1.36	0.52	3.63	-8	0	0	0.14	3.12	-3.11	2.47
83	1.36	0.52	3.63	-8	0	0	0.14	3.12	-3.11	2.47
84	0	1.95	2.2	-9.43	-1.43	0	1.57	4.55	-4.54	3.18
85	0	1.95	2.2	-9.43	-1.43	0	1.57	4.55	-4.54	3.18
86	0	1.95	2.2	-9.43	-1.43	0	1.57	4.55	-4.54	3.18
87	0	1.95	2.2	-9.43	-1.43	0	1.57	4.55	-4.54	3.18
88	0	1.95	2.2	-9.43	-1.43	0	1.57	4.55	-4.54	3.18
89	0	1.95	2.2	-9.43	-1.43	0	1.57	4.55	-4.54	3.18
90	0	1.95	2.2	-9.43	-1.43	0	1.57	4.55	-4.54	3.18
91	0	1.95	2.2	-9.43	-1.43	0	1.57	4.55	-4.54	3.18
92	0	1.95	2.2	-9.43	-1.43	0	1.57	4.55	-4.54	3.18
93	0	1.95	2.2	-9.43	-1.43	0	1.57	4.55	-4.54	3.18
94	0	1.95	2.2	-9.43	-1.43	0	1.57	4.55	-4.54	3.18
95	0	1.95	2.2	-9.43	-1.43	0	1.57	4.55	-4.54	3.18
96	0	1.95	2.2	-9.43	-1.43	0	1.57	4.55	-4.54	3.18
97	1.36	0.52	3.63	-8	0	0	0.14	3.12	-3.11	3.97

Iteration	w99cc0	w99cc1	w99cc2	w99cc3	w99cc4	w99cc5	w99cc7	w99cc8	coopDecel	RMSE
98	1.36	0.52	3.63	-8	0	0	0.14	3.12	-3.11	3.97
99	1.36	0.52	3.63	-8	0	0	0.14	3.12	-3.11	3.97
100	1.36	0.52	3.63	-8	0	0	0.14	3.12	-3.11	3.97

7.3.2.2 Convergence of objective function

The fitness value of SPSA shows a noisy trajectory during the first few iterations and then follows the gradient approximation on the graph (Figure. 7.2). The convergence of SPSA in respect of calibrated parameters and the objective function are shown in following figures. Optimal parameter set has been obtained at 76 iteration of SPSA.

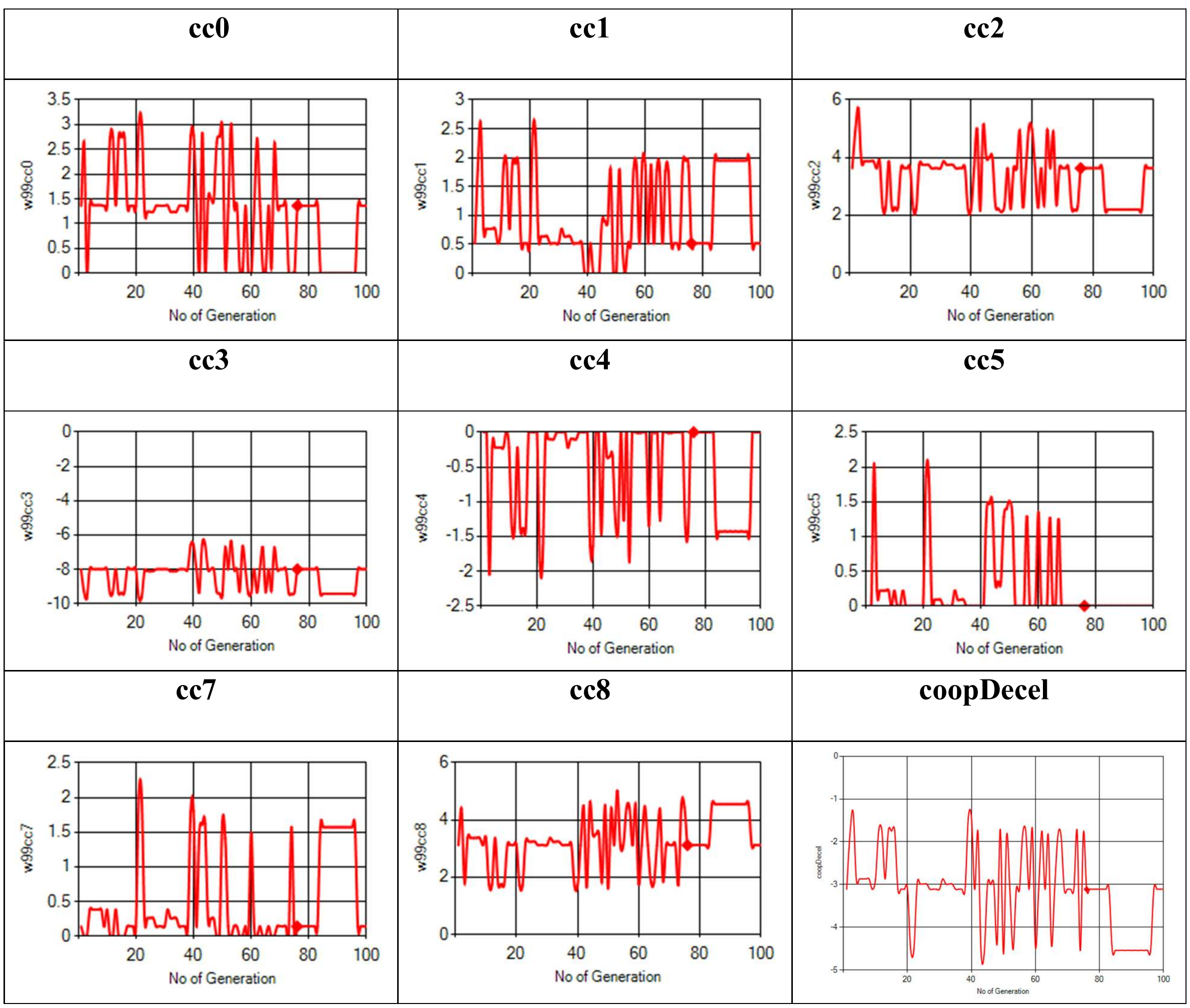

Objective Function (Headway Difference during Lane Change)

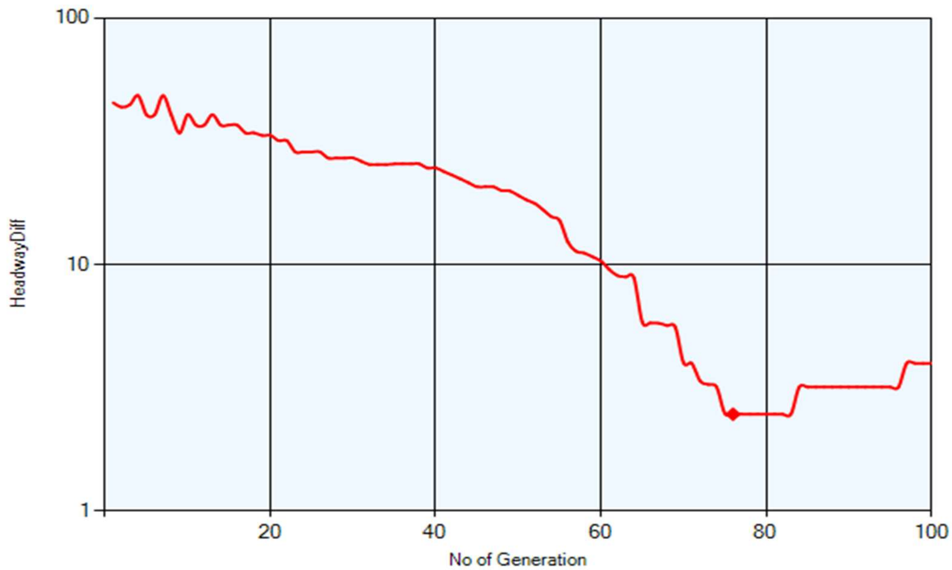

Figure 7.2: Convergence of SPSA Parameters and Objective Function (Generated from CALVIS)

7.3.3 Simultaneous Annealing (SA)

7.3.3.1 Measurement of objective function

The measurement of RMSE of space headway during lane change in each cycle of SA is presented in Table 7-3. The initial value of the objective function was 15.09 meter and after calibration process the RMSE decreased to 1.85 meter (87.74% reduction). In comparison with default parameters this change is equivalent to a decrement of 93.90% RMSE. Table 7-3 shows the calibrated parameters and RMSE values at each cycle of SA.

Table 7.3: RMSE Values at each Cycle of SA

Cycle	w99cc0	w99cc1	w99cc2	w99cc3	w99cc4	w99cc5	w99cc7	w99cc8	coopDecel	RMSE
1	1.5	0	4.05	-8	-0.93	0.7	0.48	2.53	-4.12	15.09
2	1.12	0	4.03	-8	-0.74	1	0.24	3.29	-4.71	18.27
3	0.71	1.25	1.53	-9.08	-0.44	0.3	0	5.88	-6.1	16.68
4	0.74	1.6	1.65	-8.18	-0.09	0.33	0	5.66	-5.58	2.41
5	0.65	2.18	1.89	-8	-1	0.85	1	6.8	-5.02	2.38
6	0.7	1.51	1.54	-8.66	-1	0.3	0.69	6.32	-6	3.18
7	2.17	1.64	1.04	-8.57	-0.97	0.34	0	3.73	-5.15	3.2
8	2.21	1.94	1.2	-8	-0.21	0.19	0.51	4.29	-4.78	4.34
9	3.65	1.92	0	-8.61	-0.47	0.95	0.58	5.04	-5.53	2.38
10	3.87	3.54	0	-9.94	-1	0	0.43	3.48	-4.34	2497.99
11	3.22	3.4	0.22	-10.04	-0.23	1	0	2.02	-2.81	2494.02
12	2.65	3.5	1.52	-10.25	-1	0.99	0.2	1.87	-2.44	2490.84
13	0.27	1.86	1.16	-12.4	0	1	0.61	5.66	-3.24	1.85
14	1.44	2.42	1.57	-10.79	-0.82	0	1	3.34	-3.67	4.9
15	1.73	1.85	0.55	-9.83	0	0.42	0.53	4.65	-4.66	2.38
16	0.86	1.84	0.84	-10.66	0	0	0.76	4.8	-5.14	3.97
17	0.79	1.6	0.18	-10.13	-0.37	0.58	0	4.96	-4.97	3.97
18	0.26	1.92	0.89	-12.43	-0.19	0.63	0	5.2	-2.8	4.04
19	0.27	1.86	1.16	-12.4	0	1	0.61	5.66	-3.24	1.85
20	0.27	1.86	1.16	-12.4	0	1	0.61	5.66	-3.24	1.85

7.3.3.2 Convergence of objective function

The evolution of model parameters during each iterations of SA is presented in figure 7.3. The progression of the parameters shows numerous local optima marked by small "valleys", indicating that the lowest FV is within the close vicinity of the local minima. Presence of these small valleys prove that SA has a provision to accept a fraction of inferior solutions to escape local optima in search of global optima. The convergence of SA in respect of calibrated parameters and the objective function are shown in following figures. Optimal parameter set has been obtained at 13 cycles of SA.

cc0

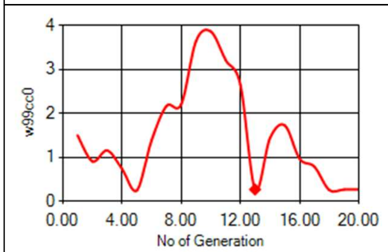

cc1

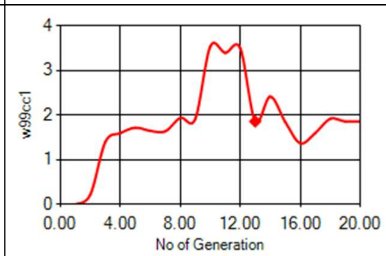

cc2

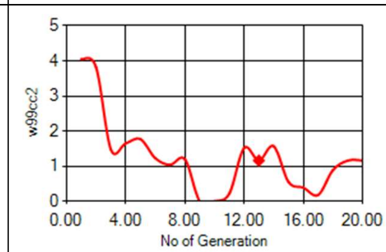

cc3

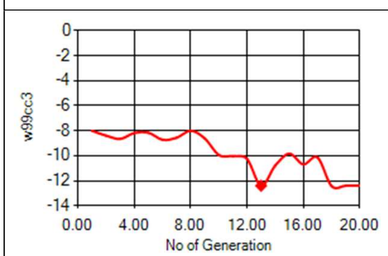

cc4

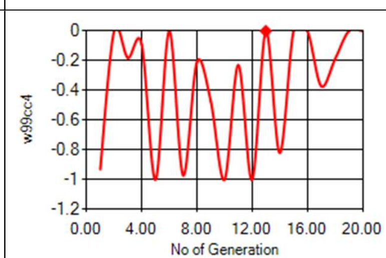

cc5

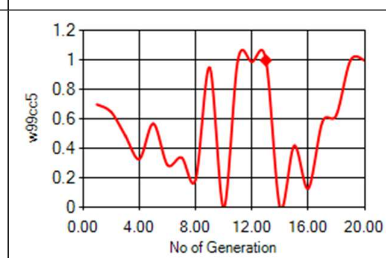

cc7

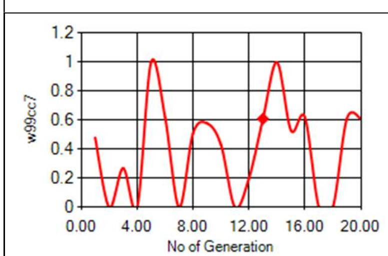

cc8

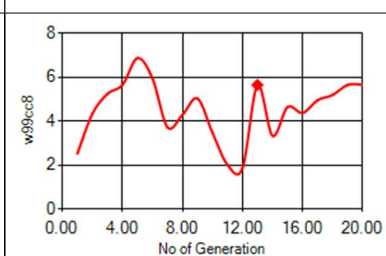

coopDecel

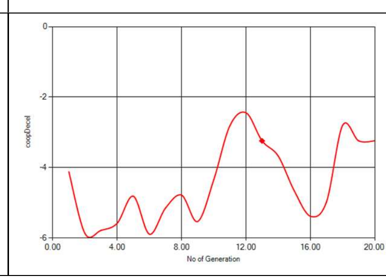

Objective Function (Headway Difference during Lane Change)

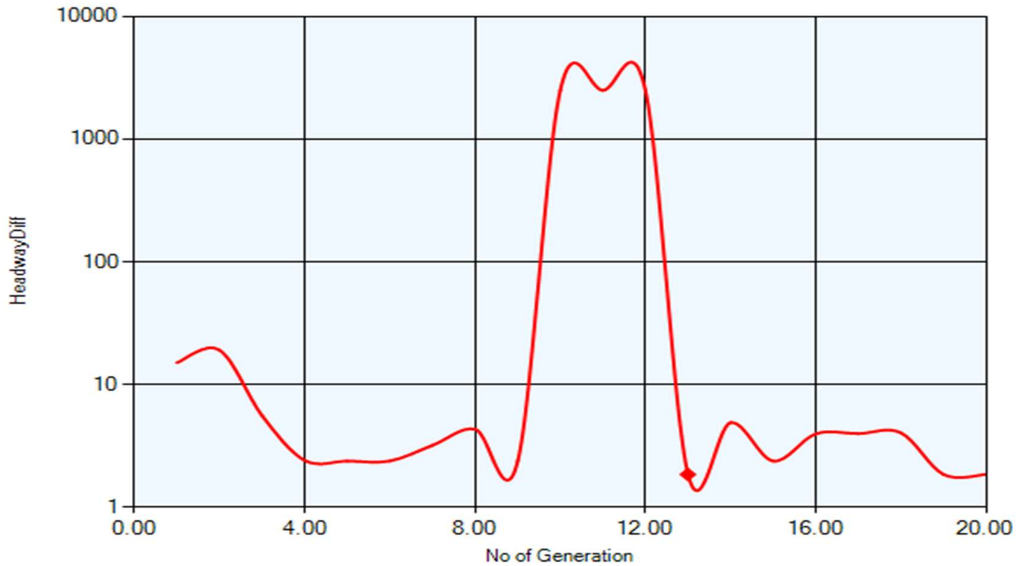

Figure 7.3: Convergence of SA Parameters and Objective Function (Generated from CALVIS)

7.4 Comparison of Calibration Results

7.4.1 Optimal parameters

The optimization operation of GA, SPSA and SA is performed on the same search space to draw a comparison between the outcomes. Comparative set of optimal parameters obtained by GA, SPSA and SA in respect of headway during lane change MOP are shown in Table 7.4:

Table 7.4: Optimal Parameters in respect of three Optimization Techniques

Serial	Driving Behavior Parameters	Unit	GA	SPSA	SA
1	CC0 (Standstill distance)	meter	0.77	1.36	0.27
2	CC1 (Headway time)	second	2.13	0.52	1.86
3	CC2 (‘Following’ variation)	meter	0	3.63	1.16

Serial	Driving Behavior Parameters	Unit	GA	SPSA	SA
4	CC3 (Threshold for entering ‘Following’)	-	-28.58	-8.0	-12.4
5	CC4 (Negative ‘Following’ thresholds)	-	-0.27	0	0
6	CC5 (Positive ‘Following’ thresholds)	-	0.13	0	1.0
7	CC7 (Oscillation acceleration)	m/s^2	0.57	0.14	0.61
8	CC8 (Standstill acceleration)	m/s^2	1.0	3.2	5.66
9	coopDecel (Max Deceleration for cooperative braking)	m/s^2	-4.01	-3.11	-3.24

7.4.2 Convergence of objective functions

Comparative calibration result and the improvement of the objective function at each iteration of the calibration process of GA, SPSA and SA as generated from the CALVIS are presented in figure 7.4 and 7.5:

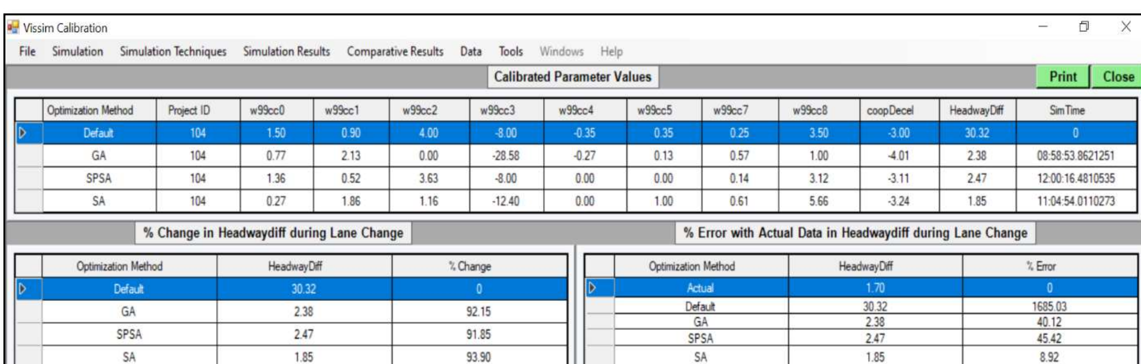
Vissim Calibration

File Simulation Simulation Techniques Simulation Results Comparative Results Data Tools Windows Help

Calibrated Parameter Values

Print Close

Optimization Method	Project ID	w99cc0	w99cc1	w99cc2	w99cc3	w99cc4	w99cc5	w99cc7	w99cc8	coopDecel	HeadwayDiff	SimTime
Default	104	1.50	0.90	4.00	-8.00	-0.35	0.35	0.25	3.50	-3.00	30.32	0
GA	104	0.77	2.13	0.00	-28.58	-0.27	0.13	0.57	1.00	-4.01	2.38	08:58:53.8621251
SPSA	104	1.36	0.52	3.63	-8.00	0.00	0.00	0.14	3.12	-3.11	2.47	12:00:16.4810535
SA	104	0.27	1.86	1.16	-12.40	0.00	1.00	0.61	5.66	-3.24	1.85	11:04:54.0110273

% Change in Headwaydiff during Lane Change

Optimization Method	HeadwayDiff	% Change
Default	30.32	0
GA	2.38	92.15
SPSA	2.47	91.85
SA	1.85	93.90

% Error with Actual Data in Headwaydiff during Lane Change

Optimization Method	HeadwayDiff	% Error
Actual	1.70	0
Default	30.32	1685.03
GA	2.38	40.12
SPSA	2.47	45.42
SA	1.85	8.92

Figure 7.4: Summary of Comparative Calibration Result (Generated from CALVIS)

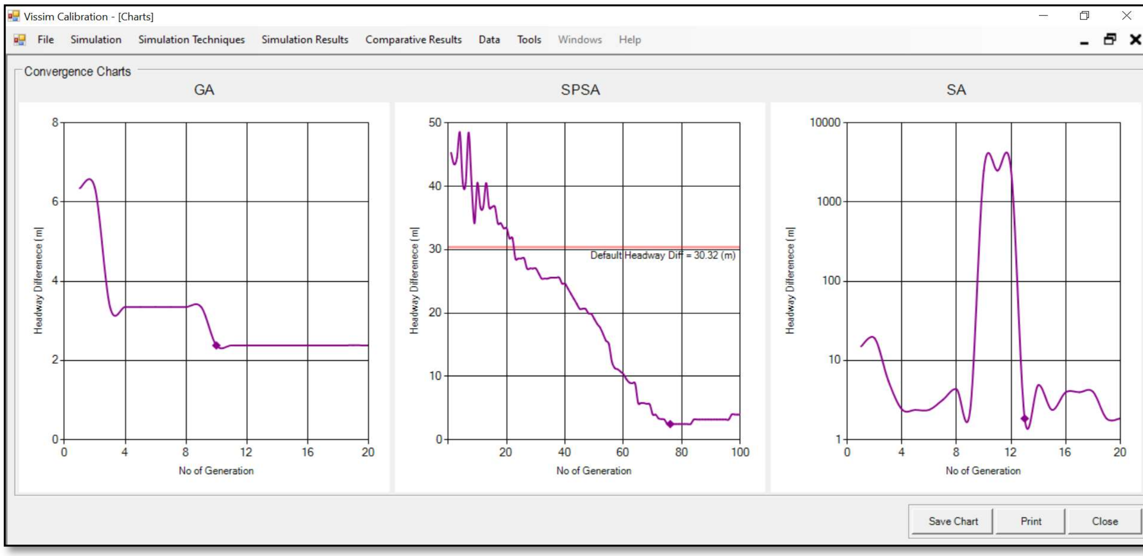

Figure 7.5: Comparative Convergence Charts (Generated from CALVIS)

The average space headway difference during lane change is 1.7 meter as measured from the field data captured from a drone. But the value of the objective function with the default parameter set is 30.32 meter which is unusual as compared to the field data. Results shows that SA reaches best fitness value (FV) of 1.85 meter at 13^{th} cycles (256 iterations) with 93.90% improvement from default parameters and 8.92% deviation from actual data, GA displays a FV of 2.36 meter at 11^{th} generation (173 iterations) with 92.15% improvement from default parameters and 40.12% deviation from actual data, and SPSA shows the worst FV of 2.47 meter with 91.85% improvement from default parameters and 45.42% error from actual data at 76 iterations. Visualization of the fitness values shows that SPSA remains oscillatory and follow a steep gradient of FV during the convergence process, GA shows a gradual convergence with very little oscillation of the FV whereas SA shows frequent fall and rise before converging towards the optimal parameter set (Figure. 7.5). SA outperformed GA and SPSA for the current calibration process.

7.4.3 Computational complexity

Generally, there is a trade-off between the quality of the solution and the time available for calibration. Often in research projects and studies there is a time limit that is directly related to cost from practical considerations. CALVIS gives the user such flexibility that the entire calibration process can be oriented towards the quality of the solution while compromising time or vice versa. This trade-off between time and quality is reflected in the case study of the freeway scenario. For instance, Table 7.5 shows that SPSA converged to an optimal solution by 76 iterations compared to other two techniques (173 for GA and 256 for SA). However, the quality of the output, FV in this case is found to be the least from others. As per as the computational time is concerned, GA proves to be economical with reasonable FV. The complexity of the calibration process depends on the number of involved micro-simulation parameters. This implies that the increase of the number of parameters has a substantial effect on the computational time and outcome of the calibration process.

Table 7.5: Computational Complexity

Optimization Algorithm	Number of Iteration	Optimal Converge at	Optimal FV (m)	Computational Time (Hr:Min)
GA	320	173	2.38	08:59
SPSA	100	76	2.47	12:01
SA	400	256	1.85	11:05

7.5 Validation

As discussed before, the model was calibrated based on micro simulation vehicle trajectory data. The calibrated model was then evaluated against aggregated MOP based on macro traffic data for validation. Average space headway for every 10 seconds of interval along every 10 meters segments of roadway has been considered as the aggregated MOP for validation. With respective optimal parameters obtained from GA, SPSA and SA the model was again simulated for validation and the differences in result with the field data in relation to sum of absolute headway difference as objective function are shown in the figure 7.6 below (generated from CALVIS):

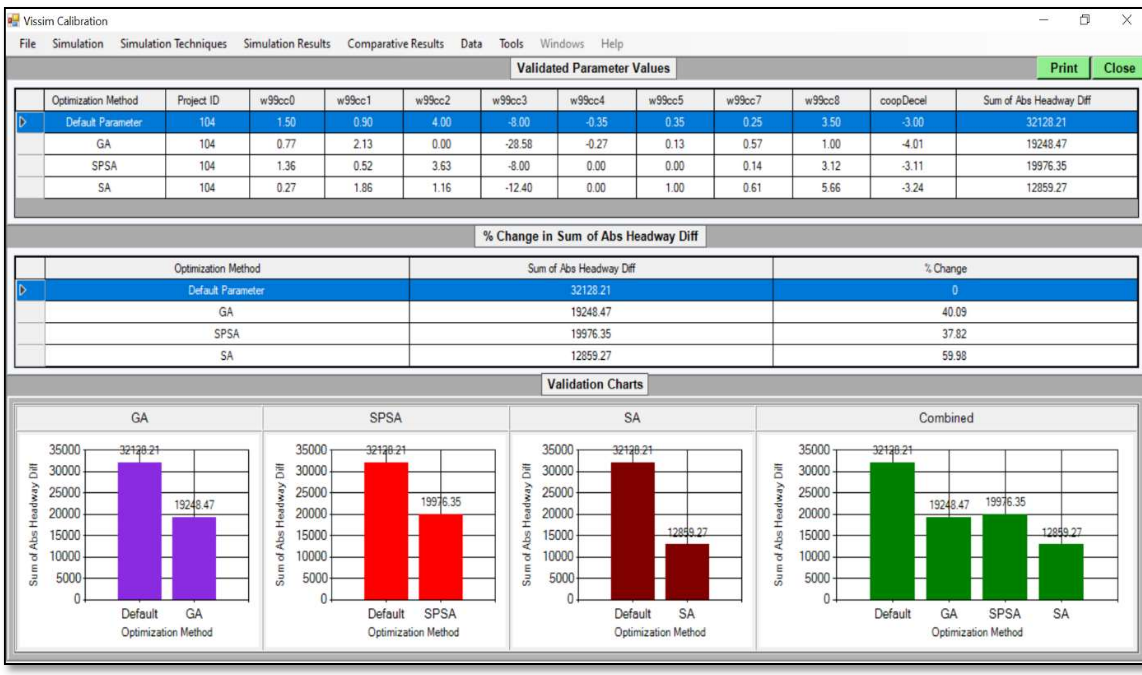

Figure 7.6: Validation Result (Generated from CALVIS)

With default parameters the sum of absolute headway difference between the actual observed traffic data and the simulated data was 32,128.21 meter. SA optimized parameters reduced the difference to 59.98% (12,859.27 meter) whereas, GA based parameters reduced to 40.09%

(19,248.47 meter) and SPSA based parameters to 37.82% (19,976.35 meter). The validation result indicates that the simulation parameters calibrated by analyzing micro traffic trajectory data have significant impact on macro measurement of traffic data in depicting aggregated values close to the observed field data.

7.6 Summary

The graphical and tabular representations of the calibration and validation results are presented in this chapter. While comparing with default parameters, the calibration results yielded an error minimization by 93.90% in SA algorithm, 92.15% in GA algorithm and 91.85% in SPSA algorithm. While comparing with actual data, the error is minimized to only 8.92% in SA algorithm which is remarkable. Again, the validation charts clearly amplify the justification of the calibration and satisfactorily validate the calibration of the model.

CHAPTER 8

CONCLUSION AND RECOMMENDATIONS

8.1 Conclusion

Use of micro simulation model has become an inseparable element in traffic management, and there are no other good options than that of adopting such state-of-art technology. The purpose of this research was three-fold: a) to propose a simulation methodology by simultaneous calibration of car following and lane changing parameters, b) to formulate an objective function by the fusion of macroscopic and microscopic traffic data, and c) To investigate a robust heuristic optimization algorithm to be used for mixed traffic condition. This research addresses all three objectives mentioned above.

This thesis proposed a seven steps procedure for calibrating microscopic simulation models: 1) field data collection and processing, 2) VISSIM model development, 3) determination of MOPs and Objective function, 4) selection of parameter and range, 5) sensitivity analysis, 6) parameter calibration using optimization techniques, and 7) model validation. The main innovation of the proposed calibration procedure lies in the simultaneous calibration of car following and lane changing parameters, mathematical formulation of new equation for the objective function, fusion of macroscopic and microscopic vehicle trajectory data and comparison of the performance of three optimization techniques in calibration of parameters. Calibration approaches based on GA, SPSA and SA were also elaborately discussed.

While comparing with default parameters, the calibration results yielded an error minimization by 93.90% in SA algorithm, 92.15% in GA algorithm and 91.85% in SPSA algorithm. SA outperformed GA and SPSA for the current calibration process. Again, the validation charts clearly amplify the justification of the calibration and satisfactorily validate the calibration of the model. The calibration procedure demonstrated in this thesis was successful in finding parameter sets that improved the accuracy of the model, relative to the default parameter values.

Calibration is a complex and tedious process involving large set of micro-simulation parameters for a particular network. Previously several studies have added new techniques and automation to the calibration process (Balakrishna 2007, Ma 2007). However, the use of generic calibration tool for any micro-simulation model is very limited in the literature that is particularly important and invaluable to any practitioner or researcher considering the complexity, cost, and time associated with the calibration process. This study develops a generic calibration tool, CALVIS for microscopic simulation parameters in VISSIM environment. The optimization system of the tool is based on three heuristic algorithms: (1) GA, (2) SPSA, (3) SA. This tool offers greater flexibility to the user by providing control on every aspect of the calibration process. CALVIS includes significant features consisting of the ability to test the significance of the appropriate decision parameter set to check the suitability of any of the three heuristic optimization algorithms for a particular network. Note that CALVIS can be used to calibrate any type (rural, urban and etc.) and extent (large, medium and etc.) of network. However, in this study the operation of the tool is tested by a dataset obtained by a drone from a 400 meter stretched freeway of Dhaka, Bangladesh which is representative of 2.6 km segment of the freeway.

8.2 Recommendations for Future Study

Although traffic simulation models have been studied for more than two decades in the developed world, research on this topic in Bangladesh as well as in other south-east Asian countries is extremely scarce and challenging. This is mainly due to the complexity of data collection and processing and the wide variations of driver population, vehicle components and traffic environment. The current study of calibration process cannot be applied equally to different roadway conditions and highly complex heterogeneous traffic operation. In fact, it should be kept in mind that there is not a single set of calibrated parameters that applies to all traffic situations. In this section some recommendations are provided for future research following the studies carried out in this dissertation. These are listed below.

a) Scope of this thesis was limited to freeways only. Calibration process for unban roadways and intersection in context of Bangladesh should also be devised.

b) Exploration on the possibility of online calibration in context of Bangladesh may be done for more accurate and automated calibration process.

c) Finally, further and extensive expansion of the computer programmed interface to include all possible variations of traffic and roadway conditions that supports all micro simulation tools presently in vogue.

Total Pages: 137

Word Count: 28,500

REFERENCES

[1] Aerde, V. and Rakha, H. (1995), "Multivariate calibration of single regime speed-flow-density relationships", *Proceedings of the 6th Vehicle Navigation and Information Systems Conference*, pp. 334-341.

[2] Balal, E., Cheu, R.L. and Gyan, T.S. (2015), "A binary decision model for discretionary lane changing move based on fuzzy inference system", Transportation Research Part C, vol. 67 (2016), pp. 47–56.

[3] Caliper (2011), "TransModeler user's guide, version 2.6", Caliper Corp., Newton, MA.

[4] Cheu, R., Jin, X., Ng, K., Ng, Y. and Srinivasan, D. (1998), "Calibration of FRESIM for Singapore expressway using GA", ASCE Journal of Transport Engineering, vol. 124(6), pp. 526–535.

[5] Crowe, J. M. (2009), "The calibration, validation, and comparison of VISSIM simulations using the two-fluid model", M. Sc. Engg. Thesis, Department of Civil and Environmental Engineering in the College of Engineering and Computer Science at the University of Central Florida Orlando, Florida.

[6] Cunto, F. and Saccomanno, F.F. (2008), "Calibration and validation of simulated vehicle safety performance at signalized intersections", Accident Analysis and Prevention, vol. 40, pp. 1171-1179.

[7] Dowling, R., Skabardonis, A., Halkias, J., McHale, G. and Zammit, G. (2004), "Guidelines for calibration of microsimulation models", Transportation Research Record: Journal of the Transportation Research Board, vol. 1976, pp. 1–9.

[8] Duong, D., Saccomanno, F. and Hellinga, B. (2010), "Calibration of traffic model for simulating safety performance", Transportation Research Board 89th Annual Meeting, Paper #10-0858.

[9] Egami, C., Mon-Ma, M., Setti, J. and Rilett, L. (2006), "Automatic calibration of two-lane highway traffic simulation models using a GA", Applications of Advanced Technology in Transportation, pp. 510-515.

[10] Emmanouil, N.B., Eleni, I. V., Golias, J. C. and Adam, B. (2017), "How accurate are small drones for measuring microscopic traffic parameters?", Transportation Letters, The international journal of transportation research, vol. 11, issue. 6, pp. 332-340.

[11] Essa, M. and Sayed, T. (2015), "Simulated traffic conflicts do they accurately represent field-measured conflicts?", Transportation Research Record: Journal of the Transportation Research Board, vol. 2514, pp. 48–57.

[12] Fellendorf, M. and Vortisch, P. (2001), “Validation of the microscopic traffic flow model VISSIM in different real-world situations”, Transportation Research Board 80th Annual Meeting 2001.

[13] FHWA (1995), “The FRESIM user’s guide”, Office of Traffic Safety and Operations R&D, Federal Highway Administration.

[14] Gao, Y. (2008), “Calibration and comparison of the VISSIM and INTEGRATION microscopic traffic simulation models”, M. Sc. Engg. Thesis, Virginia Polytechnic Institute and State University.

[15] Goldberg, D. E. (1989), “Genetic Algorithms in search, optimization, and machine learning”, Addison-Wesley Publishing Co. Inc., Reading, MA.

[16] Gomes, G., May, A. and Horowitz R. (2004), “Congested freeway microsimulation model using VISSIM”, Transportation Research Record: Journal of the Transportation Research Board, vol. 1876, pp. 71–81.

[17] Hee-Sang, K., Kwang, Y.L. and Ho-Chan, K.D. (2008), “A Simultaneous Perturbation Stochastic Approximation (SPSA)-based model approximation and its Application for power system stabilizers”, International Journal of Control, Automation, and Systems, vol. 6, no. 4, pp. 506-514.

[18] Holland, J. H. (1975), “Adaptation in natural and artificial systems”, The University of Michigan Press, Ann Arbor.

[19] Hourdakis, J., Michalopoulos, P.G. and Kottommannil, J. (2003), “Practical procedure for calibrating microscopic traffic simulation models”, Transportation Research Record: Journal of Transportation Research Board, vol. 1852(1), pp. 130-139.

[20] Karakikesa, I., Spanglera, M. and Margreiter, M. (2017), “Designing a VISSIM-Model for a motorway network with systematic calibration on the basis of travel time measurements”, Transportation Research Procedia, vol. 24, pp. 171-179.

[21] Kim, K. and Rilett, L.R. (2001), “Genetic Algorithm based approach for calibrating microscopic simulation models”, Proceedings of IEEE International Conference on Intelligent Transportation Systems, pp. 698-704.

[22] Kim, S. J., Kim, W. and Rilett, L. R. (2005), “Calibration of micro simulation models using non-parametric statistical techniques”, Transportation Research Record: Journal of Transportation Research Board, vol. 1935, pp. 111-119.

[23] Kim, S. J, Kim, W., and Rilett, L.R. (2004), “A Genetic Algorithm based approach to traffic microsimulation calibration using ITS data”, Transportation Research Board 83rd Annual Meeting 2004.

[24] Kirkpatrick, S., Gelatt, C.D. and Vecchi, M.P. (1983), “Optimization by Simulated Annealing”, Science, New Series, vol. 220, no. 4598, pp. 671-680.

[25] Kuo, Yiyo, Luo and Chi-Ming, D. (2011), “Optimization of circular type routes for a shuttle bus service”, Transportation Research Board Annual Meeting, Paper #11-0154.

[26] Laval, J. A. and Daganzo, C. F. (2006), “Lane-changing in traffic stream”, Transportation Research Part B: Methodological, vol. 40, issue. 3, pp. 251-264.

[27] Leyn, U. and Vortisch, P. (2015), “Calibrating VISSIM for the German highway capacity manual”, Transportation Research Record: Journal of the Transportation Research Board, vol. 2483, pp. 74–79.

[28] Ledesma, S., Aviña, G. and Sanchez, R. (2008), “Practical considerations for Simulated Annealing implementation”, Simulated Annealing, Cher Ming Tan (Ed.), ISBN: 978-953-7619-07-7, InTech, Available at: http://www.intechopen.com/books/simulated_annealing/practical_considerations_for_simulated_annealing_implementation, Accessed 17 April 2019.

[29] Lee, D. H., Xu, Y. and Chandrasekar, P. (2001), “Parameter calibration for PARAMICS using Genetic Algorithm”, Transportation Research Board 80th Annual Meeting 2001.

[30] Lidbe, A. D, Hainen, A. M. and Jones, S. L. (2017), “Comparative study of simulated annealing, tabu search, and the genetic algorithm for calibration of the microsimulation model”, Simulation: Transactions of the Society for Modeling and Simulation International, vol. 93(1), pp. 21–33.

[31] Lownes, N. E. and Machemehl, R. B. (2006), “VISSIM: A multi-parameter sensitivity analysis”, Proceedings of the 38th Winter Simulation Conference, pp. 1406-1413.

[32] Ma, T. and Abdulhai, B. (2002), “GA based optimization approach and generic tools for calibrating traffic microscopic simulation parameters”, Transportation Research Record: Journal of the Transportation Research Board, vol.1800: pp. 6-15.

[33] Manjunatha, P., Mathew, T. V. and Vortisch, P. (2012), “Methodology for the calibration of VISSIM in mixed traffic”, Transportation Research Board 92nd Annual Meeting 2013, Paper #13-3677.

[34] Mathew, T.V. and Radhakrishnan, P. (2010), “Calibration of microsimulation models for non-lane based heterogeneous traffic at signalized intersections”, Journal of Urban Planning and Development, vol. 136, no. 1, pp. 59-66.

[35] Menneni, S., Sun, C. and Vortisch, P. (2008), “Microsimulation calibration using speed-flow relationships”, Transportation Research Record: Journal of the Transportation Research Board, vol. 2088(1), pp. 1-9.

[36] Miller, D. M. (2009), “Developing a procedure to identify parameters for calibration of a VISSIM model”, M. Sc. Engg. Thesis, School of Civil & Environmental Engineering, Georgia Institute of Technology.

[37] Mizanur, R., Mashrur, C., Xie, Y. and He, Y. (2013), “Review of microscopic lane changing models and future research opportunities”, IEEE Transactions on intelligent transportation systems, vol. 14, no. 4, pp. 1942 – 1956.

[38] Metropolis, N., Rosenbluth, A. and Rosenbluth, M. (1953), “Equations of state calculations by fast computing machines”, Journal of Chemical Physics, vol. 21 (6), pp. 1087-1092.

[39] Omrani, R. and Kattan, L. (2013), “Simultaneous calibration of microscopic traffic simulation model and estimation of origin-destination (OD) flows based on GAs in a high-performance computer”, Proceedings of IEEE 16th International Conference on Intelligent Transportation Systems - (ITSC), pp. 2316-2321.

[40] Park, B. and Kwak, J. (2011), “Calibration and validation of TRANSIMS microsimulator for an urban arterial network”, KSCE Journal of Civil Engineering, vol. 15(6), pp. 1091-1100.

[41] Park, B. and Qi, H. (2005), “Development and evaluation of simulation model calibration procedure”, Transportation Research Record: Journal of Transportation Research Board, vol. 1934, pp. 208-217.

[42] Park, B. and Schneeberger, J. D. (2003), “Microscopic simulation model calibration and validation: Case study of VISSIM simulation model for a coordinated actuated signal system”, Transportation Research Record: Journal of the Transportation Research Board, vol. 1856, pp. 185–192.

[43] Park, B., Won, J. and Yun, I. (2006), “Application of microscopic simulation model calibration and validation procedure: Case study of coordinated actuated signal system”, Transportation Research Record: Journal of the Transportation Research Board, vol. 1978, pp. 113–122.

[44] Payne, H.J. (1979), “FREFLO: A macroscopic simulation model of freeway traffic”, Transportation Research Record: Journal of the Transportation Research Board, vol. 722, pp. 68-77.

[45] PTV (2014), “VISSIM 7.00 User Manual”, PTV AG, Karlsruhe, Germany.

[46] Quadstone (2009), “Paramics user and reference manual version 6.6.1”, Quadstone Ltd., Edinburgh, UK.

[47] Sanjana, H. (2015), “Developing metanet-based macro traffic model for Dhaka city with modified link- specific and global driver parameters”, M. Sc. Engg. Thesis, Bangladesh University of Engineering Technology.

[48] Sanwal, K. K., Petty, K., Walrand, J. and Fawaz, Y. (1996), "An extended macroscopic model for traffic flow", Transportation Research Part B: Methodological, vol. 30(1), pp. 1-9.

[49] Schultz, G.G. and Rilett L.R. (2004), "Analysis of distribution and calibration of car following sensitivity parameters in microscopic traffic simulation models", Transportation Research Record: Journal of Transportation Research Board, vol. 1876, pp.41-51.

[50] Siam, M.R.K, Nasrin, S., Hadiuzzaman, M., Muniruzzaman, S.M. and Nazmul, H. (2017), "VISCAL: Heuristic algorithm based application tool to calibrate microscopic simulation parameters", Journal of the traffic and transportation engineering (English edition) 2018, vol 5(1), pp. 28-43.

[51] Siddharth, S. M. P. and Ramadurai, G. (2013), "Calibration of VISSIM for Indian heterogeneous traffic conditions", 2nd Conference of Transportation Research Group of India (2nd CTRG), Procedia - Social and Behavioral Sciences, vol. 104, pp. 380 – 389.

[52] Skabardonis, A. (1999), "Assessment of Traffic Simulation Models", University of California, Berkley, Institute of Transportation Studies.

[53] Spall, J.C. (1998), "Implementation of the simultaneous perturbation algorithm for stochastic optimization", IEEE Transactions on Aerospace and Electronic Systems, vol. 34 (3), pp. 817-823.

[54] Spall, J.C. (1992), "Multivariate stochastic approximation using a simultaneous perturbation gradient approximation", IEEE Transactions on Automatic Control, vol. 37 (3), pp. 332-341.

[55] Spiliopoulou, A., Kontorinaki, M., Papageorgiou, M. and Kopelias, P. (2014), "Macroscopic traffic flow model validation at congested freeway off-ramp areas", Transportation Research Part C: Emerging Technologies, vol. 41, pp. 18-29.

[56] Toledo, T. and Koutsopoulos, H.N. (2004), "Statistical validation of traffic simulation models", Transportation Research Record: Journal of the Transportation Research Board, vol. 1876, pp. 142–150

[57] Toledo, T. (2007), "Driving behavior: models and challenges", Transport Reviews, vol. 27(1), pp. 65-84.

[58] Transport Research Board (2000), "Highway Capacity Manual – HCM 2000", Transport Research Board, National Research Council, Washington, D.C., 2000.

[59] TSS (2002), "AIMSUN 4.1 user manual", TSS Transport Simulation System, Barcelona, Spain.

[60] Turley, C. (2007), “Calibration procedure for a microscopic traffic simulation model”, M. Sc. Engg. Thesis, Ira A. Fulton College of Engineering and Technology, Available at: http://scholarsarchive.byu.edu/etd/846, Accessed 17 April 2018.

[61] US Department of Transportation (2007), “NGSIM - Next Generation Simulation”, Available at http://www.ngsim.fhwa.dot.gov, Accessed 17 April 2018.

[62] Venkataraman, P. (2001), “Applied optimization with MATLAB programming”, John Wiley & Sons, Hoboken.

[63] Yeom, C., Rouphail, N. M., Rasdorf, W. and Schroeder, B. J. (2016), “Simulation guidance for calibration of freeway lane closure capacity”, Transportation Research Record: Journal of the Transportation Research Board, vol. 2553, pp. 82–89.

[64] Yu, L., Li, X. and Zhuo, W. (2006), “A Genetic Algorithm-based Approach to the Calibration of VISSIM Using GPS Data”, Advances in Transportation Studies an international Journal, vol. 8, pp. 57-69.

[65] Wang, Jian, S., Guanglin, H. and Xiaowei, D. (2013), “Optimization of transit operation strategies: Case Study of Guangzhou, China”, Transportation Research Board Annual Meeting, Paper #13-5002.

[66] Wilson, R.E. and Ward, J.A. (2011), “Car-following models: fifty years of linear stability analysis–a mathematical perspective”, Transportation Planning and Technology, vol. 34(1), pp. 3-18.

[67] Wu, N. (2002), “Application and verification of macroscopic and microscopic simulation models-case study for NETCELL and VISSIM on congested freeway”, Proceedings of the International Conference on Traffic and Transportation Studies, Beijing, China.

[68] Zhizhou, W., Jian, S. and Xiaoguang, Y. (2005). “Calibration of VISSIM for Shanghai Expressway using Genetic Algorithm”, Proceedings of the 2005 Winter Simulation Conference, pp. 2645-2648.

ANNEXURE A

RELATIONSHIP BETWEEN HEADWAY AND SPEED OBTAINED FROM MICROSCOPIC VEHICLE TRAJECTORY DATA

A relationship between headway and speed of following vehicle has been established by analyzing each pair of Leader-Follower vehicles trajectory data obtained from each VISSIM simulation output file. A comparison of such relationship pattern has been explained in following figure (Figure-A.1) considering one of the VISSIM simulated output files.

Linear Relationship	2nd Degree Polynominal Relationship	3rd Degree Polynominal Relationship

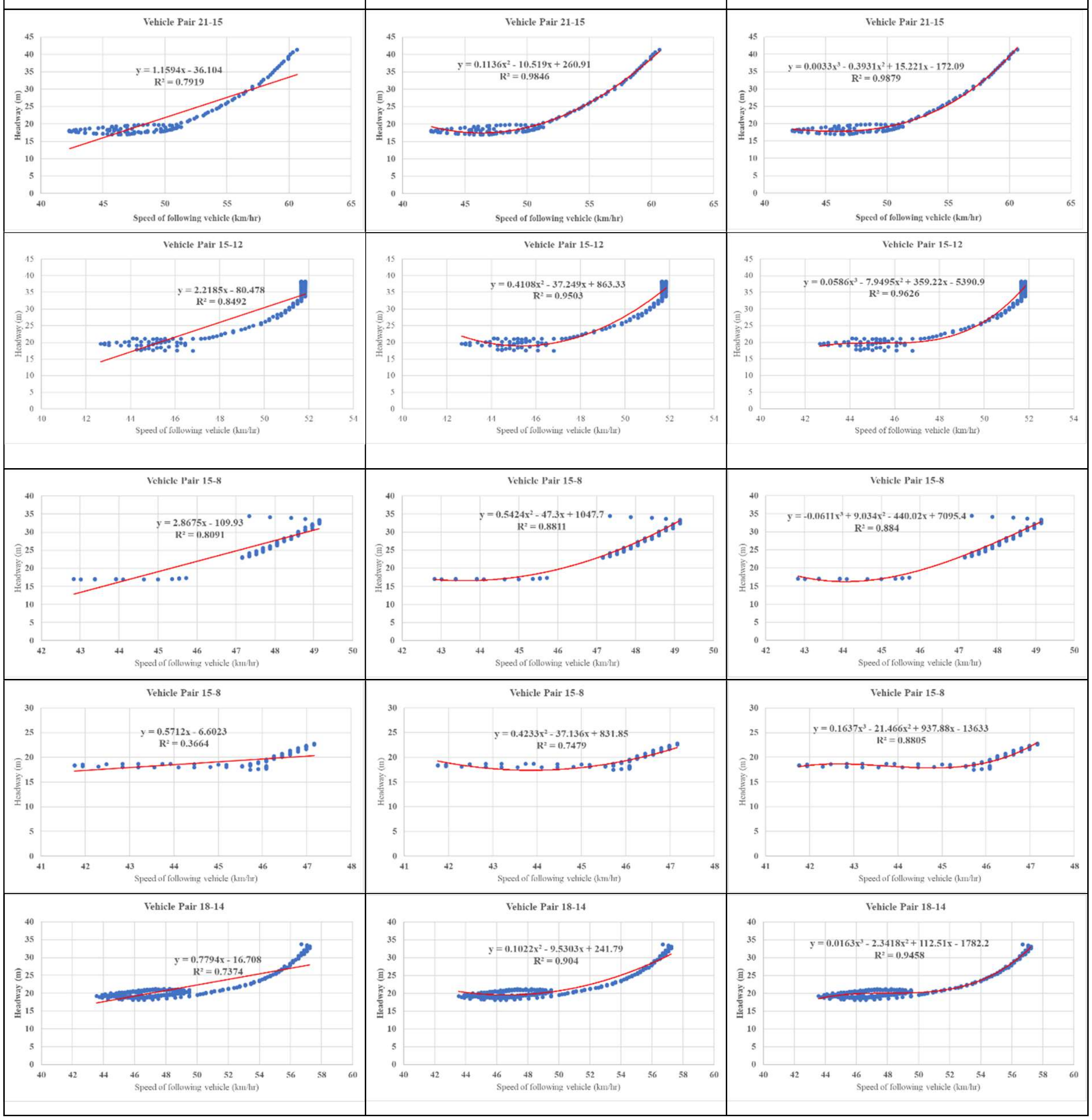

Figure A.1: Comparison of relationship between Headway and Speed

The coefficient values obtained from the mathematical equation derived from the relationship of headway and speed of each pair of Leader-Follower vehicle along with reliability values of one of the simulated output files is given in Table-A.1 and A.2.

Table A.1: Coefficient Values with Degree of Reliability (2nd Degree Polynomial)

a_0	a_1	a_2	R^2
0.0109	0.7392	-0.0056	89.67%
4.8717	-1.7846	0.0565	83.97%
0.8697	-1.155	0.0348	88.35%
0.111	-1.8205	0.0497	86.39%
0.6764	-2.1939	0.0664	91.12%
2.6267	-0.3804	0.0151	84.04%
-0.0616	3.0276	-0.0269	91.01%
1.9819	-0.3097	0.0148	84.45%
1.0168	0.1322	0.0055	85.02%
0.0624	0.3559	0.0031	84.31%
0.0387	-2.8108	0.081	97.76%
0.4372	0.1242	0.0096	88.36%
0.0104	0.2377	0.0045	89.79%
2.097	-1.5366	0.0445	89.09%
0.0285	0.5636	-0.003	89.37%
2.0591	-1.4378	0.0433	81.97%
-0.0636	0.4957	-0.0024	81.10%
0.0115	0.7672	-0.0095	87.77%
0.0418	0.6949	-0.0061	85.91%
-0.0013	0.9773	-0.0086	94.30%
0.738	-1.3008	0.045	83.87%
0.0017	0.7423	-0.0071	86.76%
0.0533	-0.4685	0.0207	88.19%
0.1061	-0.1601	0.0116	82.61%
-0.0619	0.1778	0.0062	80.95%
-0.0028	0.767	-0.0089	84.90%
0.003	0.5229	-0.0033	88.18%
2.0918	-0.9343	0.0316	91.08%
1.2321	-1.0474	0.0389	81.67%
0.0315	0.7644	-0.0066	90.68%
0.5354	-1.0602	0.0375	95.25%
0.2018	0.9747	-0.009	81.27%
0.0017	0.7961	-0.0066	95.84%
-0.0075	0.6493	-0.005	90.86%
0.218	-0.39	0.0147	84.50%
0.0251	0.5155	-0.0017	89.23%

Table A.2: Coefficient Values with Degree of Reliability (3rd Degree Polynomial)

a_0	a_1	a_2	a_3	R^2
-0.0003	2.9545	-0.0755	0.0005	88.62%
0.0047	12.2768	-0.6477	0.0088	97.73%
0.0159	9.6785	-0.4193	0.0047	89.17%
-0.2109	4.1395	-0.1821	0.0022	91.13%
-0.0067	18.5339	-0.7694	0.0081	88.64%
-0.0104	16.134	-0.6847	0.0075	96.49%
0.0015	18.4913	-0.829	0.0095	91.07%
-0.0011	17.0148	-0.7477	0.0084	84.23%
-0.0107	21.5584	-1.0467	0.013	97.08%
-0.0586	5.055	-0.1898	0.0019	89.24%
-0.0217	4.9633	-0.1905	0.002	97.45%
-0.001	1.5034	0.0231	-0.0004	90.81%
-0.0234	7.2047	-0.2832	0.003	95.75%
-0.0175	2.5927	-0.0903	0.0009	90.51%
-0.0019	6.8961	-0.2031	0.0016	88.46%
0.0008	2.2699	-0.1465	0.0025	97.65%
-0.0044	11.3269	-0.4315	0.0043	96.20%
0.0026	0.5895	-0.0106	0.0002	86.27%
0.0088	2.8665	-0.1244	0.0015	81.14%
0.0085	10.4862	-0.4834	0.0058	97.69%
0.0003	2.5431	-0.0942	0.001	90.87%
0.0038	15.9885	-0.7579	0.0092	96.37%
0.0015	-1.1448	0.0648	-0.0007	83.17%
-0.0001	3.8541	-0.1604	0.0018	82.81%
0.004	1.4262	-0.0339	0.0003	86.26%
-0.0009	0.9375	-0.0069	0	93.24%
0.0063	11.918	-0.6223	0.0084	96.40%
-0.0004	0.9762	-0.0185	0.0001	85.98%
0.0026	3.8356	-0.1284	0.0012	80.28%
0.0002	9.9744	-0.4471	0.0052	89.27%
-0.0009	16.9971	-0.7035	0.0074	94.88%
-0.0004	0.3407	0.0111	-0.0002	87.12%
0.0003	1.098	-0.0262	0.0002	86.20%
-0.033	4.9611	-0.226	0.0028	98.50%
0.0016	14.2726	-0.7483	0.0101	95.15%
0.0008	1.4978	-0.0349	0.0003	91.39%

a_0	a_1	a_2	R^2
0.0029	0.4596	-0.0001	85.43%
0.0256	0.5619	-0.0039	81.60%
0.0088	-1.1423	0.0387	96.36%
2.5235	-1.9616	0.062	81.31%
-0.0012	0.6779	-0.0054	88.21%
-0.002	0.8442	-0.0106	88.13%
11.4651	-0.5286	0.0172	88.89%
0.9058	-1.479	0.0493	92.25%
0.0164	-3.4845	0.0831	92.98%
14.7186	-1.2247	0.0324	92.59%
-0.0002	1.0114	-0.0159	89.11%
-0.0784	-1.7161	0.0418	80.66%
0.0302	0.6476	-0.0051	85.36%
0	10.5175	-0.2119	92.55%
0.3382	-0.8391	0.0247	92.38%
0.0053	-2.5727	0.0667	82.83%
4.0981	-3.6576	0.0976	84.89%
0.0166	-4.1375	0.1025	91.27%
0.7533	-0.9316	0.0319	83.85%
0.1926	-3.9649	0.1036	81.09%
4.2837	-1.8536	0.0588	90.83%
6.449	-1.3402	0.0381	93.20%
0.0351	0.6445	-0.0006	85.17%
0.0028	0.3766	0.001	85.01%
0.0103	0.7953	-0.0099	88.49%
0.0244	-1.538	0.044	92.29%
0.0317	-1.5187	0.0511	80.98%
0.3991	-2.3293	0.0626	98.06%
0.0088	0.5429	-0.0042	87.87%
0.0919	-3.1889	0.0913	95.57%
0.1503	-1.8508	0.0558	87.94%
0.3171	-8.0636	0.215	81.26%
0.0162	0.8243	-0.0101	85.32%
0.0039	0.6759	-0.0058	88.14%
0.0776	0.2008	0.006	91.17%
-0.0197	0.5583	-0.003	87.14%
0.0085	0.4722	-0.0022	81.33%
0.5143	-0.0414	0.0095	83.35%
0.271	-4.5717	0.1174	90.45%
0.0116	-2.9019	0.0857	91.59%
0.2478	0.9458	-0.0083	87.33%
-0.0879	0.6105	-0.0038	94.38%
0.0197	-0.1413	0.0198	80.30%
4.0656	-0.4335	0.0164	86.59%
0.2663	0.4275	-0.0005	85.58%

a_0	a_1	a_2	a_3	R^2
0.1241	13.4734	-0.7076	0.0096	92.99%
0.0093	7.002	-0.2954	0.0034	98.55%
0.0146	1.4935	-0.0419	0.0004	82.66%
0.0067	1.4038	-0.0299	0.0003	80.46%
0	2.1749	-0.0525	0.0004	90.98%
0.0001	-1.391	0.0864	-0.001	90.66%
0.0009	11.0558	-0.3894	0.0036	94.49%
0.0078	0.6633	-0.0078	0.0001	87.57%
0	19.6435	-0.9969	0.0131	86.90%
-0.0003	1.4215	-0.0509	0.0007	87.25%
0	15.955	-0.6859	0.0075	88.48%
0	3.6563	-0.195	0.0028	94.73%
0.0221	15.4907	-0.816	0.011	91.11%
-0.0519	2.3914	-0.0909	0.001	87.82%
-0.0004	4.9549	-0.2232	0.0027	80.65%
0	-29.2543	1.3416	-0.0152	89.20%
-0.0257	2.3278	-0.0886	0.001	96.05%
0.0032	6.1085	-0.3202	0.0045	98.53%
0.0961	-23.603	1.1045	-0.0124	81.15%
0	20.289	-0.8965	0.0101	92.48%
0.0475	3.3348	-0.1435	0.0018	99.15%
-0.0003	1.051	-0.0181	0	92.68%
0.0014	-31.0108	1.0289	-0.0083	81.67%
0.0001	1.3281	-0.035	0.0003	85.56%
-0.0018	9.1157	-0.396	0.0045	81.43%
-0.0148	7.9895	-0.3716	0.0047	83.15%
-0.0019	6.2563	-0.2507	0.0027	96.79%
0.0001	8.4055	-0.4064	0.0051	81.87%
-0.0491	23.4481	-1.1573	0.0145	95.29%
-0.0001	41.2135	-1.8872	0.0218	92.86%
-0.0023	11.4225	-0.5355	0.0065	96.94%
0.0127	4.1894	-0.2594	0.004	81.69%
0.0397	9.0618	-0.482	0.0067	98.96%
-0.0198	2.6742	-0.1009	0.0011	82.53%
0.0644	5.089	-0.2256	0.0027	99.31%
-0.0148	1.6995	-0.0533	0.0005	83.39%
-0.0006	6.8377	-0.2937	0.0035	85.46%
-0.174	30.3749	-1.4186	0.0167	83.48%
-0.007	21.9566	-0.9419	0.0104	82.19%
-0.2696	5.4542	-0.2216	0.0024	86.72%
-0.0009	6.3089	-0.2988	0.0038	83.80%
0.0059	0.3056	0.004	0	86.43%
-0.0001	3.5191	-0.1397	0.0015	80.80%
0.0004	10.6835	-0.4921	0.0059	93.50%
-0.2459	11.1088	-0.529	0.0065	85.76%

a_0	a_1	a_2	R^2
6.3802	-1.2579	0.0399	92.02%
-0.0011	0.5888	-0.0049	88.04%
0.2156	-5.2079	0.1445	95.67%
0.0002	-3.9417	0.0998	96.31%
0.0514	-4.2823	0.1119	92.44%
2.0246	-2.0555	0.067	80.81%
0.2792	0.6524	-0.0056	82.66%
0.1084	-2.8816	0.0725	85.15%
-0.0007	0.4877	-0.0022	88.30%
0.0104	0.7414	-0.0083	85.30%
-0.0006	0.6755	-0.0076	84.88%
0.0536	0.5939	-0.0032	93.55%
-0.0072	0.7358	-0.0082	88.95%
1.1178	-0.4588	0.0224	86.72%
0.0038	0.6958	-0.0063	81.86%
0.017	0.707	-0.0055	86.28%
0.0161	0.7133	-0.0061	88.13%
0.0317	-0.0886	0.0102	88.79%
0.0287	-1.4412	0.0378	92.93%
0.4454	-0.8001	0.0317	87.68%
0.0408	-3.3068	0.089	84.89%
0.1566	0.5246	-0.0019	81.98%
-0.0047	0.616	-0.0051	88.94%
0.5945	-1.9522	0.0609	93.85%
-0.0061	0.4988	-0.0029	85.12%
0.3323	-0.965	0.0276	90.82%
0.1661	-3.4049	0.099	97.31%
0.7637	-0.8179	0.0241	84.69%
2.0521	-1.5741	0.0449	90.48%
0.4207	-1.4079	0.0305	91.86%
0.0645	-1.1339	0.038	93.82%
0.0064	-2.8124	0.0734	91.10%
5.5536	-1.7685	0.0558	81.51%
0.0046	0.638	-0.0051	82.93%
2.1454	-0.0507	0.0093	87.63%
-0.0077	0.6705	-0.0062	83.68%
-0.0343	0.4111	-0.0009	83.08%
-0.0056	0.5614	-0.003	86.70%
0.4034	0.512	-0.0023	89.64%
0.186	-1.0318	0.0387	80.16%
0.2011	0.7754	-0.0072	87.65%
0.0193	0.4976	-0.0016	81.83%
0.2578	0.3511	0.0013	91.92%
0.0377	0.9111	-0.0075	85.07%
-0.0129	0.6092	-0.0037	80.55%

a_0	a_1	a_2	a_3	R^2
-0.0112	40.144	-1.8946	0.0225	90.12%
0.0022	4.8757	-0.2348	0.0031	98.85%
-0.0003	1.2252	-0.0333	0.0003	84.37%
0.0037	3.9018	-0.2411	0.0039	96.16%
0.0012	21.973	-1.0788	0.0135	94.29%
-0.0151	12.8592	-0.6809	0.0093	92.70%
-0.0027	89.0094	-4.4734	0.0566	83.87%
0.0011	16.0788	-0.8547	0.0116	94.57%
-0.1442	2.4264	-0.0987	0.0012	83.13%
-0.0002	4.9681	-0.2027	0.0022	85.94%
-0.0014	14.545	-0.6514	0.0075	90.78%
-0.0011	0.8947	-0.0166	0.0001	85.42%
0.0006	5.4501	-0.2448	0.003	91.98%
0.0015	8.7118	-0.4063	0.0049	90.03%
0.0036	0.0694	0.0188	-0.0002	82.39%
0	0.9999	-0.0275	0.0003	80.91%
0.0039	4.1587	-0.1848	0.0022	89.83%
-0.0023	28.0058	-1.2614	0.0146	93.69%
0.0002	2.0532	-0.1515	0.0028	91.49%
-0.0087	5.231	-0.2291	0.0028	94.25%
0.0002	-0.5326	0.0444	-0.0005	95.70%
-0.0341	4.8273	-0.1903	0.002	82.92%
0.0003	12.7329	-0.65	0.0087	82.39%
-0.0896	4.1135	-0.1583	0.0017	96.99%
-0.0078	1.3224	-0.0374	0.0004	87.38%
0.0645	4.872	-0.242	0.0033	99.06%
-0.0001	0.2205	0.0147	-0.0003	87.84%
-0.0008	39.2446	-1.9812	0.0254	98.33%
0	-3.4386	0.0786	0.0002	96.31%
-0.0005	40.5633	-1.7875	0.0201	93.40%
0.0007	19.0467	-1.0316	0.0143	94.93%
-0.0024	20.3968	-1.101	0.0152	97.02%
-0.003	2.5836	-0.0769	0.0007	87.62%
0.0007	33.8572	-1.5102	0.017	90.31%
-0.0002	0.3998	0.0016	0	85.87%
-0.1069	3.5711	-0.1612	0.002	91.41%
-0.0002	2.3551	-0.0773	0.0007	85.59%
-0.0004	0.6348	-0.0053	0	86.12%
-0.0019	0.7645	-0.0102	0.0001	90.45%
0	-1.2384	0.0782	-0.0009	86.35%
0.0126	4.9324	-0.2445	0.0033	98.20%
0	1.0649	-0.0242	0.0002	80.90%
0.0018	1.611	-0.0402	0.0003	87.23%
-0.0003	1.9409	-0.0603	0.0006	86.56%
-0.0038	28.3487	-1.2173	0.0132	88.02%

a_0	a_1	a_2	R^2
0.0571	0.7247	-0.0062	84.73%
0.0946	0.1542	0.0056	80.21%
0.1748	-4.3236	0.1017	85.82%
-0.003	0.167	0.0036	93.76%
0.0196	0.4573	-0.0004	88.23%
0.0542	0.941	-0.0072	81.61%
0.0128	0.7371	-0.0073	84.06%
0.0481	1.1685	-0.0138	90.36%
0.0061	0.8965	-0.0075	82.44%
0.0073	0.6067	-0.004	92.00%
0	2.9142	-0.0311	93.95%
0.5158	-0.393	0.0209	90.30%
3.3175	-0.4757	0.0188	90.02%
0.609	0.425	-0.0001	87.79%
0.0126	-3.2496	0.0799	91.30%
11.2378	-1.0813	0.0259	87.36%
1.2919	0.0058	0.0129	83.74%
0.3778	0.2846	0.0033	85.38%
3.327	0.3278	0.0007	80.32%
0.3743	0.1551	0.0056	87.54%
0.4053	-0.8107	0.0256	86.52%
0.006	-3.4161	0.0712	85.77%
-0.0063	0.713	-0.008	83.64%
0.1307	-0.851	0.0332	98.93%
1.7887	0.4566	-0.0015	81.46%
-0.1244	0.4091	0.0004	93.35%
0.1153	-2.8082	0.083	86.80%
0.0656	-0.6017	0.0221	89.05%
0.1692	-2.7496	0.0782	96.92%
0.0882	0.2953	0.0072	95.82%
0.0647	0.3607	0.0012	82.56%
0.7804	-5.1074	0.1374	88.20%
0.0155	0.776	-0.0089	90.28%
0.0052	-1.623	0.0464	89.47%
0.0014	0.8115	-0.0111	81.26%
2.1697	-1.563	0.053	89.53%
5.2128	-1.2561	0.0386	92.86%
0.0495	-0.6702	0.0261	91.64%
11.2275	-2.1918	0.0591	85.32%
1.1721	-1.7323	0.0478	97.08%
0.2654	-1.3499	0.0448	86.83%
0	3.9719	-0.0504	82.08%
-0.0084	0.8614	-0.0129	92.49%
2.7719	-0.3399	0.0172	88.35%
0.0682	-1.8307	0.0468	86.50%

a_0	a_1	a_2	a_3	R^2
-0.002	23.4563	-1.2062	0.0158	92.36%
0.0013	6.4861	-0.2516	0.0026	91.48%
0	35.4732	-1.4011	0.014	94.88%
-0.0035	4.6582	-0.1731	0.0018	89.10%
-0.0053	14.8456	-0.7586	0.0099	89.33%
0.007	4.5803	-0.2241	0.003	92.09%
0.0005	12.0347	-0.6078	0.0079	87.29%
0	0.1748	0.012	-0.0002	87.09%
0.0151	3.6963	-0.1771	0.0025	94.56%
0.0003	0.1362	0.0113	-0.0001	83.02%
-0.002	11.1974	-0.4337	0.0044	95.58%
0.0014	7.5173	-0.388	0.0054	97.89%
0.0085	10.5376	-0.4172	0.0043	96.33%
0.0048	11.6167	-0.5241	0.0061	97.88%
0.0099	2.2431	-0.0768	0.0008	92.53%
0.0009	9.2743	-0.4557	0.0058	96.86%
-0.0028	12.6317	-0.4845	0.0048	88.75%
0	35.7941	-1.6408	0.019	91.46%
-0.0076	26.3004	-1.224	0.0144	91.61%
-0.0406	18.1307	-0.8035	0.0091	90.72%
0.011	15.1996	-0.8199	0.0114	85.44%
-0.0003	1.9027	-0.0709	0.0008	84.79%
0.1329	5.4061	-0.2894	0.0042	85.99%
1.1462	1.0037	-0.024	0.0002	82.84%
0.0003	2.2459	-0.0717	0.0007	82.93%
-0.0382	3.7805	-0.1401	0.0015	97.56%
-0.0003	-1.1815	0.0666	-0.0007	84.51%
0.003	-0.6916	0.0426	-0.0004	82.50%
0.0003	0.1129	0.0147	-0.0002	87.39%
-0.041	1.0588	-0.0224	0.0002	88.54%
-0.0079	21.5376	-1.1919	0.0168	88.82%
0.0008	11.3576	-0.6018	0.0083	93.04%
0.0027	8.9703	-0.4734	0.0065	85.95%
-0.0313	0.8795	-0.012	0.0001	88.76%
0.002	0.7652	-0.0122	0.0001	80.58%
-0.0035	2.2637	-0.0719	0.0007	94.07%
0.0023	1.2081	-0.0213	0.0002	86.99%
-0.0425	0.7714	-0.0082	0	83.17%
-0.0014	7.4261	-0.3369	0.004	87.92%
-0.001	40.5012	-1.7314	0.0187	89.81%
0	-0.6108	0.0291	-0.0002	94.53%
0.0056	0.5631	-0.0056	0.0001	89.16%
-0.0048	2.8715	-0.0966	0.001	82.33%
-0.0004	4.27	-0.1742	0.002	85.62%
-0.0009	17.574	-0.8342	0.0101	82.34%

a_0	a_1	a_2	R^2
0.0291	-1.6901	0.0442	98.99%
0.0003	5.404	-0.0613	99.85%
0.0116	-3.2778	0.0752	96.96%
0.0158	-2.999	0.0892	96.94%
0.67	-0.2966	0.0166	82.89%
0.0134	-3.1588	0.0923	92.86%
0.1997	-0.0641	0.0083	90.67%
0	-3.3418	0.0989	86.76%
0.0566	-1.6957	0.0536	92.55%
-0.0037	-1.6206	0.0498	83.22%
0.2415	-0.1722	0.0154	90.80%
0.057	-0.8268	0.0346	92.38%
0.0083	-2.3088	0.0665	94.29%
0.0006	0.807	-0.0105	91.63%
-0.0042	0.8605	-0.0123	86.76%
0.0013	0.785	-0.0096	88.49%
0.0005	0.5039	-0.0016	89.11%
0.0077	0.3772	0.0006	85.99%
0.0376	0.5731	-0.0047	86.40%
0.5493	-0.233	0.015	84.04%
0.0069	0.6804	-0.006	81.16%
6.6356	-0.0338	0.0086	80.19%
0.0145	0.7339	-0.0083	92.00%
0.0133	0.6661	-0.0063	81.83%
-0.0086	0.5932	-0.0031	84.70%
0.003	-3.3468	0.0845	92.09%
-0.0053	0.7517	-0.0073	85.69%
0.3166	1.0187	-0.0103	88.23%
0.038	1.2218	-0.014	94.21%
0.0611	0.5311	-0.0024	84.41%
0.273	0.5253	-0.0025	92.49%
0.0252	-0.1545	0.0109	94.22%
21.15	-1.3809	0.0297	81.78%
0.1572	0.5788	-0.0036	85.95%
0	2.6376	-0.0367	89.03%
0	2.9599	-0.0327	80.95%
6.1623	-0.6211	0.0218	80.10%
0.0452	-2.2911	0.0666	97.90%
7.585	-1.7721	0.0497	93.45%
0.1924	-2.6157	0.0802	95.83%
0.0026	0.8645	-0.0127	84.28%
-0.0029	1.6963	-0.0195	97.84%
0.7952	-2.602	0.0739	95.35%
0.12	0.4815	-0.0028	85.71%
0.0021	0.7584	-0.0087	86.86%

a_0	a_1	a_2	a_3	R^2
0.001	10.8847	-0.5568	0.0074	93.00%
-0.0079	12.18	-0.6202	0.0082	82.04%
0.0001	3.6047	-0.1284	0.0013	90.80%
-0.0002	1.348	-0.0275	0.0002	83.44%
-0.0042	6.5541	-0.2705	0.003	86.17%
0	1.6377	-0.05	0.0005	90.27%
0.0617	13.3455	-0.6774	0.0089	80.83%
-0.0068	7.4893	-0.351	0.0044	97.15%
-0.0446	1.9725	-0.0729	0.0008	83.35%
-0.0206	16.6676	-0.7454	0.0085	97.30%
-0.0028	4.596	-0.185	0.002	98.74%
-0.0322	1.9429	-0.0679	0.0007	92.65%
-0.0121	23.0303	-0.956	0.0101	84.86%
0.0006	1.6065	-0.1122	0.0019	92.06%
-0.0767	4.2616	-0.1659	0.0018	94.40%
-0.0136	7.9016	-0.3101	0.0033	92.07%
-0.0077	2.9151	-0.11	0.0012	89.87%
-0.2153	1.6833	-0.0466	0.0004	83.74%
0.0098	0.8483	-0.0134	0.0001	80.54%
-0.0054	3.8984	-0.1434	0.0015	90.25%
0.0079	3.055	-0.1307	0.0016	88.97%
-0.0055	23.2693	-1.2821	0.018	82.51%
0	36.5267	-1.3841	0.0133	87.85%
0.0006	1.9297	-0.0806	0.0012	99.25%
-0.0277	1.9545	-0.0563	0.0005	91.02%
-0.1279	3.4058	-0.1288	0.0014	89.93%
0.0654	0.0097	0.0167	-0.0002	95.99%
0.0107	3.4118	-0.216	0.0036	88.22%
0.0011	6.129	-0.2727	0.0032	89.73%
0.0055	3.2786	-0.1935	0.0031	97.53%
0.0001	6.8714	-0.3013	0.0036	97.68%
-0.0024	13.3151	-0.7251	0.0102	93.65%
-0.0007	9.1005	-0.4776	0.0065	90.00%
-0.012	31.2104	-1.5455	0.0195	91.44%
-0.0004	3.7113	-0.1441	0.0016	83.76%
0.0001	10.1656	-0.4782	0.0058	92.55%
0.0009	0.852	-0.0131	0	82.63%
-0.0041	11.0966	-0.5823	0.0079	88.29%
0.0168	10.9308	-0.5809	0.008	98.01%
-0.0083	35.2266	-1.9231	0.0265	89.04%
0.0776	3.9678	-0.1896	0.0025	99.15%
0.0003	10.9791	-0.5215	0.0064	92.79%
-0.1565	10.5152	-0.5112	0.0064	91.71%
0.0132	3.9264	-0.1843	0.0024	99.20%
-0.0017	2.0268	-0.0805	0.001	82.35%

a_0	a_1	a_2	R^2
3.5876	-1.5701	0.0386	91.52%
0.4077	-2.2946	0.057	96.79%
10.6659	-2.6732	0.0787	85.26%
0	0.831	-0.0073	91.52%
0.0027	0.7594	-0.0078	93.44%
0.0145	0.6452	-0.006	86.33%
0.0581	-3.3527	0.0936	95.80%
1.2989	-3.7529	0.0995	91.64%
0.0008	0.7637	-0.0083	92.50%
0.8163	-1.425	0.0363	82.49%
0.0047	0.6672	-0.0057	80.82%
4.3559	-2.9276	0.0882	88.53%
-0.0201	0.8439	-0.0109	92.41%
1.2061	-1.0957	0.0352	97.55%
0.055	-2.6368	0.0706	89.97%
-0.0441	0.7646	-0.0073	86.97%
8.2835	0.094	0.0036	86.86%
2.6108	-0.3739	0.018	88.01%
0.0048	-3.1479	0.0775	92.65%
2.7231	-1.7076	0.0407	94.47%
0.009	0.8973	-0.0112	93.31%
0.0104	-4.8411	0.1138	82.92%
0.7217	-2.7516	0.0714	89.95%
0	5.7266	-0.0999	80.68%
0.0766	0.403	0.0005	88.72%
0.0094	-3.3568	0.0974	85.16%
0.0237	-2.4081	0.0685	96.55%
0.0407	0.5652	-0.0029	81.28%
0.0075	-0.3439	0.02	95.15%
0.0079	-3.1948	0.0946	81.64%
0.0116	1.0203	-0.0087	85.57%
0.0768	-4.7912	0.0944	85.02%
0.1757	-0.4954	0.0166	89.93%
0.063	-3.4897	0.0978	96.84%
-0.001	0.7157	-0.0065	88.75%
0.0133	-6.2697	0.1535	83.57%
0.2423	-1.5789	0.0475	96.89%
6.7656	-0.9773	0.0327	92.49%
0.2096	0.5239	-0.0035	81.25%
0.9375	-1.2039	0.0339	93.96%
1.0117	0.2564	0.0035	84.69%
-0.0068	0.3901	-0.0006	83.44%
-0.0032	-1.5179	0.0411	92.89%
0.0368	0.5059	-0.0017	86.55%
0.3336	0.6171	-0.004	92.39%

a_0	a_1	a_2	a_3	R^2
0.0058	8.8375	-0.439	0.0057	89.22%
-0.0002	-1.598	0.1278	-0.002	93.09%
-0.0152	4.4549	-0.2034	0.0025	96.91%
0.0032	3.3271	-0.1587	0.002	84.86%
-0.0021	-0.2656	-0.0079	0.0005	99.07%
0	11.8092	-0.3581	0.0034	99.66%
0.0002	4.1828	-0.2055	0.0026	96.70%
0.0004	4.1114	-0.2436	0.0039	96.07%
0	14.4314	-0.6951	0.0086	96.26%
-0.0083	6.3881	-0.2909	0.0035	92.72%
0.0006	5.6141	-0.3348	0.0052	93.07%
0	7.7779	-0.2774	0.0026	97.63%
-0.0012	7.7877	-0.3645	0.0045	87.04%
0.0006	12.3604	-0.6378	0.0085	93.85%
0	-23.7958	1.078	-0.0119	83.31%
0.0002	-2.0292	0.1497	-0.0023	80.24%
0.0024	5.6816	-0.2908	0.004	96.25%
0.0002	14.2814	-0.7791	0.0109	92.33%
0.0001	13.4443	-0.655	0.0083	94.93%
-0.0022	14.5793	-0.7725	0.0105	92.31%
-0.0005	1.0963	-0.0252	0.0002	90.76%
-0.0025	12.8926	-0.5876	0.0069	83.93%
-0.0001	1.144	-0.0267	0.0002	81.17%
0	11.807	-0.5128	0.0058	89.11%
-0.0001	7.1007	-0.311	0.0036	84.10%
-0.0004	4.4224	-0.1912	0.0023	85.85%
-0.0068	6.7212	-0.2886	0.0033	93.15%
-0.2167	2.5777	-0.1049	0.0013	91.89%
0.0004	1.5951	-0.0503	0.0005	86.01%
-0.0013	0.3564	0.0075	-0.0001	82.06%
0	16.4909	-0.7779	0.0094	91.88%
-0.0002	-0.0761	0.0319	-0.0005	82.76%
-0.0192	2.356	-0.0804	0.0009	89.00%
0.0003	2.7239	-0.0804	0.0007	94.78%
0.0025	1.3256	-0.0378	0.0004	84.52%
0.033	1.4058	-0.0498	0.0006	87.76%
0.002	2.4989	-0.0933	0.001	90.70%
-0.5978	4.2206	-0.1738	0.002	91.58%
-0.0049	2.7508	-0.1122	0.0013	89.10%
-0.1404	4.206	-0.186	0.0023	95.80%
0.0006	2.2313	-0.1331	0.0022	98.09%
0.0191	4.097	-0.1915	0.0025	97.60%
0.0028	9.2647	-0.5145	0.0074	96.19%
0	1.412	-0.0436	0.0004	86.82%
0	-4.9867	0.2811	-0.0034	98.13%

a_0	a_1	a_2	R^2
0.6153	0.6831	-0.0027	83.90%
1.8253	0.0879	0.0053	84.20%
0.0402	-2.2247	0.0679	94.82%
1.1244	0.0255	0.0078	96.23%
9.9063	-1.1793	0.0365	80.71%
0.0912	-5.9855	0.169	86.68%
0.0136	-3.9876	0.1172	84.04%
0	2.7897	-0.0367	97.91%
0.3068	-0.0075	0.0111	81.03%
1.037	0.2935	0.0038	90.27%
9.7692	-0.6325	0.0201	94.59%
0.0481	-2.3079	0.0625	94.12%
0.0045	-3.423	0.0929	96.78%
0.0579	0.2358	0.0041	83.90%
0.1139	-4.446	0.1196	94.62%
0.0343	-2.3242	0.0717	93.97%
0.0149	-5.2875	0.1431	84.75%
0	3.5517	-0.0413	81.67%
3.5569	-1.4993	0.0464	97.10%
0.0349	0.6798	-0.0068	88.63%
0.094	0.2769	0.0025	85.27%
0.0125	-3.3278	0.0796	88.73%
0.0178	-2.4125	0.0484	95.75%
0.1265	0.3508	0	82.53%
0.0434	-1.2647	0.0336	96.57%
0.0632	0.6278	-0.0044	92.64%
0.7827	-0.5326	0.022	87.87%
0.0802	-1.4523	0.0376	96.98%
0.1185	-3.0015	0.0856	96.92%
10.1701	-3.6989	0.1032	82.16%
-0.0193	-1.3388	0.0398	81.23%
0.0009	1.0187	-0.0107	86.58%
0.1665	0.732	-0.0038	92.85%
0.0132	-2.8559	0.0679	97.11%
0	4.1765	-0.0666	93.30%
0.0347	-3.058	0.0841	97.62%
0.0305	-5.4931	0.1274	91.59%
0.0313	-1.7501	0.0579	92.77%
1.4934	0.1516	0.0064	80.07%
10.8282	-1.3137	0.0341	88.69%
0.0153	-7.0353	0.1586	82.16%
0.0872	-2.6039	0.0698	96.99%
1.0063	-1.0562	0.0344	82.87%
0.1	-3.8677	0.0866	96.09%
2.3617	-0.3901	0.0178	86.40%

a_0	a_1	a_2	a_3	R^2
0.004	7.7355	-0.3994	0.0054	98.48%
-0.0009	1.9394	-0.0668	0.0007	86.81%
0	1.3818	-0.0357	0.0003	88.57%
0.0288	7.5038	-0.3019	0.0032	99.26%
0.0096	4.6933	-0.2106	0.0026	98.13%
-0.0075	19.7627	-1.0953	0.0155	94.29%
-0.0149	12.5189	-0.6793	0.0095	94.65%
0.0021	16.6638	-0.8969	0.0124	84.58%
-0.0002	0.8576	-0.0086	0	93.44%
-0.3793	6.9811	-0.3449	0.0045	90.66%
-0.0003	1.7565	-0.0491	0.0004	92.87%
0.0003	1.5474	-0.0468	0.0005	86.31%
0.0004	7.3892	-0.3895	0.0054	96.25%
-0.0132	12.8974	-0.6149	0.0076	93.88%
0.0001	1.072	-0.0226	0.0002	92.45%
0.0328	2.1548	-0.0953	0.0012	82.60%
-0.0023	14.1917	-0.7737	0.0109	97.99%
0	-4.7283	0.2676	-0.0035	88.45%
-0.0039	16.4847	-0.8844	0.0122	87.87%
0.0118	2.3473	-0.112	0.0016	99.10%
0.0006	8.2877	-0.4089	0.0053	90.43%
-0.0017	-0.0345	0.0303	-0.0004	85.19%
-0.4728	1.4837	-0.0435	0.0004	92.27%
-0.0048	4.3457	-0.1935	0.0024	98.78%
0.0002	17.0545	-0.821	0.0101	89.99%
0.0001	4.5656	-0.2486	0.0034	91.03%
-0.0289	6.0056	-0.2392	0.0025	99.31%
-0.0003	2.2208	-0.0728	0.0007	93.82%
0	147.7799	-6.0862	0.063	84.80%
-0.007	16.8331	-0.7713	0.009	95.63%
-0.0007	2.8147	-0.106	0.0012	91.02%
-0.0004	14.9055	-0.5829	0.0058	86.75%
0	39.0054	-2.0125	0.0263	87.78%
0.0004	4.7493	-0.254	0.0036	96.83%
-0.0002	10.1519	-0.5031	0.0065	89.98%
0.0002	3.0821	-0.0968	0.0009	82.91%
-0.0007	1.8946	-0.0761	0.001	94.63%
0.0002	13.4995	-0.6376	0.0078	83.48%
0	37.5123	-1.8898	0.0242	81.90%
-0.0014	1.6471	-0.0338	0.0003	85.28%
0.0007	24.0331	-0.8894	0.0084	86.51%
-0.0043	6.7087	-0.2543	0.0025	92.88%
0.0013	4.2279	-0.2545	0.004	97.40%
-0.0006	0.6834	-0.0051	0	89.85%
0	101.593	-4.5269	0.0508	87.16%

a_0	a_1	a_2	R^2
0.0376	-3.0874	0.0809	94.66%
0.0477	-2.7564	0.0573	95.83%
8.1424	-0.0024	0.0055	81.23%
0.0257	0.4849	-0.0016	85.79%
1.4955	-0.5978	0.0216	84.87%
0.1636	-1.1983	0.0418	80.25%
0.092	-2.3959	0.066	95.66%
4.866	-1.2195	0.0315	88.14%
5.2415	-0.4199	0.0176	96.09%
19.0898	-1.044	0.0214	93.35%
0	7.7603	-0.1084	99.18%
-0.0047	8.3555	-0.1501	93.98%

a_0	a_1	a_2	a_3	R^2
-0.0034	7.4514	-0.339	0.0041	98.49%
0.1142	3.6094	-0.1777	0.0024	99.18%
0.0014	3.4407	-0.1519	0.0019	89.95%
-0.0073	6.7969	-0.2884	0.0032	98.64%
-0.1164	2.7335	-0.0958	0.001	87.57%
-0.0112	4.1081	-0.1579	0.0017	96.13%
0	-44.698	1.6667	-0.0153	91.85%
0.0009	1.0405	-0.0251	0.0003	87.27%
0.006	1.6783	-0.043	0.0004	95.33%
-0.0202	2.2093	-0.065	0.0006	86.33%
-0.1451	11.5873	-0.5894	0.0077	92.48%
-0.0746	1.9472	-0.0671	0.0007	91.04%
-0.002	9.7785	-0.4889	0.0064	87.53%
0.0004	5.7973	-0.3186	0.0046	96.27%
0.0082	1.7955	-0.0552	0.0006	98.84%
0.0391	5.3529	-0.2708	0.0037	88.55%
0.0015	37.6796	-2.0339	0.0278	87.32%
-0.044	50.1603	-2.7491	0.0379	91.81%
0.0006	14.126	-0.8063	0.0118	84.61%
0.0005	10.6149	-0.5167	0.0065	88.39%
0	6.1153	-0.2998	0.0039	89.99%
-0.0121	2.5584	-0.1073	0.0014	95.79%
-0.0031	9.6487	-0.5155	0.0072	86.82%
0.1454	1.7716	-0.0714	0.0009	99.46%
0.0002	17.7098	-0.8267	0.0099	94.35%
0.0006	-1.6673	0.0161	0.0008	96.54%
0	10.337	-0.4724	0.0056	87.02%
0.0002	18.8706	-0.9441	0.0121	95.46%
0.0004	9.3079	-0.509	0.0072	94.84%
0.0004	19.634	-0.9969	0.013	86.47%
0.0176	2.3925	-0.1152	0.0017	99.08%
1.1774	2.8368	-0.1253	0.0016	83.25%
-0.0006	3.1197	-0.1173	0.0012	87.40%
-0.0008	8.9697	-0.4048	0.0048	94.28%
0.0005	10.3176	-0.4752	0.0056	87.49%
0.0001	14.4005	-0.5137	0.0047	97.02%
-0.0424	8.6853	-0.3378	0.0034	92.86%
0.001	2.5772	-0.1162	0.0015	96.66%
0.0012	3.979	-0.1317	0.0012	91.74%
-0.0027	6.2156	-0.2885	0.0036	97.43%
0.0007	8.4577	-0.354	0.0039	97.47%
0.1375	11.262	-0.594	0.0081	82.30%
0.001	8.1868	-0.4244	0.0058	97.55%
0.0248	13.1038	-0.6451	0.0082	84.15%
-0.2595	31.5119	-1.6492	0.0218	93.91%

a_0	a_1	a_2	R^2

a_0	a_1	a_2	a_3	R^2
0.0003	-8.8968	0.3556	-0.0033	81.07%
-0.0038	29.1322	-1.2407	0.0134	94.62%
0	1.1868	-0.0193	0.0001	83.89%
-0.0034	3.142	-0.1185	0.0014	93.69%
0.0001	0.4466	-0.057	0.0012	97.17%
-0.0379	13.1638	-0.5816	0.0066	94.52%
0.0077	6.6314	-0.3148	0.004	80.16%
0.0012	3.5373	-0.1906	0.0029	97.46%
-0.0001	54.1257	-2.2777	0.0242	93.01%
0.0003	10.5874	-0.5756	0.0081	93.92%
-0.0087	4.8953	-0.1953	0.0021	97.39%
0.3442	3.4629	-0.1407	0.0016	92.15%
-0.0001	81.403	-3.4521	0.0368	86.86%
0.0008	7.598	-0.366	0.0046	97.89%
0.0045	10.9943	-0.5106	0.0061	97.96%
-0.0003	14.3107	-0.5853	0.0062	96.62%
-0.018	4.8633	-0.2036	0.0023	96.37%
0.0015	9.3391	-0.4649	0.006	96.30%
0.0005	11.7065	-0.4436	0.0043	96.88%
0	5.3376	-0.2611	0.0034	94.98%
-0.6291	2.1254	-0.0642	0.0006	89.48%
0.0643	9.0021	-0.4818	0.0067	81.31%
0.0867	7.5477	-0.3931	0.0054	83.50%
-0.0003	6.8587	-0.289	0.0032	83.17%
0.0045	5.6772	-0.2491	0.0029	86.61%
-0.0108	5.4527	-0.2412	0.0028	94.26%
0.0008	14.5273	-0.7494	0.0099	90.19%
-0.0002	9.2542	-0.4333	0.0053	96.73%
0.0385	3.3779	-0.1368	0.0015	92.30%
0.1508	1.5178	-0.0544	0.0007	99.47%
-0.3469	1.6941	-0.0536	0.0006	96.99%
0.0018	-53.9113	1.8772	-0.0158	80.35%
-0.0001	-3.7332	0.4529	-0.0075	94.12%

Values of coefficient a_0, a_1, a_2 and a_3 are plotted against the average density of respective pair of Leader-Follower vehicle along the roadway. Box plot was used to define data population within the range of 0.75 and 0.50 quartiles. The comparative improvement of curve fitting after removal of noisy data for 2nd degree and 3rd degree polynominal relation between each coefficient and the average density is shown in Figure A.2 and A.3.

<table>
<tr><th>Coefficient</th><th>2nd Degree Polynominal Relationship</th><th>2nd Degree Polynominal Relationship after Noise Removal</th></tr>
<tr><td>a_0</td><td>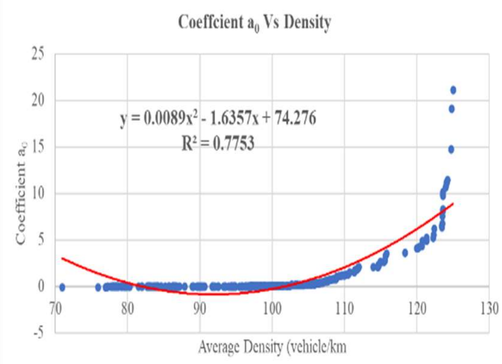
</td><td>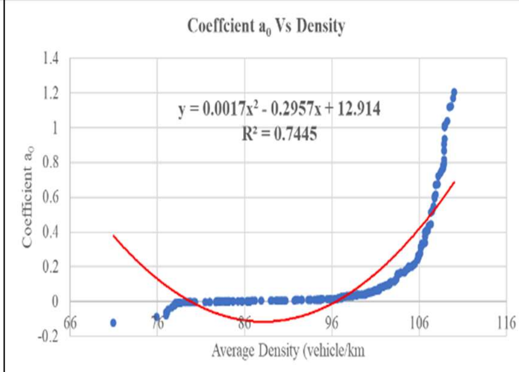
</td></tr>
<tr><td>a_1</td><td>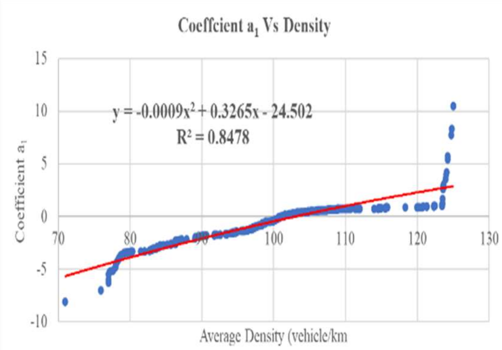
</td><td>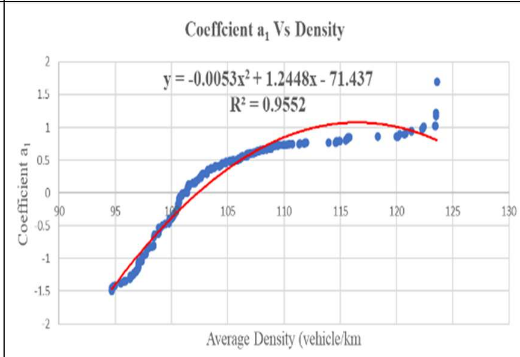
</td></tr>
<tr><td>a_2</td><td>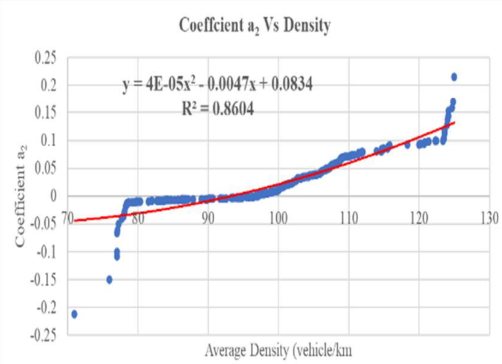
</td><td>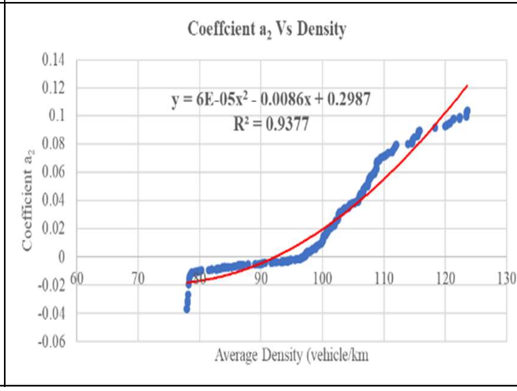
</td></tr>
</table>

Figure A.2: 2nd Order Polynominal Relationship

<table>
<tr><th>Coefficient</th><th>3rd Degree Polynominal Relationship</th><th>3rd Degree Polynominal Relationship after Noise Removal</th></tr>
<tr><td>a0</td><td>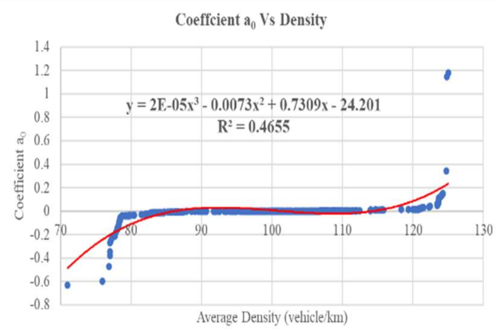
</td><td>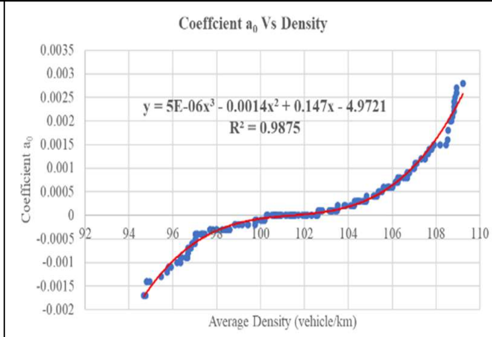
</td></tr>
<tr><td>a1</td><td>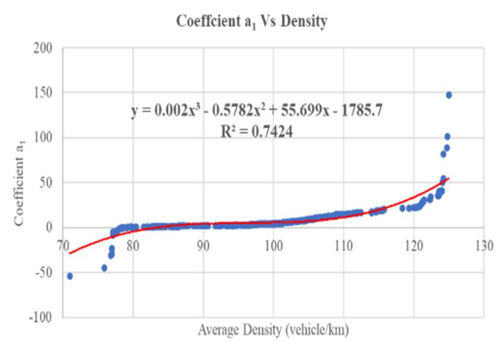
</td><td>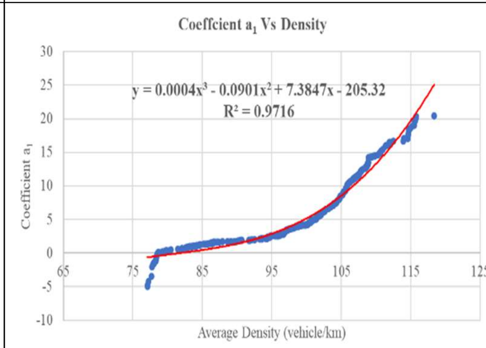
</td></tr>
<tr><td>a2</td><td>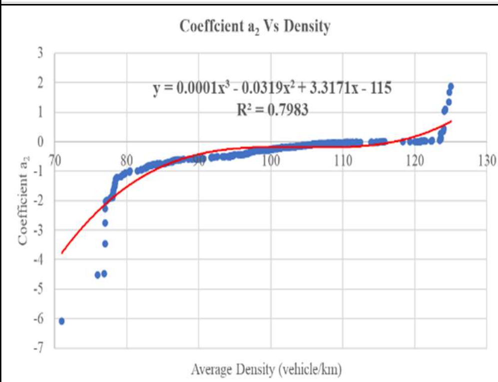
</td><td>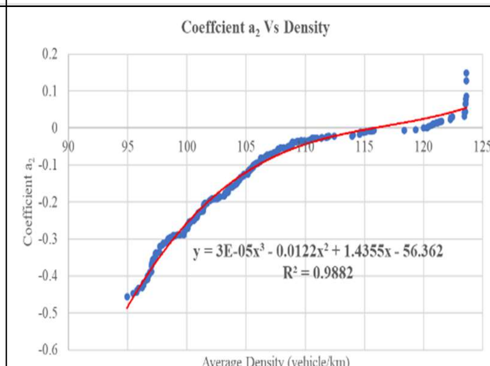
</td></tr>
<tr><td>a3</td><td>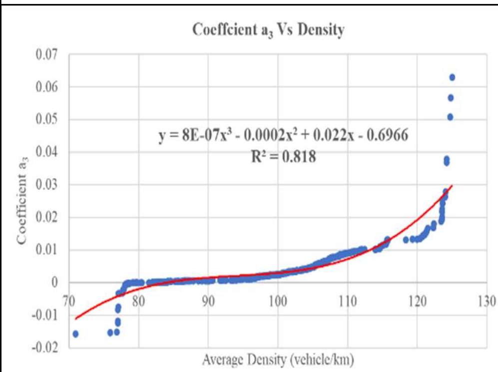
</td><td>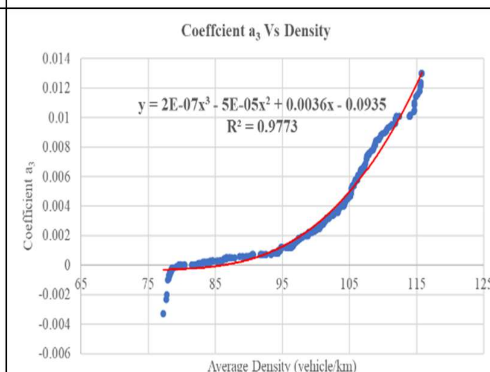
</td></tr>
</table>

Figure A.3: 3rd Order Polynominal Relationship

Table A.3: Default, Min and Max Values of Car Following Parameters

Serial	Driving Behavior Parameters	Unit	Default Values	Min Value	Max Value
1	CC0 (Standstill distance)	meter	1.50	0.00	4.00
2	CC1 (Headway time)	second	0.90	0.00	4.00
3	CC2 (‘Following’ variation)	meter	4.00	0.00	10.00
4	CC3 (Threshold for entering ‘Following’)	-	-8.00	-30.00	-8.00
5	CC4 (Negative ‘Following’ thresholds)	-	-0.35	-1.00	0.00
6	CC5 (Positive ‘Following’ thresholds)	-	0.35	0.00	1.00
7	CC6 (Speed dependency of oscillation)	-	11.44	0.00	20.00
8	CC7 (Oscillation acceleration)	m/s^2	0.25	0.00	1.00
9	CC8 (Standstill acceleration)	m/s^2	3.50	1.00	8.00
10	CC9 (Acceleration at 80 km/h)	m/s^2	1.50	0.50	3.00
11	Minimum look ahead distance	meter	0.00		
12	Maximum look ahead distance	meter	250.00		
13	No of observed vehicles	number	2		
14	Minimum look back distance	meter	0.00		
15	Maximum look back distance	meter	150.00		
16	Temporary lack of attention duration	Second	0.00		
17	Temporary lack of attention probability	%	0.00		

Table A.4: Default, Min and Max Values of Lane Changing Parameters

Serial	Driving Behavior Parameters	Unit	Default Values	Min Value	Max Value
1	Maximum deceleration (own)	m/s^2	-4.00	-4.57	-3.66
2	:−1 m/s^2 per distance (own)	meter	100.00	100	250
3	Accepted deceleration (own)	m/s^2	-1.00	-3.66	-0.76
4	Maximum deceleration (trailing veh)	m/s^2	-3.00	-4.57	-2.44
5	:−1 m/s^2 per distance (trailing veh)	meter	100.00	100	250
6	Accepted deceleration (trailing veh)	m/s^2	-1.00	-3.66	-0.46
7	Waiting time before diffusion	second	60.00	30.00	200.00
8	Min headway (front/rear)	meter	0.50	0.46	0.61
9	Safety distance reduction factor	-	0.60	0.10	1.00
10	Maximum deceleration for cooperative braking	m/s^2	-3.00	-6.10	-2.44

ANNEXURE B
'CALVIS' AN OPTIMIZATION PROGRAM CONTROL INTERFACE (OPCI)

B.1 Motivation for Development of OPCI 'CALVIS'

The proposed procedure of calibration discussed in this study involves a sequence of complex actions which requires priori knowledge on traffic microsimulation model and optimization algorithms. Extraction of real time video data and analyzing, derivation of regression equation from the relationship between space headway and speed, and between coefficients, obtained from previous relation, and average density, generation of new set of parameters as directed by the optimization algorithm to converge for optimal values of fitness function and finally analyzing, comparing and displaying the result, which all are colossal jobs and require tremendous effort and time. Manual experimentation with model parameters appears to be impractical because users have to undergo potentially endless trials to fine-tune parameter values to fit the simulation output with observed data. That provoked for development of an automated and robust optimization tool for calibration of microscopic traffic simulation parameters in VISSIM.

To automate such calibration process, CALVIS (Calibration of VISSIM), a Windows-based Optimization Program Control Interface, has been developed in Visual Basic 2015 so that the user can easily and automatically optimize the parameter values for the simulation model. CALVIS integrates the Visual Basic 2015 and VISSIM 7.0 to implement the calibration approach by three optimization methods. New algorithm for GA, SPSA and SA has been coded in Visual Basic 15 for the OPCI. CALVIS capture the observed video data, analyze and organize the vehicle trajectory data for comparison with simulation data. It communicates with VISSIM through COM interface, customize the input parameters and run simulation for specific number of iterations as per user's choice. After every simulation, CALVIS gets the simulation result from VISSIM, analyze and formulate equation for MOP, and compare with observed data as per objective function. Guided by the selected optimization algorithm it suggests new set of parameters for the subsequent simulation. Finally, CALVIS produces the output of optimal parameters resulting from lowest value of objective function. CALVIS also has the provision of preserving vehicle trajectory data and displays result in the forms of graphs and charts for further analysis.

B.2 Features of CALVIS

B.2.1 Extraction of video data to desired format

CALVIS uses OpenCV Background Subtraction technique of image processing for extracting vehicle trajectory data with each vehicle's position at 0.2 seconds of interval along the roadway in the format as shown in Table 6.1 and 6.2 of Chapter 6.

(a)

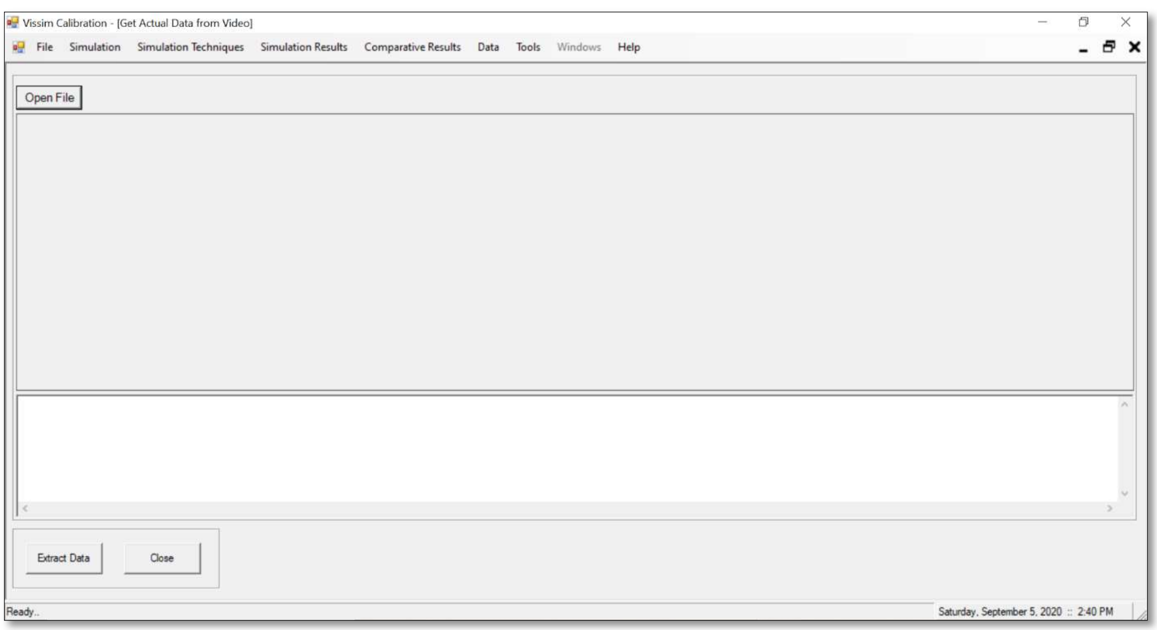

(b)

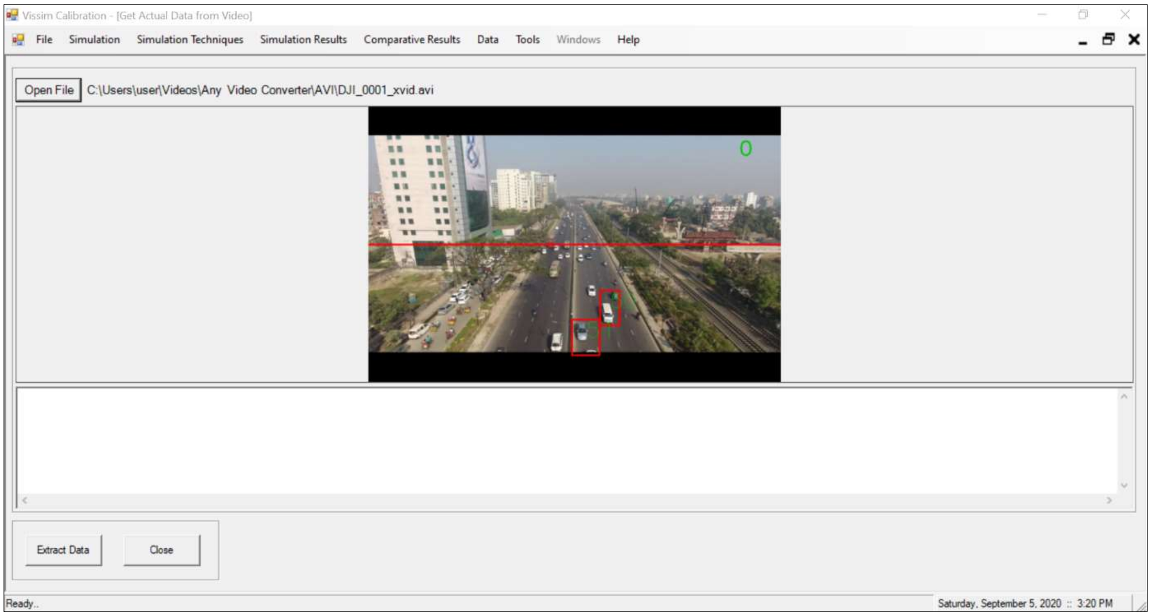

Vissim Calibration - [Get Actual Data from Video]
File Simulation Simulation Techniques Simulation Results Comparative Results Data Tools Windows Help
Open File C:\Users\user\Videos\Any Video Converter\AVI\DJI_0001_xvid.avi
Extract Data
Close
Ready..
Saturday, September 5, 2020 :: 3:20 PM

(c)

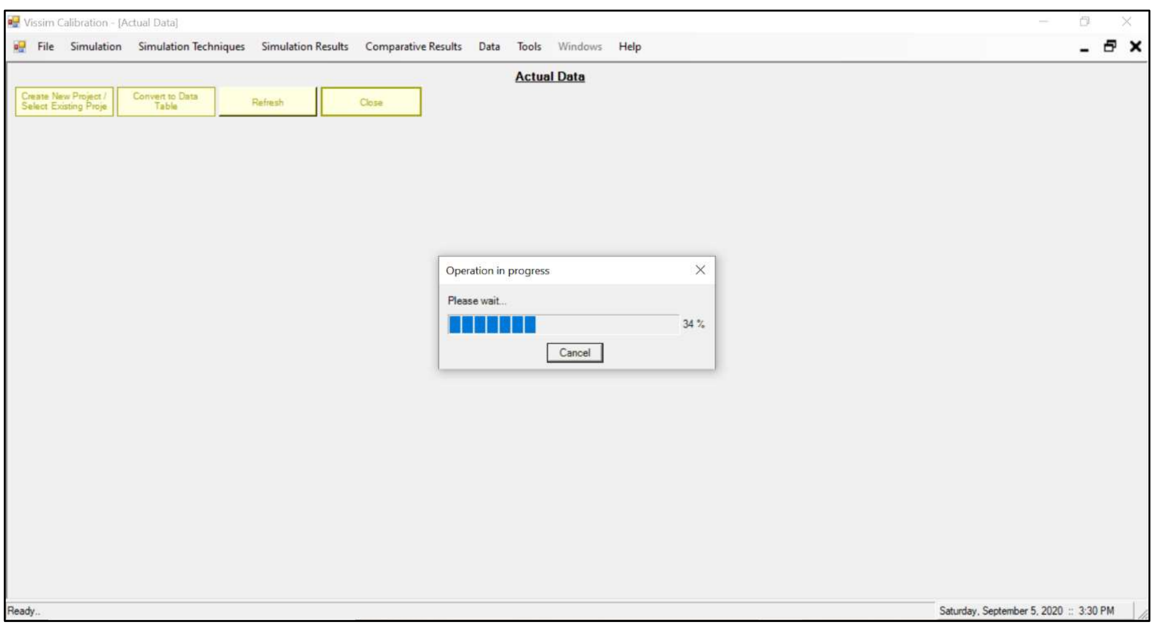

Vissim Calibration - [Actual Data]
File Simulation Simulation Techniques Simulation Results Comparative Results Data Tools Windows Help
Actual Data
Create New Project / Select Existing Proje
Convert to Data Table
Refresh
Close
Operation in progress
Please wait...
34 %
Cancel
Ready..
Saturday, September 5, 2020 :: 3:30 PM

(d)

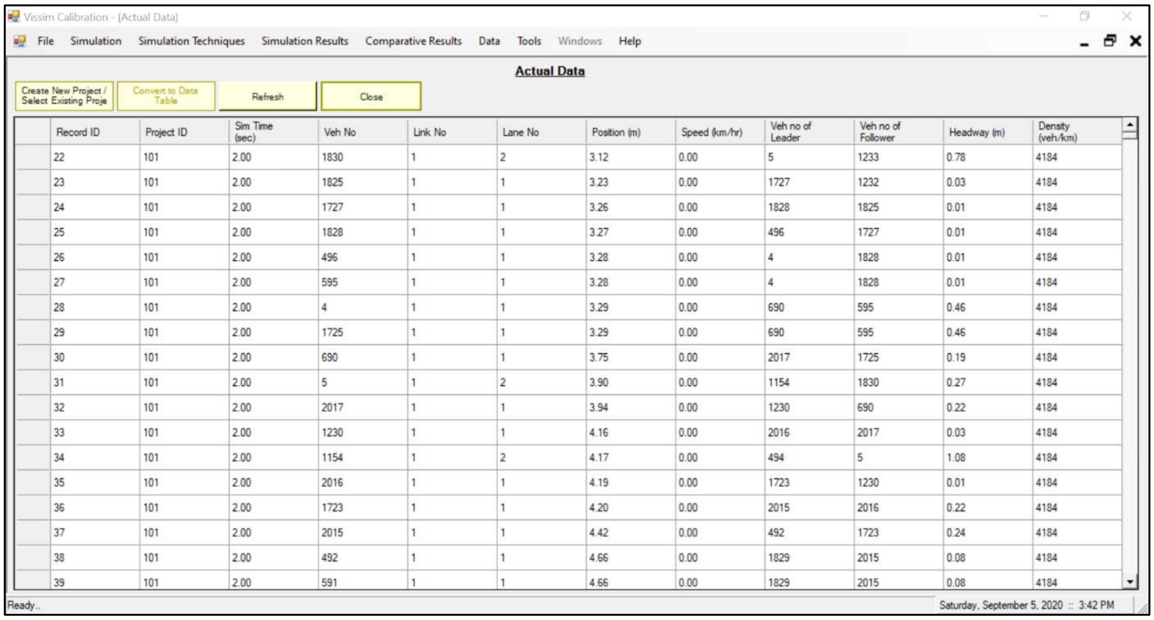

Record ID	Project ID	Sim Time (sec)	Veh No	Link No	Lane No	Position (m)	Speed (km/hr)	Veh no of Leader	Veh no of Follower	Headway (m)	Density (veh/km)
22	101	2.00	1830	1	2	3.12	0.00	5	1233	0.78	4184
23	101	2.00	1825	1	1	3.23	0.00	1727	1232	0.03	4184
24	101	2.00	1727	1	1	3.26	0.00	1828	1825	0.01	4184
25	101	2.00	1828	1	1	3.27	0.00	496	1727	0.01	4184
26	101	2.00	496	1	1	3.28	0.00	4	1828	0.01	4184
27	101	2.00	595	1	1	3.28	0.00	4	1828	0.01	4184
28	101	2.00	4	1	1	3.29	0.00	690	595	0.46	4184
29	101	2.00	1725	1	1	3.29	0.00	690	595	0.46	4184
30	101	2.00	690	1	1	3.75	0.00	2017	1725	0.19	4184
31	101	2.00	5	1	2	3.90	0.00	1154	1830	0.27	4184
32	101	2.00	2017	1	1	3.94	0.00	1230	690	0.22	4184
33	101	2.00	1230	1	1	4.16	0.00	2016	2017	0.03	4184
34	101	2.00	1154	1	2	4.17	0.00	494	5	1.08	4184
35	101	2.00	2016	1	1	4.19	0.00	1723	1230	0.01	4184
36	101	2.00	1723	1	1	4.20	0.00	2015	2016	0.22	4184
37	101	2.00	2015	1	1	4.42	0.00	492	1723	0.24	4184
38	101	2.00	492	1	1	4.66	0.00	1829	2015	0.08	4184
39	101	2.00	591	1	1	4.66	0.00	1829	2015	0.08	4184

Figure B.1: Screenshot of CALVIS for Extraction of Video data.
(a) Initial Screen of Video Extraction (b) Video Capturing Process Ongoing
(c) Processing of Data (d) Data Extracted to Desired Format

B.2.2 Simulation with default parameters

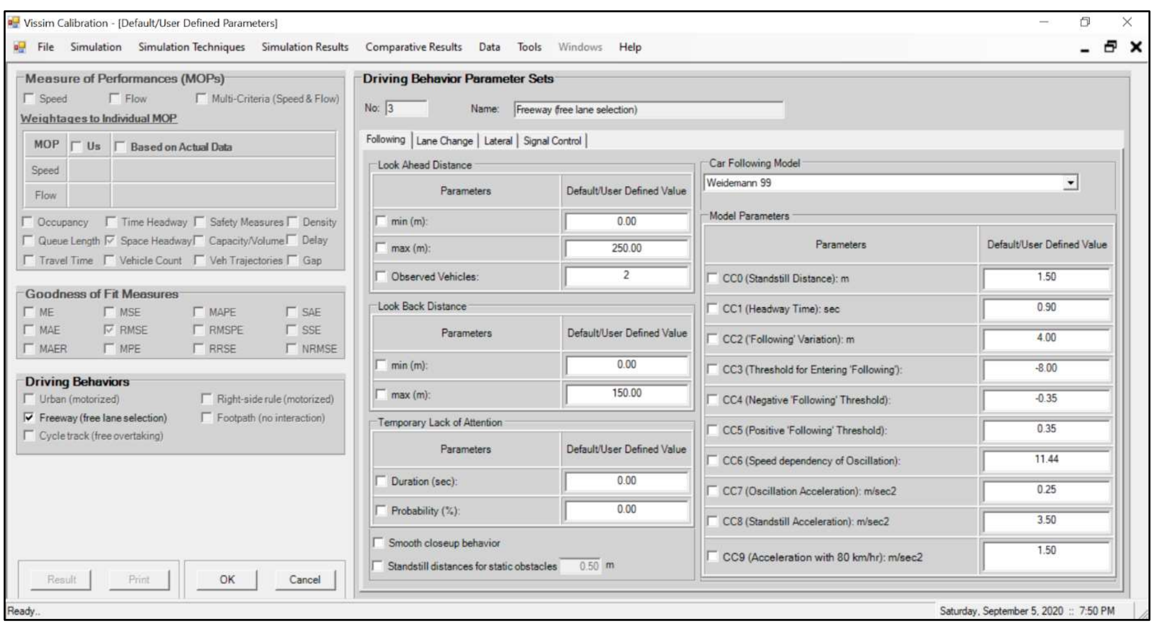

Figure B.2: CLAVIS Panel Screenshot for Simulation with Default Parameters

B.2.3 Perform sensitivity analysis

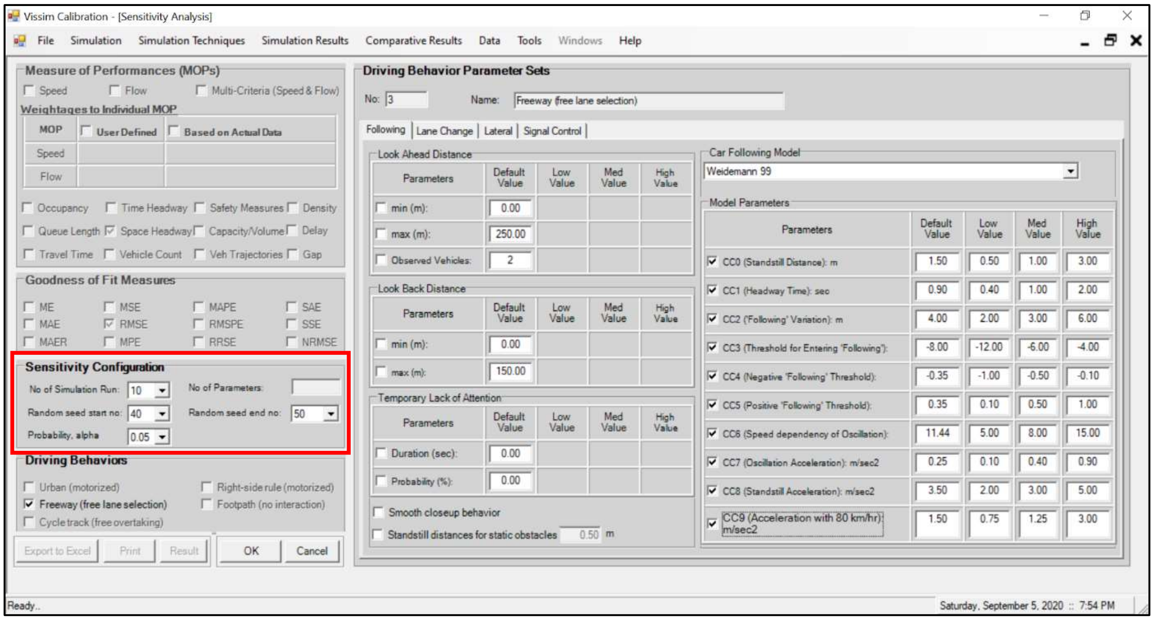

Figure B.3: CLAVIS Panel Screenshot for Sensitivity Analysis

B.2.4 Result of sensitivity analysis

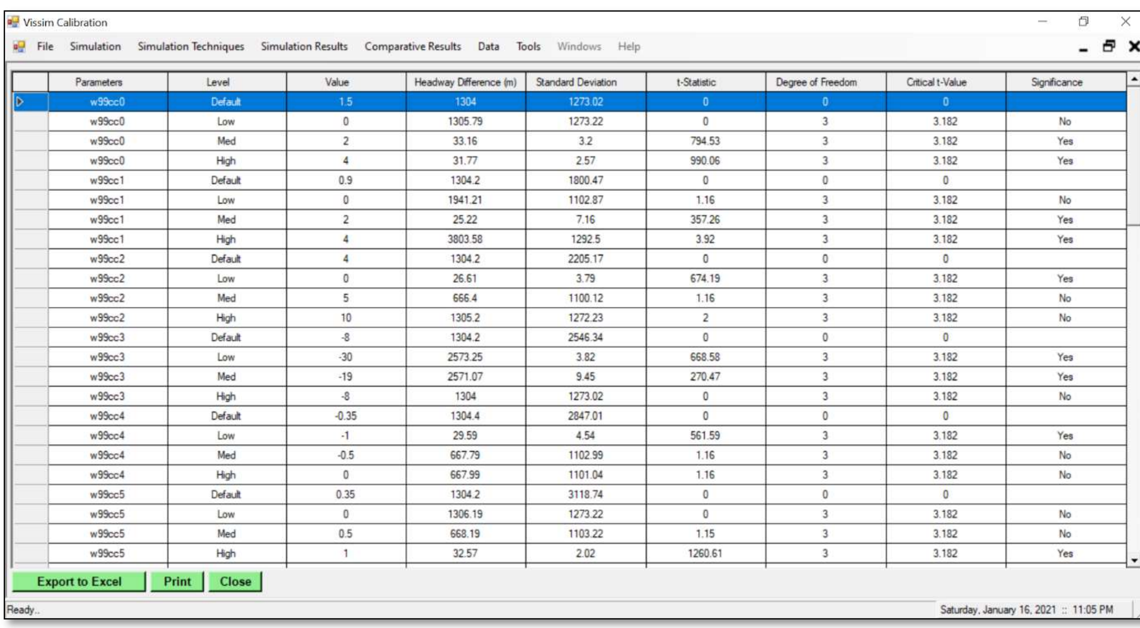

Parameters	Level	Value	Headway Difference (m)	Standard Deviation	t-Statistic	Degree of Freedom	Critical t-Value	Significance
w99cc0	Default	1.5	1304	1273.02	0	0	0	
w99cc0	Low	0	1305.79	1273.22	0	3	3.182	No
w99cc0	Med	2	33.16	3.2	794.53	3	3.182	Yes
w99cc0	High	4	31.77	2.57	990.06	3	3.182	Yes
w99cc1	Default	0.9	1304.2	1800.47	0	0	0	
w99cc1	Low	0	1941.21	1102.87	1.16	3	3.182	No
w99cc1	Med	2	25.22	7.16	357.26	3	3.182	Yes
w99cc1	High	4	3803.58	1292.5	3.92	3	3.182	Yes
w99cc2	Default	4	1304.2	2205.17	0	0	0	
w99cc2	Low	0	26.61	3.79	674.19	3	3.182	Yes
w99cc2	Med	5	666.4	1100.12	1.16	3	3.182	No
w99cc2	High	10	1305.2	1272.23	2	3	3.182	No
w99cc3	Default	-8	1304.2	2546.34	0	0	0	
w99cc3	Low	-30	2573.25	3.82	668.58	3	3.182	Yes
w99cc3	Med	-19	2571.07	9.45	270.47	3	3.182	Yes
w99cc3	High	-8	1304	1273.02	0	3	3.182	No
w99cc4	Default	-0.35	1304.4	2847.01	0	0	0	
w99cc4	Low	-1	29.59	4.54	561.59	3	3.182	Yes
w99cc4	Med	-0.5	667.79	1102.99	1.16	3	3.182	No
w99cc4	High	0	667.99	1101.04	1.16	3	3.182	No
w99cc5	Default	0.35	1304.2	3118.74	0	0	0	
w99cc5	Low	0	1306.19	1273.22	0	3	3.182	No
w99cc5	Med	0.5	668.19	1103.22	1.15	3	3.182	No
w99cc5	High	1	32.57	2.02	1260.61	3	3.182	Yes

Figure B.4: CLAVIS Panel Screenshot for Result of Sensitivity Analysis

B.2.5 Simulation techniques

B.2.5.1 GA optimization control panel

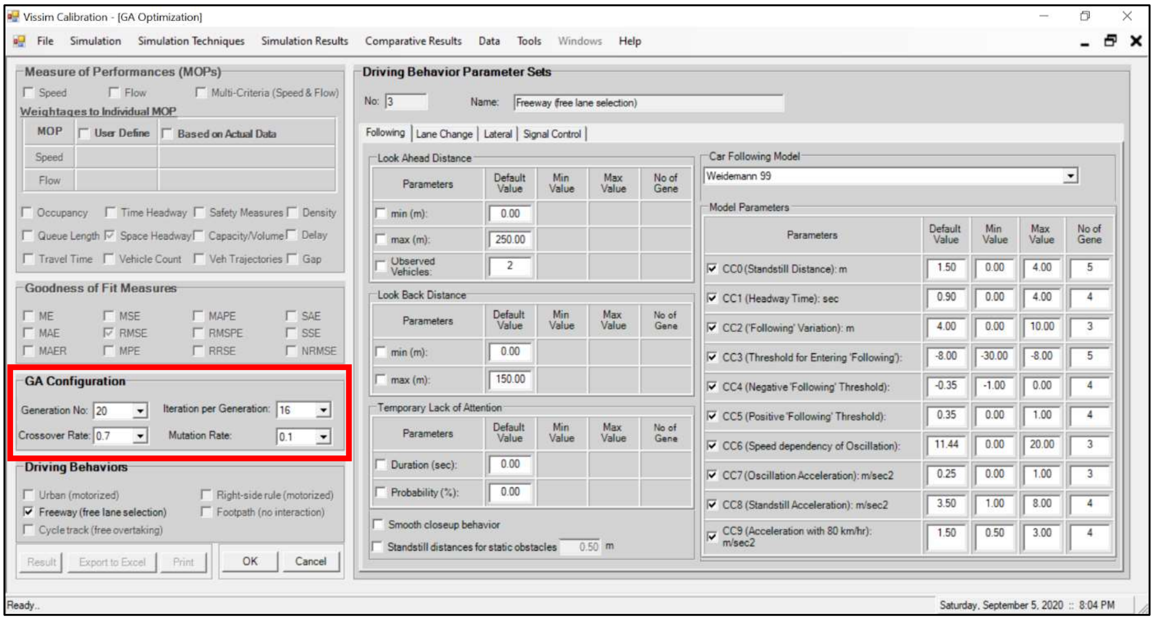

Figure B.5: CLAVIS Panel Screenshot for GA Optimization

B.2.5.2 SPSA optimization control panel

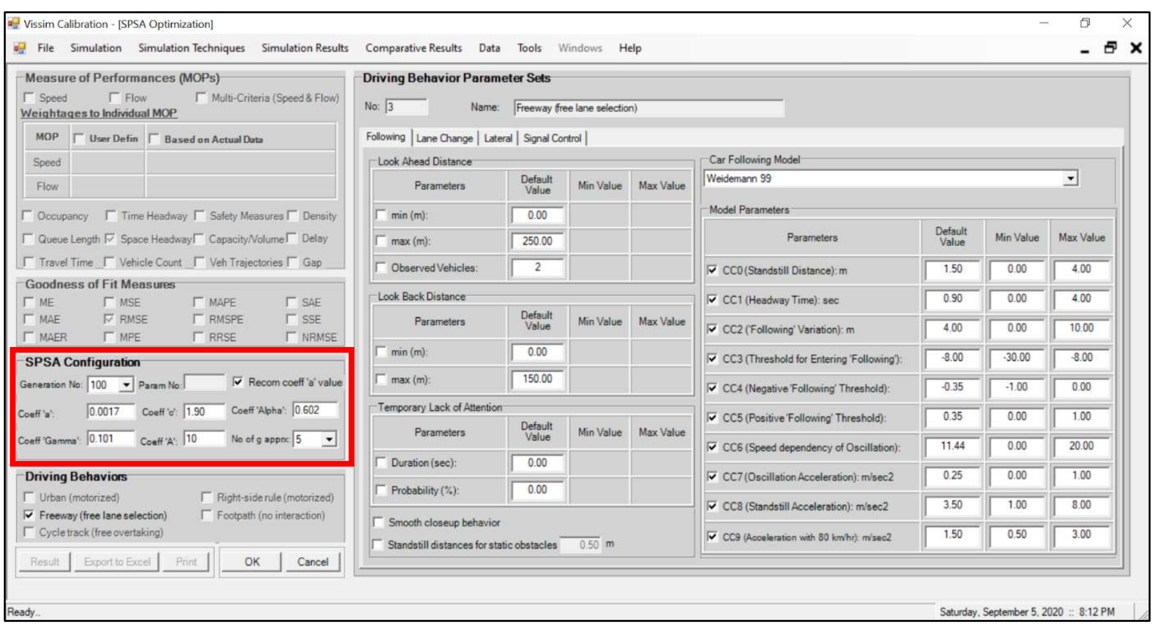

Figure B.6: CLAVIS Panel Screenshot for SPSA Optimization

B.2.5.3 SA optimization control panel

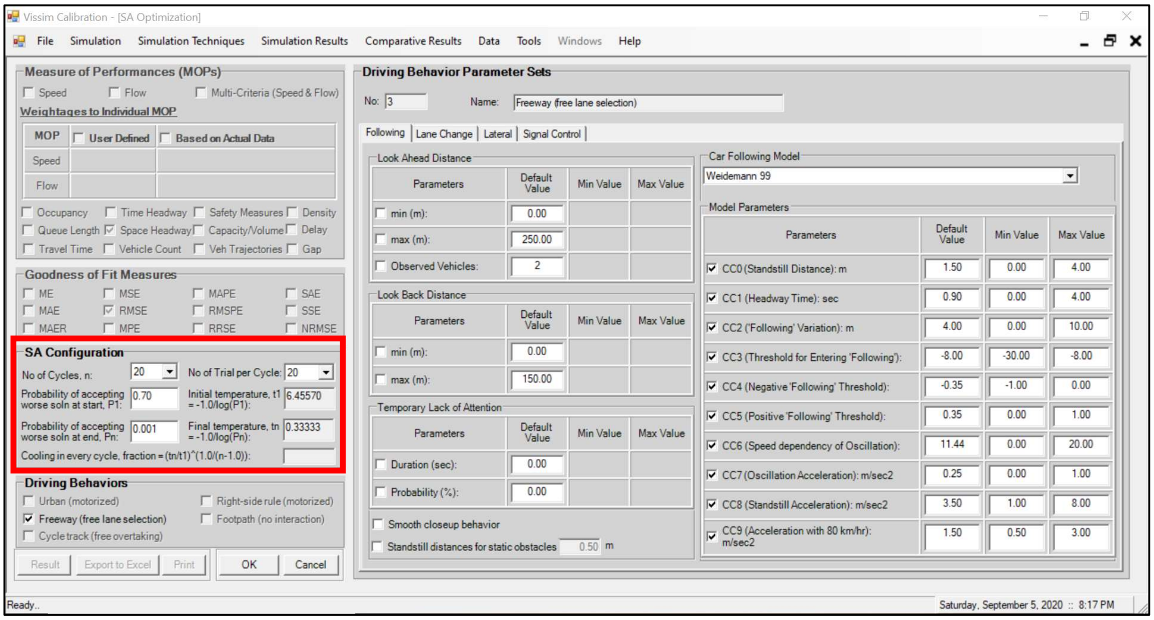

Figure B.7: CLAVIS Panel Screenshot for SA Optimization

B.2.6 Validation control panel

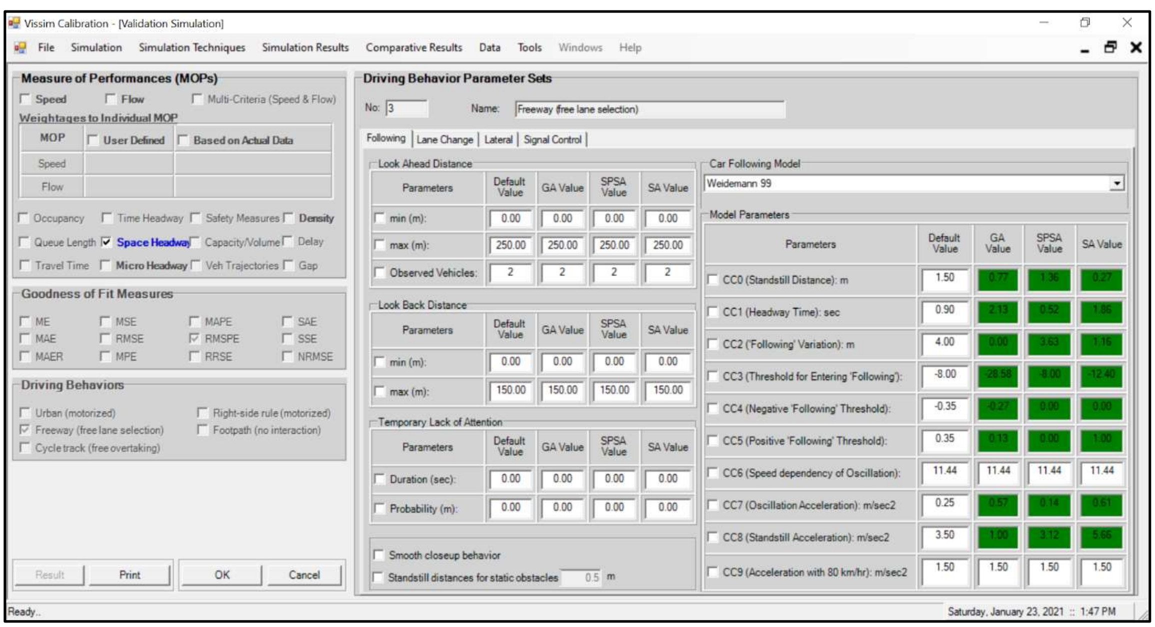

Figure B.8: CLAVIS Panel Screenshot for Validation

B.2.7 Results

B.2.7.1 All results

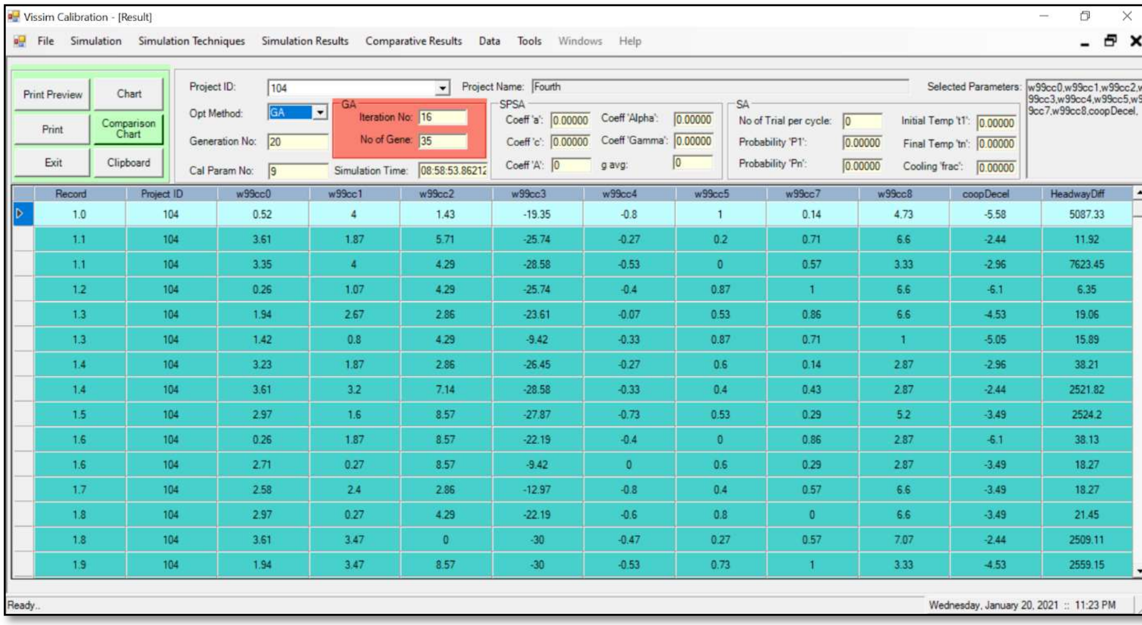

Figure B.9: CLAVIS Panel Screenshot for Results of Detail Iteration and Charts

B.2.7.2 Calibrated parameters

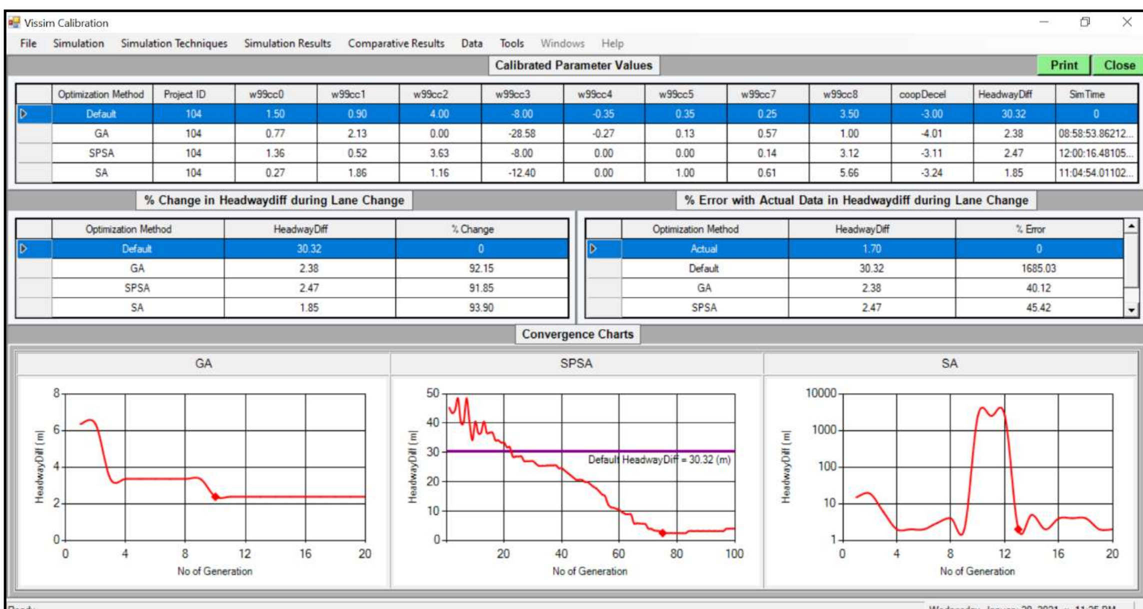

Figure B.10: CLAVIS Panel Screenshot for Results of Calibrated Parameters

B.2.7.3 Validation result

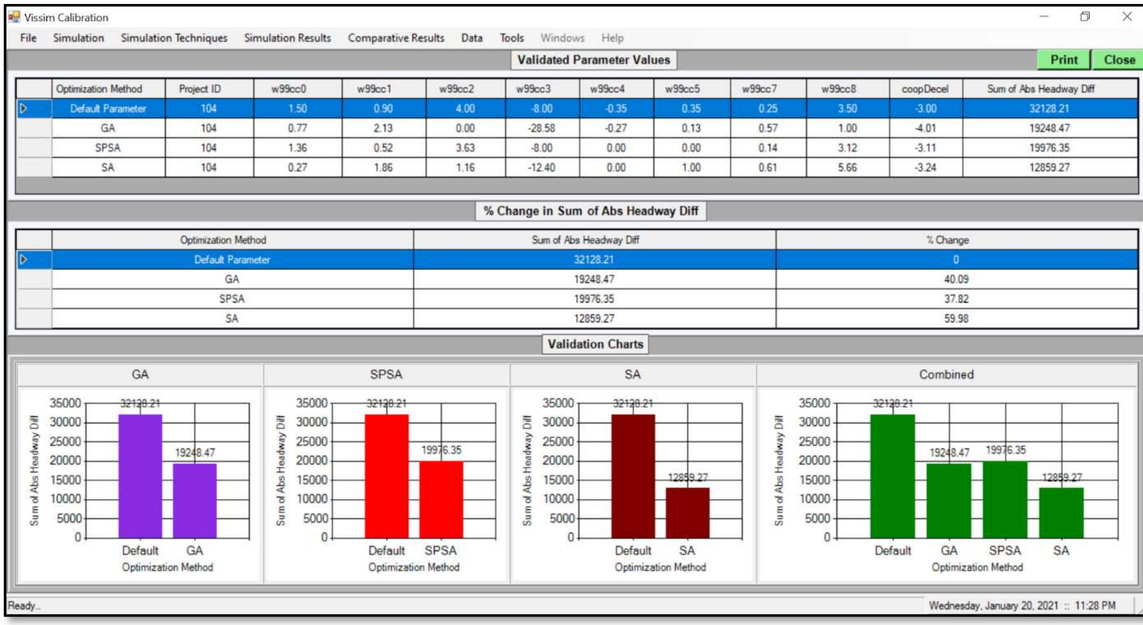

Figure B.11: CLAVIS Panel Screenshot for Validation Result